DOCTOR OF PHILOSOPHY

Novel roles of the Canadian clock protein neuronal PAS domain protein 2 (NPAS2) in the response to oxidative and heat stress

Gammash, Mohammed Matuq

Award date:
2017

Awarding institution:
Bangor University

PRIFYSGOL
BANGOR
UNIVERSITY

Novel Roles of the Circadian Clock Protein Neuronal PAS Domain Protein 2 (NPAS2) in the Response to Oxidative and Heat Stress

A Dissertation presented to

School of Biological School

College of Natural Science

Bangor University

In Partial Fulfillment

Of the Requirements for the

Degree Doctor of Philosophy

Mohammed. Matuq. Gammash

Dr. Thomas Manfred Helmut Caspari, Dissertation Supervisor

April 2017

Summary

Human NPAS2 is a basic-helix-loop-helix (BHLH) transcription factor with two N-terminal PAS domains that forms a hetero-dimeric complex with BMAL1/ARNTL to regulate the transcription of key circadian clock genes like *Period* and *Cryptochrome*. NPAS2 is unique in higher eukaryotic cells as both PAS domains contain one heme group each, which bind carbon monoxide. Although NPAS2 has been linked to cancer and neurological disorders, very little is known about its cellular roles. The results obtained in this study support a model in which NPAS2 responds to oxidative and heat stress in distinct manners. While oxidative stress results in the post-translational modification of NPAS2 and the formation of high molecular weight complexes, heat stress reduces the protein levels of NPAS2. These differences are also reflected in the changes to the *NPAS2* mRNA levels. While oxidative stress increases expression of *NPAS2*, heat stress causes a drop in mRNA levels. The responses are cell line specific as, for example, the drop in NPAS2 protein levels after a heat shock was observed in MCF-7 breast cancer cells and HeLa cervical cancer cells, but not in non-malignant HEK-293 cells which may be of neuronal origin. Since both stress types are known to affect the peripheral clocks in human tissues in a manner which may be regulated by the MAP kinase p38β, it is proposed that NPAS2 is a novel target of this kinase. Why NPAS2 is regulated differently depending on the type of stress, could be linked with the different ways the p38 MAP kinase pathway responds to heat and oxidative stress. While heat activation is dependent on upstream kinases, heat activation may be dependent on the heat-induced increase in carbon monoxide in human cells.

The works shows also that NPAS2 mRNA levels drop in the response to serum starvation and that the neuroblastoma KELLY cell line does not, or only at a very reduced level, express *NPAS2* although an analysis of a large panel of human tissues shows high *NPAS2* expression in the brain. A bioinformatical analysis of missense single nucleotide polymorphisms (SNPs) located the N-terminal domain of NPAS2 identifies two SNPs (S204P, rs750277651 and T252N, rs555063320) which may affect a p38 (S202) and DYRK1A (T252) kinase modification site, respectively. This is of interest as p38β may regulate NPAS2 and the dual-specific DYRK1A kinase is known to regulate the protein turnover of Cryptochrome.

In summary, the work makes a strong case for NPAS2 as a novel target of the p38β MAP kinase pathway in the cellular response to oxidative and heat stress.

Acknowledgment

In the name of Allah (God), the Most Gracious and the Most Merciful, all praises to Allah (God) for the strengths and his blessing that he blessed upon me.

Accomplishment is a word, which always sounds good. It is really a pleasure to see things done in a perfect and orderly manner. No one is an island and so a helping hand is needed in every step we take to accomplish a goal.

My heartfelt appreciation goes to my supervisor **Dr.Thomas Caspari**, for his supervision, guidance, and support throughout the course of my study.

I feel very privileged to have the opportunity to work in a wonderful lab where I have received everyday assistance and useful discussions from everyone. I'm grateful to my colleagues Saad Al-Johani, Rabiaa Oun, Yasir Al-Mehdi and every one else in D2 lab for everyday useful discussions throughout the project and science.

Also, I would like to express my gratitude to my family for the support they provided me through my entire life. In particular, I'm very grateful to my uncle **Abdulaziz Gammash (**God bless his soul**)** who took care of me since childhood and who I saw him the father I had lost.

Father in law **Khalid Al-Hussaini**, my wife **Mashael Al-Hussaini** and my kids Hassan, Mila and Abdulaziz, without your encouragement, love, patience, backing me for all the decisions I have made. I simply can't believe how lucky I am to having you all as part of my life.

In not least, I recognize that, this research would not have been possible without the financial assistance of Ministry of Higher Education, Saudi Arabia.

Finally, all people whose helped me directly or indirectly to make this experience amazing. I am grateful to you to be as part of this achievement.

Mohammed Matuq Gammash

Table of Contents

LIST of Figures

LIST of Tables

CHAPTER 1

GENERAL INTRODUCTION

Chapter 1: General Introduction

1.1 Introduction to the circadian clock.

1.1.1 Circadian genes.

The circadian system plays a fundamental role in synchronising a range of biological processes in organisms thereby coordinating them with the environment. Changes in both the behaviour and physiology of organisms may result. In humans, biological processes that are influenced by circadian clock include hormone secretions, body temperature, heartbeat, energy metabolism sleep and wakefulness, the cell cycle and DNA repair (Kondratov et al. 2006). The location of the master circadian clock in mammals is in the suprachiasmatic nuclei (SCN) a small group of neurons situated in the anterior hypothalamus. The SCN is able to respond to light input from the visual system such as the light-dark cycle and coordinate tissue-specific rhythms (Albrecht, Eichele 2003). As well as the circadian clock in the SCN that acts as a central pacemaker, mammals also possess multiple individual clocks in peripheral tissues (Schibler, Sassone-Corsi 2002). For example, expression analysis of eight canonical clock genes in seven peripheral tissues showed robust circadian expression of each mRNA in liver, heart, lung, spleen, kidney and stomach but not testis (Yamamoto et al. 2004). The SCN clock is composed of multiple, single-cell oscillators with a period of oscillation of around 24 hours. Generation of synchronized circadian outputs from the SCN regulates rhythms of individual clocks in peripheral tissues (Schibler, Sassone-Corsi 2002, Reppert, Weaver 2001).

The mammalian clock is regulated at the cellular level by feedback loops acting at transcriptional and translational levels. This is shown diagrammatically in (Figure 1-1). Heterodimers of the ARNTL (aryl hydrocarbon receptor nuclear translocator-like; formerly BMAL1) and CLOCK (circadian locomotor output cycles kaput) transcription complex activate the expression of the Period (*Per1* – period homolog 1 *Drosophila*; and *Per 2* period homolog 2 *Drosophila* and cryptochrome 1 (photolyase-like) (*Cry1*) genes. The ARNTL-CLOCK complex binds to the *Per* and *Cry* promoters via Enhancer Box (E-box) elements. Both CLOCK and ARNTL (BMAL1) proteins contain a basic helix-loop-helix-PAS domain, which is important for their function (Yu, Weaver 2011). NPAS2 (Neuronal PAS domain protein 2), which is the focus of this study, is closely related to CLOCK and can replace CLOCK in the ARNTL/BMAL1 transcription complex (Reick et al. 2001).

The transcriptional activity of the CLOCK-ARNTL complex is counteracted by increasing levels of the PER proteins which complex with the CRY proteins in the cytoplasm and are post-translationally modified by CKIe (casein kinase 1, epsilon; CSNK1E) and CKId (casein kinase 1, delta; CSNK1D). Phosphorylation of the Period-Cryptochrome complexes by CKIe results first in their nuclear localization to down-regulate the activity of the CLOCK-ARNTL complex. Further phosphorylation of the Per-Cry complexes inside the nucleus triggers then their attachment to ubiquitin and subsequent degradation there by re-activating the CLOCK-ARNTL complex (Keesler et al. 2000, Vielhaber et al. 2000). This creates a cycle that drives the circadian clock. Similar phosphorylation-dependent regulations are executed by CKId and CKIe in human cells affecting both PER1 and PER2 (Camacho et al. 2001). Recently, it was shown that the balance between phosphorylation by casein kinase 1 and dephosphorylation by protein phosphatase 1 (PP1) is the main determinant of the period length of the circadian oscillator (Lee et al. 2011). Interestingly, a decrease in human CK1e expression has been linked with schizophrenia (Pinacho et al. 2016).

The negative feedback loop of PER-CRY and CLOCK-ARNTL is further regulated by the retinoic acid receptor-related orphan receptor α (RORα) and the nuclear receptor subfamily 1, group D, member 1 (NR1D1/ Rev-Erbα) which are two nuclear receptors that target a *RORE*-response element in the promoter of the *ARNTL/Bmal1* gene (Reick et al. 2001, Delerive, Chin & Suen 2002, Reppert, Weaver 2002, Crumbley et al. 2010).

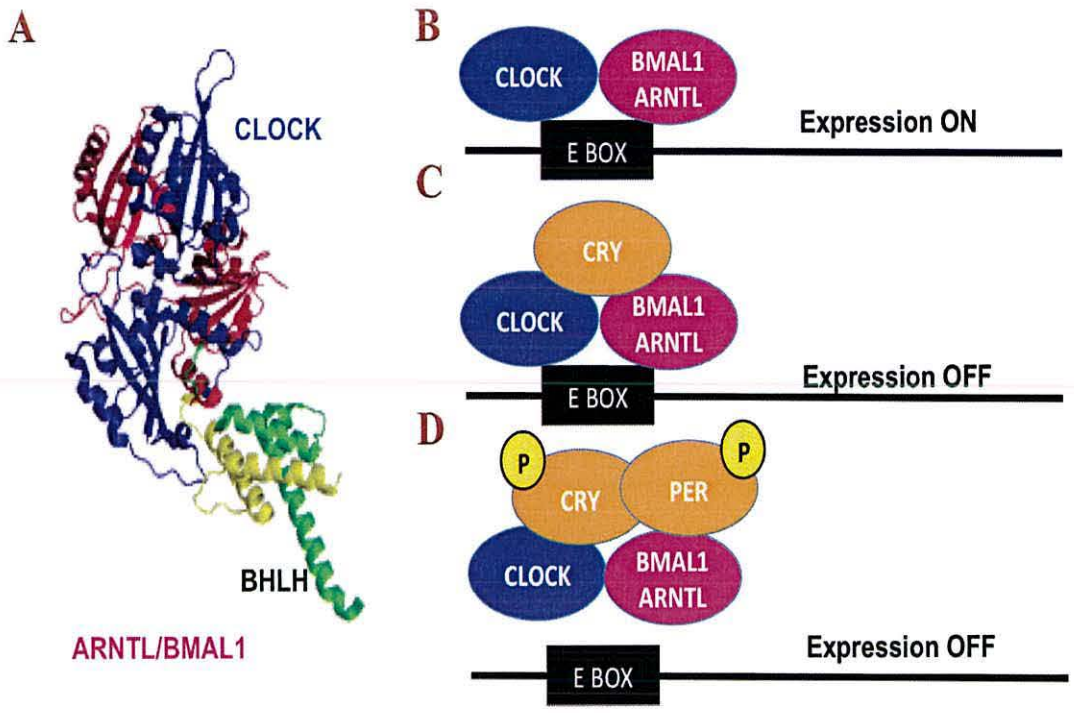

Figure 1-1: Structure of the CLOCK (NAPS2)-ARNTL/BMAL1 transcription complex and regulation of the complex by Period and cryptochrome.

A: Structure of the N-terminal section of the mouse CLOCK (NPAS2)-ANTL/BMAL1 transcription complex (ID: 4F3L, (Huang et al. 2012)). The image was generated with Polyview3D. The Basic-HELIX-Loop-Helix (BHLH) domain of CLOCK is shown in yellow, the corresponding BHLH domain of ARNTL/BMAL1 is shown in green. The BHLH domains bind to the E box upstream of the Period (PER) and Cryptochrome (CRY) genes. The CLOCK protein is shown in blue and the ARNTL/BMAL1 protein is shown in red.

B: Activation of gene expression by the CLOCK-ARNTL/BMAL1 complex at the E box domain in the promotor region.

C: Cryptochrome on its own can bind and inactivate the CLOCK-ARNTL complex while bound to the E box.

D: The phosphorylated Period-Cryptochrome complex removes the CLOCK-ARNTL from the DNA.

In the nucleus, the phosphorylated PER-Cry complex displaces the CLOCK-ARNTL/BMAL1-heterodimer from the DNA to repress transcription (negative feedback loop) from the E box sections of the *Period* and *Cryptochrome* genes (Figure 1-1). Interestingly, while Period proteins on their own do have no effect on the CLOCK-ARNTL complex, Cryptochrome on its own binds to the complex at the DNA to inactivate its activity (Ye et al. 2014). Expression of ARNTL/BMAL1 is regulated by the competitive binding of RORα and REV-ERB (NR1D1) to the *RORE* element in the Bmal1 promoter. While REV-ERB blocks ARNTL/BMAL1 transcription, ROR induces it thereby creating a stabilizing loop (Reppert, Weaver 2002, Partch, Green & Takahashi 2014).

Neuronal PAS domain protein 2 (NPAS2) is closely related to CLOCK (King et al. 1997) and is predominantly expressed in the forebrain of mammals (Reick et al. 2001). NPAS2, like CLOCK, forms a heterodimer with ARNTLl (BMAL1) and, has a similar function to CLOCK, inducing transcription of *PER1, PER2* and *CRY* genes by binding to E-box elements (CACGTG) within their promoters (Reick et al. 2001, Rutter et al. 2001). It has recently been shown that NPAS2, like its paralog CLOCK, is also a RORα and NR1D1 (REV-ERBα) target thereby enabling the regulation of the expression of the *NPAS2* gene (Crumbley et al. 2010).

Generation of BMAL1 (ARNTL) null mice has shown that the gene is non-redundant and an essential component of the circadian pacemaker in mammals as its knockout produced an immediate and complete loss of circadian rhythmicity when the mice were kept in the dark without the light trigger (Bunger et al. 2000). In contrast, the phenotype observed with homozygous *CLOCK* mutant mice, generated with the Cre-LoxP conditional knockout system, was less severe since the mice only showed altered responses to light but robust circadian rhythms as demonstrated by locomotion activity (DeBruyne et al. 2006). The most likely reason for these results is that NPAS2 can compensate for the absence of CLOCK. Homozygous *NPAS2* mutant mice showed a similar phenotype as *CLOCK* null mice with a robust circadian rhythm which was demonstrated by their the frequency of wheel-running activity (DeBruyne, Weaver & Reppert 2007). In addition, *NPAS2* null mice, like *CLOCK* null mice, show a slightly abbreviated circadian period and also an altered response to changes in the light-dark cycle. Interbreeding of Clock-deficient mice (*Clock-/-*) with mice heterozygous for NPAS2 (*NPAS2+/-*) showed that the resulting mice which were homozygous null for both *CLOCK* and *NPAS2* showed immediate arrhythmic locomotion behaviour. This shows that a functional circadian rhythm requires either NPAS2 or CLOCK to form a complex with ARNTL/BMAL1. In contrast, mice that were *Clock-/-* and *NPAS2+/-* showed a less severe circadian phenotype with progressive rhythmic instability and circadian periods which were substantially shorter in constant darkness in comparison to wild-type mice. The results strongly suggest that NPAS2 has a direct function in the SCN jointly with CLOCK with both proteins

being able to independently form heterodimers with ARNTLl (BMAL1) in the SCN to maintain behavioral rhythmicity (DeBruyne, Weaver & Reppert 2007).

Dysfunctions of the circadian system have been reported to be associated with the development of a number of pathological conditions. For example, a number of circadian clock genes have been implicated in carcinogenesis (Yu, Weaver 2011, Savvidis, Koutsilieris 2012). The CLOCK protein is also implicated in the ageing process, as the average lifespan in homozygous *Clock* deficient mice is around 15% less compared to wild type mice, and their maximum lifespan in comparison to wild type mice is reduced by more than 20%. CLOCK appears to be involved in the regulation of aging in the skin and lens dermatitis and cataracts develop in *Clock* deficient mice (Dubrovsky, Samsa & Kondratov 2010). Since NPAS2 can substitute for CLOCK in the ARNTLl (BMAL1) heterodimer it remains to be seen whether NPAS2 plays a similar role in ageing. Down-regulation of human NPAS2 has been linked with cell growth and invasion in the context colorectal cancer (Xue et al. 2014).

1.1.2 Structure and function of NPAS2 Protein.

1.1.2.1 The Basic Helix-Loop-Helix-PAS domain protein.

Like ARNTLl (BMAL1) and CLOCK, NPAS2 (PASD4, bHLHe9, BHLHE9, MOP4) is also a member of the basic-helix-loop-helix-PAS (BHLH-PAS) domain group of transcription factors (Reppert, Weaver 2002, Debruyne 2008). NPAS2 has one BHLH domain (9aa-59aa) and two Per-Arnt-Sim (PAS) domains termed PAS-A (82aa-145aa) and PAS-B (260aa-307aa) in its N-terminal region (Ishida, Ueha & Sagami 2008) (Figure 1-2).

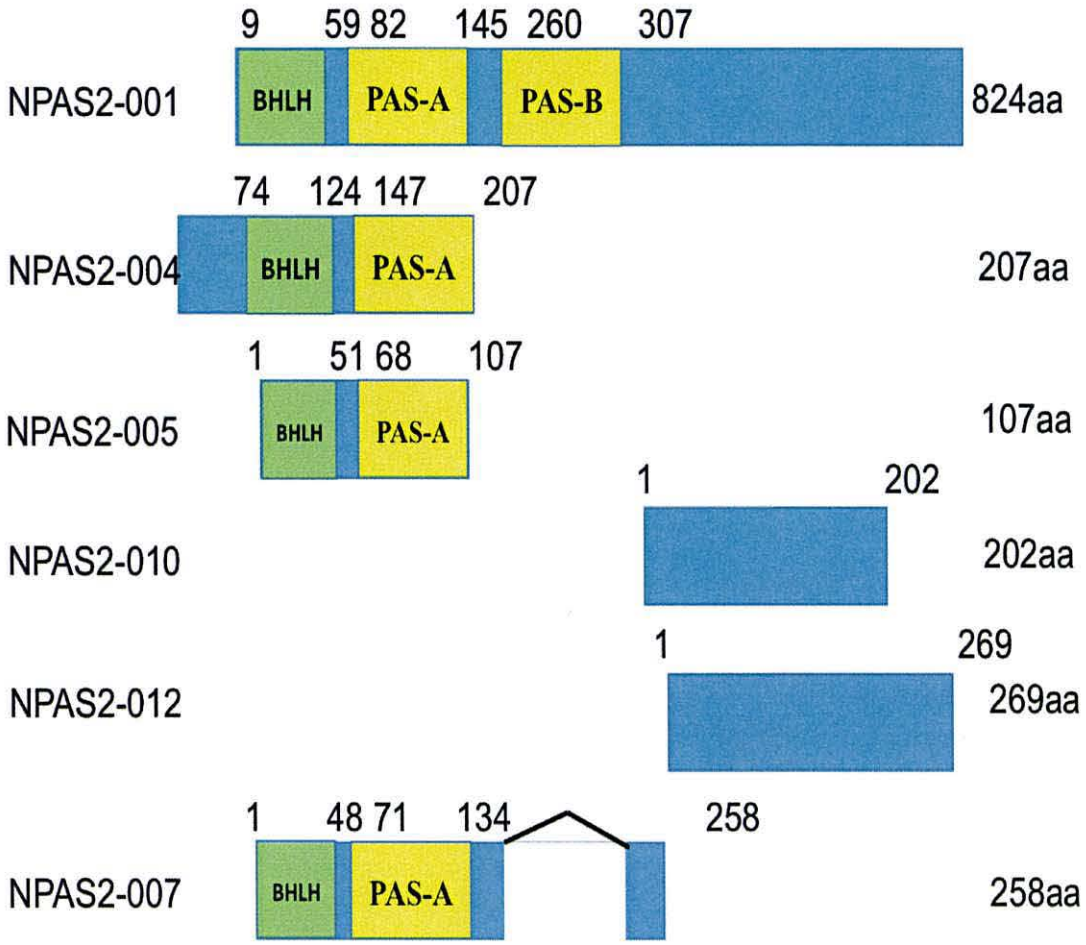

Figure 1-2: Protein Variants of human NPAS2.

The human NPAS2 gene encodes 6 protein variants as listed in the Ensembl database. NPAS2-001 is the full-length protein. NPAS2-004, 005 and 007 are C-terminally truncated proteins all containing the BHLH and first PAS domain. NPAS2-010 and 012 are N-terminally truncated proteins lacking the BLHL and PAS domains. NPAS2-007 has an in frame deletion of the second PAS domain.

Complementary DNA (cDNA) sequences of *NPAS2* along with *NPAS1* were first isolated from mouse and human bacteriophage cDNA libraries (Zhou et al. 1997). Although NPAS1 and NPAS2 are closely related, NPAS1 binds to ARNT whereas NPAS2 binds to ARNTL/BMAL1 (Zhou et al. 1997). ARNT (AhR nuclear translocator) is also a BHLH-PAS domain transcription factor and the NPAS1-ARNT complex may act as a transcriptional repressor rather than a transcriptional activator like the NPAS2-ARNTL complex. Expression of NPAS1 is restricted to some brain areas and linked with brain development and Schizophrenia (Teh et al. 2006).

NPAS3 plays a role in brain development and is linked with inherited forms of Schizophrenia (Yu et al. 2014). NPAS4 expression is induced in the response to neuronal activity and the transcription factor is linked with memory in the working brain (Sun, Lin 2016).

The structure of the N-terminal region of the mouse CLOCK – ARNTL/BMAL1 heterodimer has recently been determined by X-ray crystallography and it shows the formation of a heterodimer via interactions between the BHLH and the PAS domains (Figure 1-3 A). Three domains of each protein (BHLH, PAS-A and PAS-B) interact with the other subunit of the heterodimer (Huang et al. 2012) (Figure 1-3, Figure 1-4). The second alpha-helix of the BHLH domain of CLOCK is in contact with the first PAS-A domain leaving the first helix free to associate with the DNA. The N-terminal helices of the BHLH domains of CLOCK and ARNTL/BMAL1 bind to the E box motive at the DNA (Ma et al. 1994). The exposed surfaces of the two PAS domains in CLOCK are very negatively charged whereas the corresponding PAS domains in ARNTL/BMAl1 are mainly positively charged. Like CLOCK (pI: 5.8), NPAS2 has an acidic isoelectric point (pI: 6.0) which indicates a similar negative charge of the accessible surfaces of the PAS domains in NPAS2.

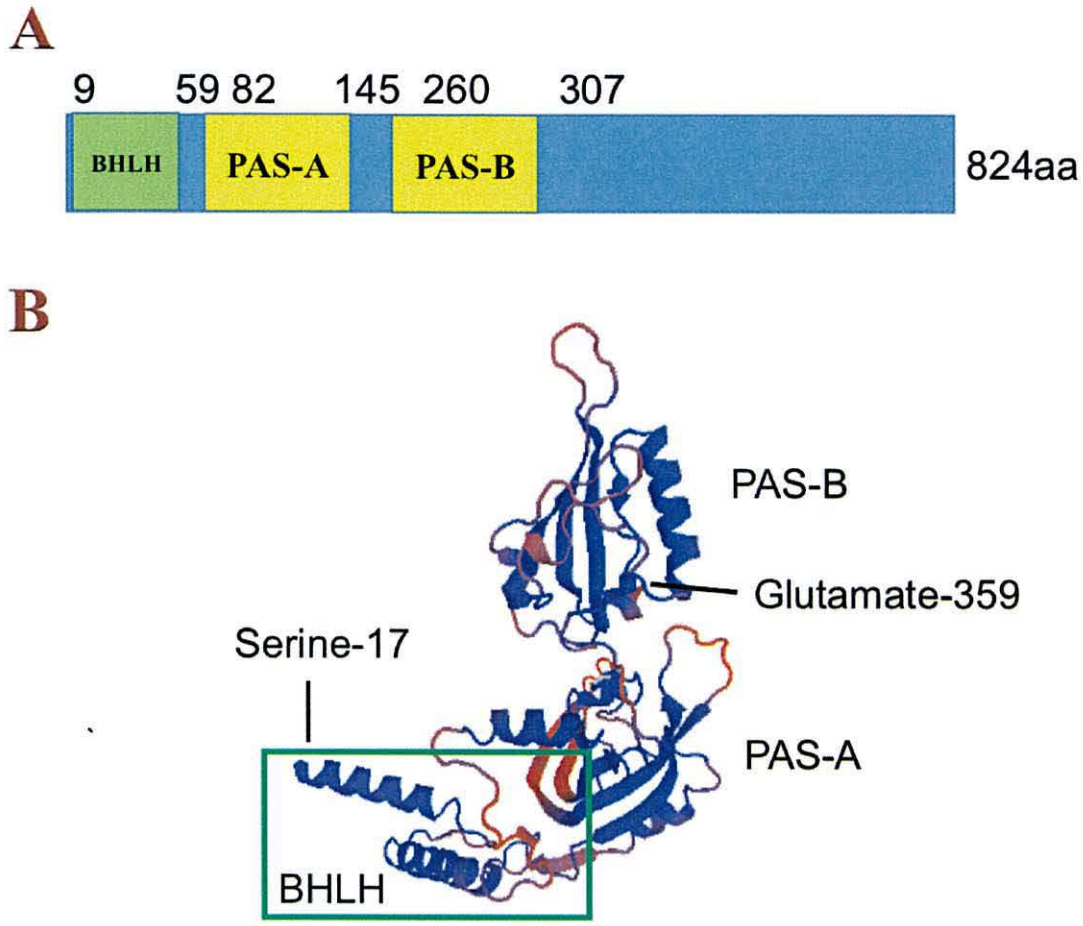

Figure 1-3: Domain organization and model of human NPAS2.

A: Domain organization of human NPAS2.

B: Model of the N-terminal section of human NPAS2 (17aa-359aa) generated with Swiss Model based on the crystal structure of CLOCK (ID 4f3l.1) (Huang et al. 2012). The Basic Helix-Loop-Helix (BHLH) domain is highlighted. This domain binds to DNA. The two PAS domains consist of alpha-helical domains packed against beta-sheets.

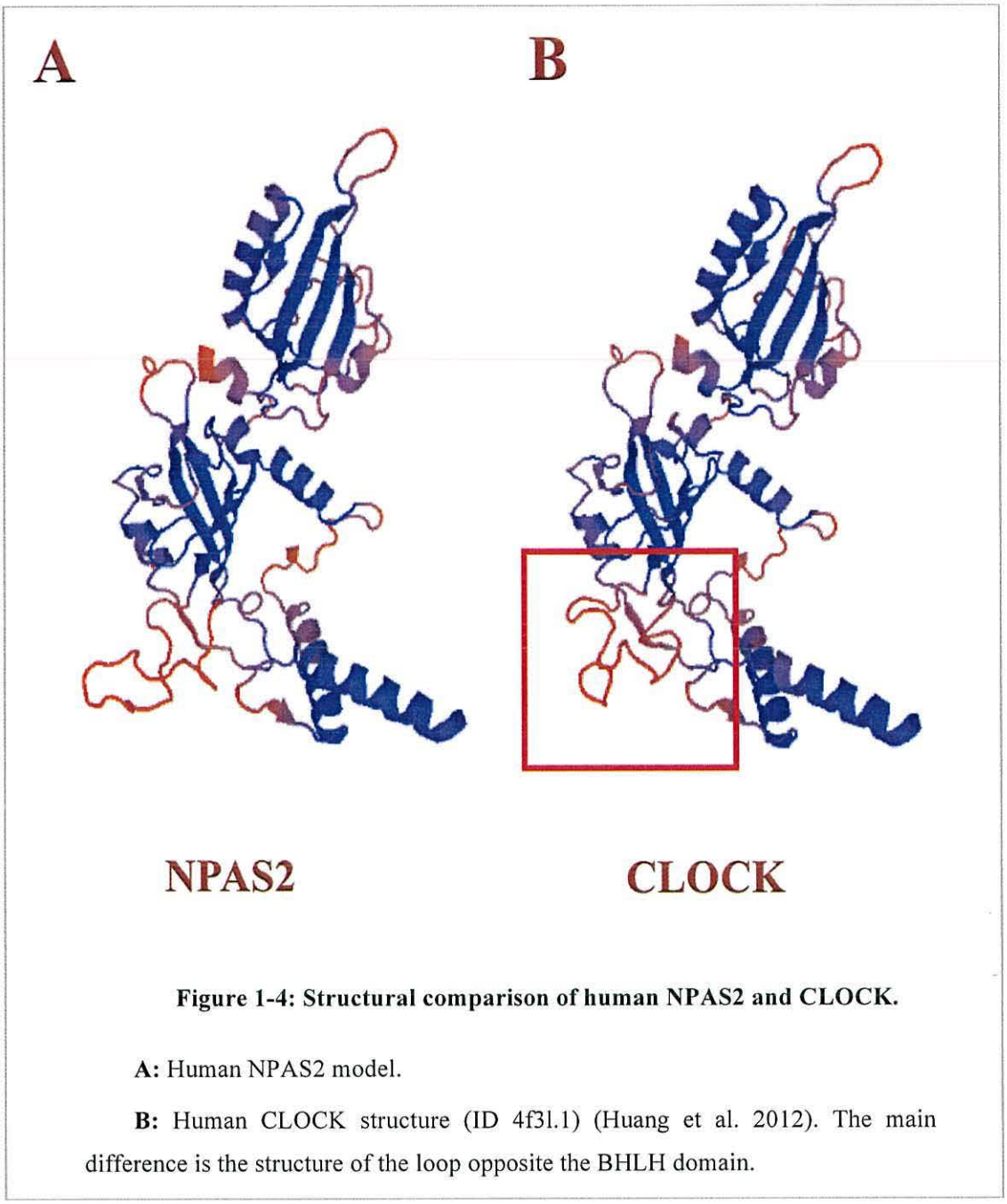

Figure 1-4: Structural comparison of human NPAS2 and CLOCK.

A: Human NPAS2 model.

B: Human CLOCK structure (ID 4f3l.1) (Huang et al. 2012). The main difference is the structure of the loop opposite the BHLH domain.

The model of the structure of human NPAS2 is very similar to the structure of mouse CLOCK which is to be expected since the model is based on the crystal structure of CLOCK. What is however interesting is the difference in the structure of the loop opposite the second helix of the BHLH domain (Figure 1-4).

1.1.2.2 The Heme Binding Motif.

NPAS2 is so far the only PAS domain protein in higher organisms for which the presence of a heme group (Figure 1-5) at the PAS domain has been confirmed (Dioum et al. 2002). Heme group containing PAS domains are frequently found in prokaryotic proteins which respond to gases like carbon monoxide or oxygen. Human NPAS2 exists in a heme-free and heme-containing form. Binding of carbon monoxide to the heme group of NPAS2 decreases its DNA binding activity and releases NPAS2 from its partner ARNTL/BMAl1 which forms inactive homo-dimeric complexes rather than active hetero-dimeric complexes with CO-bound NPAS2 (Dioum et al. 2002). Carbon monoxide is produced in cells and tissues as a result of endogenous metabolic processes involving heme oxygenases (Ryter, Otterbein 2004). The PAS-A domain of NPAS2 has approximately ten times the affinity for carbon monoxide compared to the PAS-B domain indicating that the PAS-A domain is likely to be functionally more important than the B domain for carbon monoxide inhibition (Ishida *et al.*, 2008). Carbon monoxide at micro-molar concentrations was found to inhibit the DNA binding activity of heme-bound NPAS2, but not heme-free NPAS2. Given the that NPAS2 is a gas sensitive transcription factor with binds to E boxes, it will be interesting to see whether the proposed DNA damage response activity of NPAS2 is also regulated by gases like carbon monoxide. In this context it is noteworthy that carbon monoxide stimulates DNA break repair and cell survival in mice through the ATM kinase DNA damage checkpoint pathway (Otterbein et al. 2011).

It is also interesting that heme biosynthesis is controlled by the circadian clock through its regulation of the rate-limiting mitochondrial enzyme aminolevulinate synthase 1 (ALAS1). Mitochondrial ALAS1 is in turn down-regulated by high levels of heme and up-regulated by low levels. Heme has been shown to differentially regulate the expression of the mouse Period genes *Per1* and *Per2* in vivo (Kaasik, Lee 2004). Interestingly, the activity of the ARNTLl (BMAL1)-NPAS2 transcription complex is stimulated by the PER2 protein and in a feedback loop *ALAS1* expression is transcriptionally regulated by NPAS2 (Kaasik, Lee 2004). This suggests a close functional relationship of heme biosynthesis and NPAS2 activity.

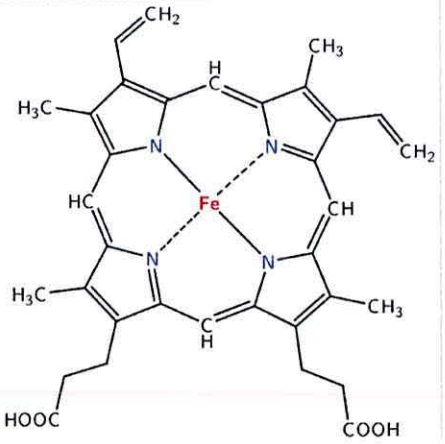

Figure 1-5: Structure of the heme group showing the porphorin ring structure with a central iron ion (Fe2+).

Adapted from: chemistry.about.com

A series of mutations in the PAS-A domain of NPAS2 were assessed for activation of the *Per1* gene in a luciferase reporter gene assays in NIH3T3 mouse cells. A substantial reduction in transcriptional activity was found with two mutants (H119A or H171A) in the heme containing PAS-A domain of NPAS2 (Figure 1-6) illustrating the importance of the heme group for NPAS2 function. Using gel-shift assays, both mutants showed impaired heterodimer formation with ARNTL1 (BMAL1), and consequently loss of DNA binding to the E-box elements (Ishida, Ueha & Sagami 2008).

The redox state of nicotinamide adenine dinucleotide (NAD) cofactors has also been shown to regulate the DNA binding of NPAS2/ARNTL1 (BMAL1) and CLOCK/ARNTL1 (BMAL1) heterodimers *in vitro* suggesting that NPAS2 and CLOCK may function as intracellular redox sensors. Reduced forms of the redox cofactors, NADH and NADPH, strongly induced DNA binding of NPAS2/ARNTL1 (BMAL1) and CLOCK/ARNTL1 (BMAL1) heterodimers. In contrast, the oxidised forms (NAD and NADP) inhibited DNA binding of both pairs of heterodimers (Rutter et al. 2001). The authors suggest that the circadian clock could be modulated by changes the redox state as a result of food intake or neuronal activity (Stokkan et al. 2001). Although circadian rhythms are determined by the light-dark cycle, restrictions in feeding rapidly shifted rhythmicity in the liver and other organs. It is tempting to speculate that effects of feeding could be mediated by NPAS2 and CLOCK functioning as redox sensors in the liver. However in vivo data are needed to confirm the role of the redox cofactors in mediating these effects. Interestingly, the NAD/NADP pool is not only a measure for food availability, but has also an important effect on cell cycle progression and DNA repair (Chiarugi et al. 2012). Hence, changes in the

redox equilibrium of NAD and NADP, like changes in carbon monoxide may affect the ability of NPAS2 to regulate DNA repair at the chromatin.

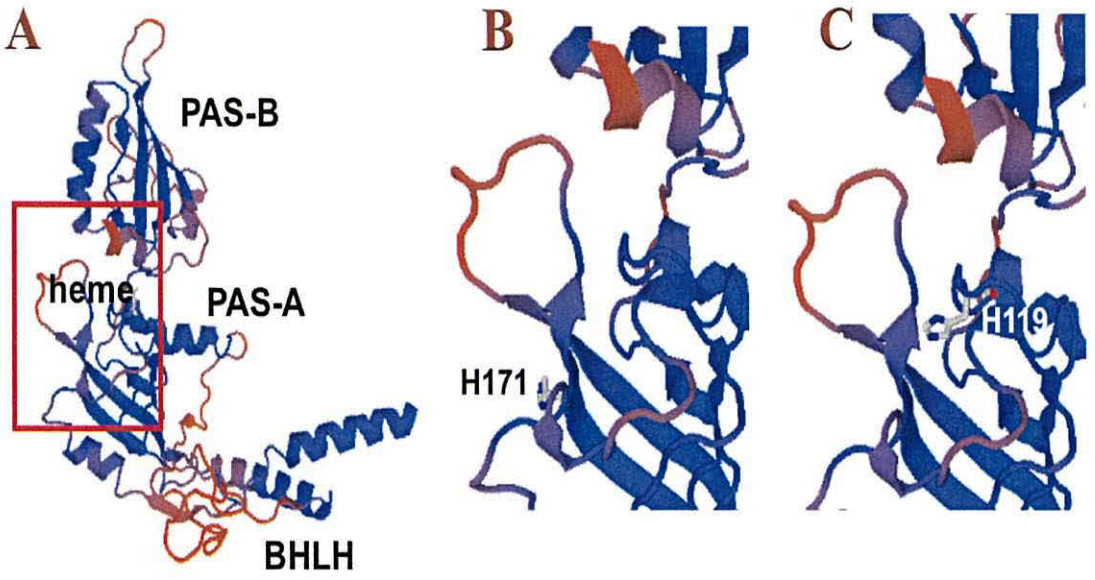

Figure 1-6: Structure of the heme-binding site in human NPAS2.

The heme-binding site in the PAS-A domain is highlighted **(A)**. The heme group binds to histidine 171 **(B)** and histidine 119 **(C)** sitting at the opposite ends of a groove formed by two loops located at the upper end of the PAS-A domain. The model of human NPAS2 is based on the CLOCK structure (ID 4f3l.1) (Huang et al. 2012).

1.1.3 Involvement of NPAS2 in the DNA damage response.

The main cellular pathways in the response to DNA damage consist of DNA repair, DNA damage checkpoints, transcriptional reprogramming and apoptosis with the circadian clock regulating a number of the pathways involved (Sancar et al. 2010). Evidence for a role of NPAS2 in the DNA damage response has come from *in vitro* experiments in which human MCF-7 (breast cancer) and HCT-15 (colon carcinoma) cell lines were transfected with small interfering RNA (siRNA) oligonucleotides targeting the *NPAS2* gene (Hoffman et al. 2008). Expression profiling of these NPAS2 knockdown experiments focused on 84 genes with known roles in DNA damage signaling. In knockdown experiments with the MCF-7 breast cancer cell line, seven genes with significant changes ($p < 0.05$) in expression, in comparison to control levels, and a two-fold or more change in expression were identified. Each of these genes were significantly down-regulated by the *NPAS2* siRNA oligonucleotides and were classified by known function: damaged DNA binding (*DMC1*, *DDB1*, *MSH2*), mismatch repair (*EXO1*), double-strand break repair (*PRKDC*), cell cycle checkpoint control (*FANCG*) and cell cycle arrest (*MAPK12*). The repeat experiment with the HCT-15 colon carcinoma cell line identified three genes of the seven genes (*DMC1*, *MSH2* and *EXO1*) which were also significantly down-regulated in the MCF-7 cell line although changes in expression were less than with the breast cancer cell line. DMC1 is an ATP-dependent recombinase involved in the repair of broken chromosomes, MSH2 is involved in mismatch repair and EXO1 is an exonuclease required for DNA processing during repair. The chemical mutagen methyl methanesulphonate (MMS) was added to *NPAS2* silenced MCF-7 cells or wild-type cells to assess a possible role of NPAS2 in the DNA damage response to methylated DNA. NPAS2 silenced MCF-7 cells failed to display the cell cycle delay in response to MMS treatment, which was observed in wild-type cells. In addition to this cell cycle defect, the repair of DNA breaks was impaired (Hoffman et al. 2008). This suggests a role for NPAS2 or of a gene product controlled by NPAS2 in the response to broken chromosomes, but these experiments are far from definitive. It would be of great interest to evaluate the effects of carbon monoxide and the redox level (NAD, NADH) on the ability of NPAS2 to impose a cell cycle arrest and to aid DNA repair in the presence of DNA damage.

NPAS2 may also impact on the DNA damage response indirectly as an element of the circadian clock. Signaling similarities in the regulation of DNA damage and the circadian clock has been discussed (Uchida, Hirayama & Nishina 2010). In particular, the observation that Wee1 kinase, a main negative regulator of the cell cycle, is a key target of the circadian clock suggests that the clock has a direct impact on cell cycle progression (Matsuo et al. 2003). The circadian clock also regulates DNA excision repair (Kang, Sancar 2009). In particular the expression of the *Xpa* gene in mouse which contains two E-boxes in its promotor region (Kang et al. 2010). Whether is regulation extends also to human cells is not yet

clear.

As in the case of the *Xpa* promoter, the mouse *c-Myc* gene, which encodes the transcription factor c-MYC that is involved in cellular proliferation, contains also a canonical E-box enabling heterodimers of ARNTL (BMAL1) with NPAS2 or CLOCK to bind and to regulate c-Myc expression (Sancar *et al.*, 2010). Another important protein under the regulation of the circadian clock is the CDK inhibitor p21/WAF1 (CDKN1A). The p21 protein binds to Cdk2 and inhibits its activity thereby playing a critical role in the maintenance of G1/S DNA damage checkpoint. P21 binds also to PCNA and is involved in DNA repair (Soria, Gottifredi 2010). Expression of *p21* is negatively regulated by Rev-Erbα (NR1D1) which is positively regulated by the heterodimer complex of Clock (NPAS2)-ARNTL/BMAL1 (Grechez-Cassiau et al. 2008). The circadian protein Period 2 (PER2) stabilizes the transcription factor p53 and because p53 up-regulates p21, Per2 may be involved in the expression of this protein in addition to Rev-Erbα (Gotoh et al. 2014).

Evidence for a direct link between circadian clock proteins and the DNA damage checkpoints is limited to TIMELESS in the ATR-CHK1 kinase pathway and Period 1 (PER1) in the ATM-CHK2 kinase signaling pathway in the response to irradiation (Sancar et al. 2010). Timeless binds to DNA replication forks and associates with cryptochrome 1 and cryptochrome 2 in a manner regulated by Per2 (Cho et al. 2013). DNA replication fork damage activates the ATR-Chk1 kinase cascade to protect the stalled fork and to arrest cell cycle progression in a way which requires the Timeless-Cry1/2 complex (Smith, Fu & Brown 2009). Period 1 associates with the ATM and Chk2 kinases at broken DNA lesions to induce repair and to stop cell cycle progression (Gery et al. 2006). So far no evidence has been reported that establishes a direct link between NPAS2 and DNA checkpoint proteins.

1.1.3.1 NPAS2 and Breast Cancer.

Epidemiological studies have shown that there is a clear correlation between the incidence of breast cancer and a disruption of circadian rhythms, with, for example, exposure to night shift work being a significant risk factor for breast cancer (Saha, Sassone-Corsi 2007, Leonardi et al. 2012). Several studies have investigated the possible role of NPAS2 in breast cancer. In an association study of 431 breast cancer cases and 476 controls, three non-synonymous polymorphisms (Ala394Thr, Ser471Leu and Pro690Ala) in the gene were genotyped. Each of these polymorphisms affects amino acids located outside of the conserved BHLH, PAS-A and PAS-B domains of NPAS2. Comparison of the heterozygous Ala394Thr genotype with the common homozygous Ala394Ala genotype showed a significant association of heterozygotes with breast cancer risk but there was no association of the homozygous Thr394Thr genotype with breast cancer risk (Zhu et al. 2008). These results are difficult to reconcile, as a

homozygote for both risk alleles (Thr394) would be expected to show the same or increased risk for a disease as a heterozygote possessing only copy of the risk allele.

Using the MCF-7 breast cancer cell line, cancer-related transcriptional targets of NPAS2 have been identified using a genome-wide mapping approach involving chromatin immunoprecipitation combined with microarray (ChIP-on-chip) analysis. Analysis of 488,000 probes that target around 17,000 of well-defined human transcripts identified 26 genes that contained potential binding regions for NPAS2, with 16 of these genes being confirmed by real-time PCR assays. Nine of these genes (*ARHGAP29*, *CDC25A*, *CDKN2AIP*, *CX3CL1*, *ELF4*, *GNAL*, *KDELR1*, *POU4F2*, and *THRA*) are known to be involved in tumourigenesis (Yi et al. 2009). These results support the assertion that NPAS2 is involved in tumourigenesis and tumour growth and may act as a tumour suppressor gene (Hoffman et al. 2008).

Evidence from genotyping the NPAS2 Ala394Thr polymorphism and measurements of *NPAS2* expression levels in around 300 breast cancer tissue samples has indicated that NPAS2 may be a useful prognostic biomarker for breast cancer. High expression levels of *NPAS2* were associated with disease-free survival and overall survival (Yi et al. 2010).

Using a novel approach, 27 newly identified breast cancer risk alleles were analysed in 859 cases that had been exposed to occupational and medical diagnostic radiation and 1083 controls. There was suggestive evidence ($p < 0.08$) of an interaction between one *NPAS2* synonymous SNP (rs12622050) and radiation-associated breast cancer risk (Bhatti et al. 2010).

A single nucleotide polymorphism (SNP) in the 3' untranslated region (3' UTR) of the *NPAS2* gene was identified (rs3739008) which may disrupt the binding of the microRNAs 17-5p and 519e to this region. Binding of these regulatory microRNAs normally down-regulates NPAS2 expression. The SNP was used in an association study using both cases and controls from Chinese and German populations to assess a possible link with breast cancer risk. No association was found with either the Chinese population or the German population (Wang et al. 2011). Results for the involvement of NPAS2 in breast cancer are equivocal. The most compelling results for the involvement of NPAS2 in carcinogenesis comes from the study of Yi et al. 2009 described above, on the identification of transcriptional targets of NPAS2, which are known to be involved in tumourigenesis. Although results were obtained using the breast cancer cell line MCF-7, the targets identified may not be specific to breast cancer, but to a more general carcinogenesis phenotype. Repeating these results with a range of cell lines, including breast cancer lines may resolve this question.

1.1.3.2 NPAS2 in Non-Hodgkin's Lymphoma.

A population based association study of the non-synonymous polymorphism Ala394Thr (SNP rs2305160) in the *NPAS2* gene with 455 cases with non-Hodgkin's lymphoma and 527 controls has implicated this circadian clock gene in this disease. The Ala394Thr residue is localised outside the conserved regions of NPAS2. There was a strong association of variant Thr genotypes (Ala/Thr and Thr/Thr) with a reduced risk of non-Hodgkin's lymphoma (OR = 0.66, 95% confidence intervals (95% CI), 0.51 - 0.85, p = 0.001), with an increased statistical significance being obtained with the subtype B-cell lymphoma (OR = 0.61, 95% CI, 0.47 - 0.80, p = 0.0001) (Zhu et al. 2007). Whilst this study has not been replicated, a second association study of a second clock gene, *CRY2* has supported a possible role of circadian clock genes in non-Hodgkin's lymphoma. This study analysed the non-Hodgkin's lymphoma cases and controls from the original study by Zhu *et al.* (2007) using five SNPs in the *CRY2* gene (Hoffman et al. 2009). Three of these *CRY2* SNPs were found to be significantly associated with risk of non-Hodgkin's lymphoma when all subtypes of the disease were combined with p values ranging from 0.006 to 0.001 being obtained. In addition, each of the three SNPs showed significant association with B-cell lymphoma and follicular lymphoma subtypes. Both studies suggest a possible role of both *NPAS2* and *CRY2* in non-Hodgkin's lymphoma, but as they were conducted on the same cases and controls population bias cannot be excluded. Thus, additional studies using alternative populations are required.

1.1.3.3 NPAS2 in Prostate Cancer.

A study of core circadian genes including *NPAS2* in a second malignant disease, prostate cancer produced inconclusive results. The results of this large population based association study of Caucasian men with 1,308 cases and 1,266 controls, reported at least one single SNP in nine of ten core circadian genes (two SNPs in *PER1*; one SNP in each of *PER2*, *PER3*, *CSNK1E*, *CRY1*, *CRY2*, *ARNTL* and *CLOCK* and three SNPs in *NPAS2*) examined as being significantly associated with susceptibility to prostate cancer (Zhu et al. 2009). The results for the association of three SNPs in the *NPAS2* gene with prostate cancer risk were discrepant (rs895521; rs1369481; and rs17024926). Thus, two SNPs (rs895521 and rs1369481) were associated with a reduced risk of prostate cancer, whilst a third (rs17024926) was associated with an increased risk. None of these SNPs results in an amino acid change. Similarly, discrepant results were obtained for the association of two *NPAS2* SNPs with the risk of a less aggressive prostate cancer phenotype rs17024926, rs1369481) (Zhu et al. 2009). Again none of these SNPs causes a change in the amino acid sequence of NPAS2. Results with other core circadian genes were similar with no overall pattern of association, either positive or negative with the risk of prostate cancer. A link of circadian genes with prostate cancer was therefore not established, and in some cases the results are

difficult to reconcile. For example, the *NPAS2* SNP rs17024926 showed an increased risk of prostate cancer but also an increased risk of a less aggressive prostate cancer phenotype. Additional association studies on different populations of prostate cancer cases and controls may clarify these apparently conflicting results.

1.1.3.4 NPAS2 in the Kidney.

Molecular clock facilitated by PAS domain transcription factor NPAS2 is also a functional aspect of kidney's circadian adjustment. The Kidney is vital for the maintenance of ion and fluid homeostasis, and thereafter control of blood pressure (Solocinski, Gumz 2015). However, circadian aberrations in the glomerular filtration rate, blood flow in kidneys, blood pressure, and water and sodium excretion were reported by the investigators. Say, few studies have shed light on the involvement of proteins specific to the circadian clock in the control of several genes of renal transport. This indicated that the molecular clock plays a key role in the control of kidney's circadian aberrations in the overall renal function. Scientists have considered that circadian clock is an important regulator of kidney function with key implications with regard to the renal pathology treatment that involves hypertension and chronic kidney disease (Solocinski, Gumz 2015).

Renal discharge of important electrolytes and water shows a noteworthy circadian rhythm. This useful periodicity is considered to lead to an output ranging from the circadian alteration in emission/reabsorption limits of the collecting ducts and distal nephron (Zuber et al. 2009). In this regard, researchers have concentrated on the molecular pathways behind the circadian rhythms in the cortical collecting duct (CCD), connecting tubule (CNT), and the distal convoluted tubule (DCT). Here, when a temporal expression analysis was carried out on the CCD or CNT/DCT, noteworthy circadian rhythmicity in the various gene expressions playing role in the kidney's several homeostatic functions (Zuber et al. 2009).

This examination additionally uncovered that both CCD and CNT/DCT have a characteristic circadian framework portrayed by vigorous motions in the NPAS2 gene expression and clock-controlled Par bZip transcriptional elements such as thyrotroph embryonic factor (TEF), hepatic leukemia factor (HLF) and albumin D-site binding protein (DBP). Further, knockout mice with and without TEF, HLF and DBP were found to show critical changes in kidney-specific expression of key controllers of sodium or water adjustments (aquaporin-2 and 4, vasopressin V2 receptor). Practically, the depletion of clock genes in knockout mice was found to prompt a perplexing phenotype characterized by dysregulation of sodium discharge rhythms, diabetes insipidus, and a critical reduction in blood pressure (Zuber et al. 2009). This could imply that circadian clock genes like NPAS2 influence the function of the kidney

through its localization and expression. In recent study, scientists revealed the involvement of clock gene expression in the kidney cancer. According to that investigation, the most continuous dangerous kidney specific tumour in adult individuals is the renal cell carcinoma described by increased lethality linked with the nearness of metastatic illness during the diagnosis (Mazzoccoli et al. 2014). Here, the most fundamental and molecular characteristic element of sporadic renal cell carcinomas is the change of the tumour silencer gene that encodes the von Hippel-Lindau protein, with modification of controlled pathways and stimulation of hypoxia-inducible transcription components (Mazzoccoli et al. 2014).

Hypoxia-inducible transcription components are transcriptional controllers of genes that control homeostasis of mammalian oxygen, internal pH, neovascularisation, cell survival, movement, and energy metabolism and are viewed as potential promoters of tumour development (Mazzoccoli et al. 2014). As such, researchers have reported strong interrelationships between the circadian pathway and hypoxic reaction pathway. Serious gene deregulation required in the circadian clock network and reaction to hypoxia was observed in patients influenced by renal malignancy, affecting the procedure of cancer development, and also infection progression and result (Mazzoccoli et al. 2014).

With these outcomes, it was thought that studies focused on the adjustments of clock gene expression and hypoxia-related network in kidney disease may advance the perception of pathophysiological systems required in the onset of renal cell carcinoma onset and development. This was also believed to furnish insights on the successful therapeutic methodologies (Mazzoccoli et al. 2014). So, clock gene expression like NPAS2 in the kidney tissue is complex. Using this concept, researchers have taken initiatives to explore the circadian functions and pathobiology of kidney. However, much research is awaited to obtain a further confirmation regarding the attachment of NPAS2 gene with the kidney (Mazzoccoli et al. 2014).

1.1.3.5 NPAS2 in Neuroblastoma.

Neuroblastoma represents the embryonal tumour. This malignancy originates from the defects in the autonomic nervous system where one deficient precursor cell develops from the neural-crest tissues. Generally, neuroblastomas appear in children of exceptionally young age; it is mainly diagnosed when the child reaches the age of 17 months. The tumours emerge in tissues of the (ANS), ordinarily in the paraspinal ganglia or adrenal medulla. In this manner, the condition is better represented in chest, neck, stomach and pelvic region. Its clinical presentation varies from a state of no symptom to a state that has a primary tumour due to the internal invasion and broadly established illness (Maris 2010). Research interventions have highlighted that cancer development is vulnerable to circadian rhythm aberrations. As such, the role of NPAS2 which is also a kind of circadian gene was implicated (Maris 2010).

Research interventions have highlighted that cancer development is vulnerable to circadian rhythm aberrations. Rhythmicity is exhibited during the expression of transcriptionally controlled clock genes that manage several functions typical of a normal cell, for example, cell division and expansion. In this regard, deregulation of circadian clock genes was reported in the cancer development and different maladies. Interruption of circadian rhythms quickens the progression of the tumour (Maris 2010).

In one study, investigators have checked the biological role of NPAS2 in neuroblastoma tissues. For this, the study team arranged a neuroblastoma cell line fit for the contingent synthesis of heterodimer of NPAS2:BMAL1 and recognised putative target genes by Northern blotting, and DNA microarrays. Here, a co-production of NPAS2 and BMAL1 stimulated transcription of the endogenous Cry1 Per1 and Per2 genes that code for the negatively stimulating elements of the circadian regulatory network, and inhibited the transcription of the internal BMAL1 gene (Schibler, Ripperger & Brown 2001). The study team inspected the frontal cortex of mice (wild-strain) during the dim-light sessions maintained throughout the day. This experiment uncovered that the mRNA levels of Per1, Per2, and Cry1 were increased during a dark session and decrease during a light session, whereas the mRNA of BMAL1 exhibited the opposite impression (Schibler, Ripperger & Brown 2001).

Likewise, mice, subjected to *in situ* hybridization assay under prolonged darkness, have shown that the abundance of Per2 mRNA did not sway as the circadian cycle function in mice lacking NPAS2. Along these lines, NPAS2 is believed to work as a feature of molecular clock agent in the forebrain of mammals (Reick et al. 2001). This study also implied that the neuroblastoma tissues are vulnerable to NPAS2 gene expression mediated circadian cycle changes (Reick et al. 2001).

In another trial, investigators have focused on the role of NPAS2 in the nurodegeneration processes driven by the oxidative stress alterations in cancerous tissues (Musiek et al. 2013). The insight for this new line of research is due to the effect of redox balance on the neuroblastoma tissue differentiation (Silvis et al. 2016). From the fundamental biological view point, circadian rhythmicity and oxygen are vital in a spectrum of physiological procedures to look after the cellular signalling pathways, sleep/wake cycles, blood pressure that are involved in the maintenance of health and disease (Silvis et al. 2016).

In the event that the human body or cells encounter huge stress, their capacity to control inside frameworks, including redox levels and circadian rhythms, may get to be distinctly hindered. At cell and organismal levels, alterations in the redox control and circadian rhythms may lead to various unfavourable impacts, for example, heart ailments, neurodegenerative conditions, and tumour growth (Wilking et al. 2013).

Musiek and associates found that the depletion of transcriptional activators of circadian clock like NPAS2 prompted extreme age-specific astrogliosis in the hippocampus and cortex (Musiek et al. 2013). On the other hand, mice without the Per1 and Per2 genes did not show any astrogliosis. Similarly, the depletion of Bmal1 resulted in the damage to synaptic terminals and disabled connectivity in the cortical functions, and also neuronal oxidative harm and altered expression of few genes related to the redox protection. When Bmal1 was subjected to targeted deletion in glia and neurons, the study team noted the identical neuropathology. This effect contributed to a diminishment of Bmal1 expression that advanced the death of neuronal tissues in the primary cell cultures and in mice chemically exposed to the striatal neurodegeneration following the oxidative damage. This study indicated that NPAS2 in association with BMAL1complex controls the cerebral redox homeostasis and associates the altered clock gene activity to the process of neurodegeneration (Musiek et al. 2013).

1.1.3.6 NPAS2 in Psychiatric and Behavioural Disorders.

A possible role of circadian clock genes in the development of autistic disorder has been suggested with the proposal of a clock genes/social timing hypothesis. An association study of clock gene SNPs with autistic disorder genotyped SNPs from clock-related, genes using 110 trios (affected child and both parents) of subjects which comprised diagnosed autistic disorder progeny and their parents (Nicholas et al. 2007). Significant associations with the disorder ($p < 0.05$) were found for two SNPs in the *PER1* gene and two in *NPAS2*. Analysis of all the combinations of pairwise SNP haplotypes for each gene showed that in *NPAS2* 40 of 136 possible combinations significant associations with autism were found ($p < 0.05$), with the best result between two NPAS2 SNPs achieving a significance level of $p = 0.001$. Haplotype analysis within the *PER1* gene gave a solitary significant result with $p = 0.027$ (Nicholas et al. 2007). Subsequent work showed that the two SNPs in *NPAS2* are located in the first intron and affect the expression of a novel microRNA cluster (Jones, Nicholas and Caspari unpublished). This shows that the SNPs are not functionally linked with NPAS2 but may have evolved in this intron due to the tissue specific expression of NPAS2 in different areas of the brain.

On the basis of their functional circadian clock core activity three genes, *PER2*, *ARNTL* and *NPAS2* were selected for an association study of Seasonal Affective Disorder or winter depression (Partonen et al. 2007). The study compared 189 patients with 189 matched controls, using a single SNP from each gene, which were selected in silico as being the most "relevant". A further assumption of the study was that the SNPs in each of the genes combined to contribute to Seasonal Affective Disorder risk. Using combination analysis of each of the three gene variants a genetic risk profile for the disorder was identified which produced odds ratio of 4.43 when compared to the remaining genotypes, and 10.67 when compared to the "most protective" genotype (Partonen et al. 2007). Whilst these results appear to be

impressive the selection of genotypes for comparison appears to favour those that give the most impressive results and there is no correction for multiple testing.

The possible role of circadian clock genes in some psychiatric disorders has been suggested as disrupted circadian rhythms, for example in sleep, appetite, and hormonal secretions have been described in mood disorders (Mansour et al. 2009, Soria et al. 2010) and sleep disturbances in schizophrenia genotyped 209 SNPs covering 19 circadian genes in 335 cases with unipolar major mood depression, 199 with bipolar disorder, and 440 community-based screened controls. In a combined mood disorder group (unipolar plus bipolar) significant associations were found with SNPs in three different genes: *NPAS2* (rs11123857), *CRY1* and vasoactive intestinal peptide receptor 2 (*VIPR2*). Unipolar major mood depression was associated with two genes: *NPAS2* (rs11123857) and *CRY1*; whilst bipolar disorder was associated with *CLOCK* and vasoactive intestinal peptide (VIP) (Soria et al. 2010).

A second association of psychiatric disorders and circadian clock genes genotyped 21 genes in 523 patients with bipolar I disorder, 527 patients with schizophrenia or schizoaffective disorder, and 477 screened adult controls. *NPAS2* showed a weak association with the combined schizophrenia and schizoaffective disorder group ($p = 0.034$) but following correction for multiple testing this result did not achieve statistical significance (Mansour et al. 2009). The possible role of circadian clock genes, including NPAS2, in mood disorders and schizophrenia requires additional studies to confirm or rule out candidate genes. The current focus is on the CLOCK, PER1, PER3 and TIMELESS (timeless homolog (*Drosophila*)) genes in schizophrenia, and CLOCK in bipolar disorder (Boivin 2010).

1.2 Aims of research project

Neuronal PAS domain protein 2 (NPAS2) is a Basic-helix-loop-helix (BHLH) containing transcription factor which acts in the circadian clock system as a hetero-dimer with ARNTL/BMAL1. Although its important role in the circadian rhythm, very little is known about this protein other than it replaces CLOCK in the hetero-dimeric complex with ARNTL/BMAl1, binds one heme co-factor in each of its two PAS domains and belongs to a group of four related proteins (NPAS 1- 4).

This thesis set out to gather more information about the cellular activities of human NPAS2 in the context of the response to DNA damage and cellular stress. NPAS2 has not yet been directly linked with DNA damage responses, but its down-regulation affects the repair of broken chromosomes and changes in NPAS2 protein levels are linked with different cancers and neurological disorders like Schizophrenia.

CHAPTER 2

MATERIALS AND METHODS

Chapter 2: Materials and Methods

2.1 Cell line.

2.1.1 Cell line source.

2.1.1.1 HEK-293.

HEK-293 is a cell line derived from Human Embryo Kidney, which was obtained from European Collection of Authenticated Cell Cultures (ECACC) (85120602). The cells were grown in Dulbecco's Modified Eagle's Medium (DMEM) (SIGMA, D5546) supplemented with 10% Fetal Bovine Serum (FBS) (SIGMA-F2442), 1% of 10,000 units penicillin and 10mg streptomycin/mL (SIGMA-P4333), and 200mM L-Glutamine solution (SIGMA- G7513).

2.1.1.2 HeLa.

HeLa is a cell line derived from a cervical carcinoma, which was obtained from Health Protection Agency (HPA) Culture Collection (93021013). The cells were grown in Dulbecco's Modified Eagle's Medium (DMEM) (SIGMA, D5546) supplemented with 10% Fetal Bovine Serum (FBS) (SIGMA-F2442) and 1% penicillin - Streptomycin antibiotics.

2.1.1.3 MCF-7.

MCF-7 was established from the pleural effusion, from female Caucasian suffering from a breast adenocarcinoma that was obtained from Health Protection Agency (HPA) Culture Collection (86012803). The cells were grown in Dulbecco's Modified Eagle's Medium (DMEM) (SIGMA, D5546) supplemented with 10% Fetal Bovine Serum (FBS) (SIGMA-F2442), 1% penicillin - Streptomycin antibiotics and 200mM L-Glutamine solution (SIGMA- G7513).

2.1.1.4 HCT-116.

HCT-116 is a cell line from a human diagnosed with colon cancer, which was obtained from the European Collection of Authenticated Cell Cultures (ECACC) (91091005). The cells were grown in McCoy's 5A (Modified) Medium (Gibco, 16600) supplemented with 10% FBS and 1% penicillin - Streptomycin antibiotics.

2.1.1.5 KELLY.

KELLY is a human neuroblastoma cell line taken from the brain and obtained from the European Collection of Authenticated Cell Cultures (ECACC) (92110411). The cells were grown in RPMI 1640 Medium (SIGMA R0883) supplemented with 10% Fetal Bovine Serum (FBS) (SIGMA-F2442), 1% penicillin - Streptomycin antibiotics.

2.1.2 Cell line maintaining, harvesting.

All Cells were incubated at 37°C and 5% CO^2 until they reached the required cells confluence percentage. Thereafter, cells were de-attached from the plate using 1x Trypsin-EDTA solution (SIGMA, T3924). 1µl/ml of 100µg/ml Zeocin (Meford-Z2475) should add to DMEM media when it used for HEK-293 cells maintaining only.

2.1.3 Cells counting.

The cells were counted by BIO-RAD/TC10™ Automated cell counter using Bio-Rad counting slides (cat.145-0011) by mixing 10µl of the cells with 10µl of 0.4% Trypan blue solution (SIGMA, T8154).

2.1.4 The cell lines cryopreservation.

The main purpose of cryopreservation is to keep stocks of cells, prevent the need to have all cell lines in a culture at all times. There is other advantages of cryopreservation like reduced the risk of microbial contamination, cross contamination with other cell lines. Dimethyl sulfoxide (DMSO) is commonly used as a cryoprotective agent by added at a concentration of 10% to Fetal Bovine Serum (FBS). Cells were gently washed by 1% phosphate- buffered saline (PBS) then trypsinised, counted and centrifuged at 1500rpm (≈ 200xg) for 5 minutes. $1x10^6$ cells were resuspended with cryopreservation medium (10% DMSO, 90% FBS). Cells were transferred to the Mr. Frosty equipment, freeze for 24 hours in (-80°C), and transferred later to the Liquid Nitrogen.

2.1.5 Thawing Frozen Cells.

In this procedure time is significant. Therefore, it should be conducted in a short time. The vials were thawed in a 37°C water bath with gentle agitation. The cells suspensions were transferred quickly to the maintaining medium. Cells usually take at least 4 hours to attach to the plate. After 24 hours maintaining medium should be changed.

2.2 DNA damage treatment.

HEK-293, HeLa and MCF-7 cells were treated with different DNA damaging agents (**Table 2-1**).

Table 2-1: DNA damage treatments and their conditions

Agent	Abbreviation	Dose
Ultraviolet radiation B (UVP, CL-1000 254nm)	UV	$40J/m^2$
Camptothecin	CPT	1μM
Heat Shock	HS	43°C (1 hour)
Hydrogen peroxide	H_2O_2	500μM

2.3 Tricarbonyldichlororuthenium (II) dimer (CORM-2) treatment.

To test whether an increase in carbon monoxide in the cells would have an impact on the expression levels of NPAS2. Tricarbonyldichlororuthenium (II) dimer ($[RuCl_2(CO)_3]_2$) (Alpha Aesar, 10503) releases carbon monoxide when added to cells (Megias, Busserolles & Alcaraz 2007). HEK-293 cells were treated with 300μM of this chemical for 3 hour. Dishes were sealed with parafilm to trigger the release of carbonmonoxyde (CO). Total RNA and protein was isolated.

2.4 Total RNA isolation from mammalian cells.

RNA was extracted using two different protocols, Trizol reagent from Sigma (93289) and RNeasy Plus Micro and Mini Kits from Qiagen (74134). In Trizol reagent protocol, cells were harvested in 1ml of 1x Trypsin-EDTA solution and counted using T20 Automated Cell Counter (BioRad, 1450102). Then, cells were homogenized in Trizol (1ml Trizol / $5x10^7$ cells) and held at room temperature (RT) for 5 minutes. Chloroform (200µl/ 1ml of Trizol) was added to each sample and the homogenate was vigorously shaken for 15 seconds, followed by incubation for 5 minutes at RT. Samples were then centrifuged at 12,000xg for 15 minutes at 4°C. The aqueous layer was then removed to a new eppendorf tube and 500µl of isopropanol was added. After incubation at RT for 10 minutes, the samples were centrifuged again at 12,000xg for 20 minutes. The supernatant was removed and the pellet was washed with 70% ethanol and re-centrifuged at 7,500xg for 5 minutes at 4°C. The supernatant was discarded again and the cell pellet was left to dry at RT for 5-10 minutes, and then 100µl RNase free water. RNA concentration was measured with a NanoDrop (ND_1000) spectrophotometer. RNeasy Plus Mini Kit (Qiagen-74134) was used to isolate RNAs for Real time quantitative PCR (qRT-PCR). The isolation process was done according to the manufacturer's recommendation.

2.5 Reverse Transcriptase.

cDNA is a DNA copy synthesized from mRNA. The Tetro cDNA synthesis kit (BIOLINE-BIO-65042), Oligo $(dT)_{18}$ primer mix was used to transcribe RNA into single-strand cDNA that binds to the poly-A tail of mRNAs.

2.6 Polymerase chain reaction (PCR).

PCR reaction was used to amplify entire gene or to amplify the genes of interest. The PCR program was as follows:

Step	Temperature (°C)	Time	No. of cycles
Initial Denature	94°C	2 minutes	1
Denature	98°C	30 seconds	35
Annealing	55°C	30 seconds	
Extension	72°C	45 seconds	
Final Extension	72°C	10 minute	1
Final hold	4°C		

2.6.1 Primers.

The following primers were used during the project:

Table 2-2: Primers used in this study.

Primes	Sequence (5`-3`)	Order No
qPCR- NPAS2	From Qiagen, amplified exons 3-4, amplicon length 91bp.	QT00032480
qPCR- ARNTL (Bmal1)	From Qiagen, amplified exons 9-10, amplicon length 91bp.	QT00011844
qPCR- CLOCK	From Qiagen, amplified exons 21-22, amplicon length 71bp.	QT00054481
GAPDH	From Qiagen, amplified exons 6-7, amplicon length 95bp.	QT00079247

TUBULIN1 (TUBBP1)	From Qiagen, amplified exons 3-4, amplicon length 69bp.	QT00231889
FRT-F	CAA CGG GAC TTT CCA AAATGT CG	
CMV-F	CGC AAA TGG GCG GTA GGC GTG	
ACTIN-F	AGA AAA TCT GGC ACC ACA CC	
ACTIN-R	GGG GTG TTG AAG GTC TCA AA	
hNPAS2-001-pcDNA5-XhoI-F	ctacgatggaatctcgagATGGATGAAGATGAGAAAGACAG AGCC	
hNPAS2-001-pcDNA5-XhoI-R	ataatgtaacggatctcgagTTATCGGGGCGGCTGCTGGAGG	

2.6.2 PCR.

The following PCR set up samples were used during the project according to MyTaq™ HS Red Mix kit (BioLine):

Table 2-3: Standard MyTaq HS Mix Red Protocol for set up samples

Component	Volume (µl)
My Taq HS Red Mix, 2x	25µl
DNA template	≈100ng
10µM 5'-primer-F	2.5µl
10µM 5'-primer-R	2.5µl
Water (dH_2O)	Up to 50µl

2.6.3 PCR Products examination by Agarose Gel electrophoresis.

An agarose gel was used to analyze the PCR products or to clean them up by gel purification. It was usually prepared as a 1% (w/v) gel in 1x TAE buffer (40mM Tris Base, 1mM EDTA , 20mM Glacial Acetic Acid, pH = 8.5), since it is suitable for PCR examination and gel purification. PCR amplification product (≈5µl) were mixed with DNA loading dye (Promega, G1881) and run through the agarose gel in parallel with either 1Kb or 100bp DNA ladder (Promega, G5711 & G 2101 respectively). At the end of the electrophoresis time, the products were analyzed using a Gel Doc2000 at 85V for (1-1:30) hour with the assistance of Quantity One® software.

2.7 Quantitative Real time PCR (qRT-PCR).

2.7.1 Primer design for qRT-PCR.

For efficient amplification in quantitative qRT-PCR, Qiagen QuantiTect Primer Assays designed all primers. It has been taken into consideration when choosing primers that are detected to more than one exon. Also, housekeeping primer genes used in qRT-PCR were design by Qiagen (**Table 2-2**). Stock primers were diluted with RNA free distilled water (1:5 RNA: water).

2.7.2 PCR setup for qRT-PCR.

The qRT-PCR Reaction was performed using GoTaq® qPCR Master Mix (Promega-A6002). Instructions in user manual have been followed. 6µl cDNA (containing ~100 ng/µl cDNA) and 2.5µl from Qiagen commercial primers were used in a total of 50µl, anatomize the results include the standard deviation between replicates and normalizing the results was carried out using BioRad CFX Manager Software. The qPCR reactions were run using CFX96 real-time PCR detection system, and a setup program was as follow:

Step	Temperature (°C)	Time	
Pre-cycling hold	95°C	10 minutes	
Denaturation	95°C	15 seconds	39 cycles
Annealing	60°C	60 seconds	
Melt curve	60°C	5 seconds	
	95°C	5 seconds	

2.8 Protein extraction.

2.8.1 Whole cell extract.

Cells were washed, harvested and counted using T20 Automated Cell Counter (BioRad, 1450102). At least $2x10^6$/ml of cells were centrifuged at 200xg for 5 minutes at 4°C. The supernatant was discarded and the pellet was washed and centrifuged at 200xg for 1 minute at 4°C. Cell pellets were resuspended in lysis buffer (50mM Tris-HCL (pH=7.4), 200mM NaCl, 0.5% Triton-X100). The buffer was fresh supplied with 25U/ml of Benzonase (Millipore-70746), 2mM of $MgCl_2$, 1µl/100µl lysis buffer of Protease Inhibitor Cocktail III for Mammalian Cells (MELFORD- P2202) as a ratio of 100µl lysis buffer/$2x10^6$ cells. Sample kept at -20°C until it used.

2.9 Cells Fractionation.

Cells were trypsinised and counted. At least, $2x10^6$/ml cells were washed and the pellet was centrifuged at 200xg for 10 minute. Pellets were re-suspended into Hypotonic Buffer (50mM Tris-HCL (pH=7.4) and Lysis Buffer C (1% Triton-X100) in a ratio of 100µl of both buffers/ $2x10^6$ cells. Lysed cells were incubated for 30 minutes on ice. Cells were pellet at 6000xg for 2 minutes at 4°C. Supernatant (represents cytoplasmic fraction) was transferred to another pre-chilled Eppendorf tube. The remained pellets (represent Nuclei) were washed once. Pellets then were centrifuged at 6000xg for 2 minutes at 4°C. Thereafter, they were lysed in Lysis Buffer N (50mM Tris-HCL (pH=7.4), 100mM KAc). As a ratio of a 100µl/$2x10^6$ cell, cytoplasmic, Nuclei fraction was kept at -20°C until it used. All samples were supplied with 1µl/100µl lysis buffer of Protease Inhibitor Cocktail III for Mammalian Cells (MELFORD-P2202) and 2mM of $MgCl_2$. Nuclei samples were supplied with 25U/ml of Benzonase.

2.10 Size Exclusion chromatography on Superdex-200 HR gel filtration column

This experiment was done to get preliminary information about whether the recombinant proteins (NPAS2) react with other proteins to form larger complexes. The experiment was done by extracting whole cell proteins followed by a treatment for 1 hour on ice with Benzonase (125U/ml) in lysis buffer, which was supplemented with 2mM of $MgCl_2$ as a final concentration. Protein samples were centrifuged at 16.000xg for 30 minutes at 4°C, supernatant was kept at -20 °C until it used and the pellet was discarded. Proteins were eluted through the Superdex-200 HR gel filtration column. Protein fractions were concentrated later by protein precipitation procedure, and analyzed in parallel with their whole extract sample by SDS-PAGE and Western Blot.

2.10.1 TCA protein precipitation protocol

Add 1 volume of 100% TCA (**500g TCA in 350ml of dH_2O**) stock to 4 volumes of protein sample. Incubate samples at 4°C/10 minutes, then spin tubes in centrifuge at 14000rpm/5 minutes. Supernatant was removed and pellet washed with 200µl cold acetone twice. Spin tubes in centrifuge at 14000rpm/5 minutes in every wash. Dry off the pellets from acetone by placing tube in 95°C heat block for 5-10 minutes.

2.11 SDS-Polyacrylamide gel electrophoresis and Western blot.

SDS-Polyacrylamide Gel Electrophoresis was used to analyse the protein extracts. It was performed either by one or by two dimensions (2D) electrophoresis:

2.11.1 One Dimension SDS-PAGE.

Proteins were separated according to their sizes on different acrylamide-gel percentages. Regarding to our protein samples. The protocol was achieved as following:

a) Resolving gels were set at a specific percentage, cast in between the Bio- Rad Wet/Tank Blotting system's glasses and were over-laid with isopropanol to remove bubbles. Gels were left to settle down for 15 minutes at room temperature.

Acrylamide percentage	**6%**	**8%**	**10%**	**12%**	**15%**
Number of mini gels	4				
1M Tris-HCl pH8.8	7.5ml				
40% acrylamide and bis-acrylamide solution, 37.5:1	3ml	4ml	5ml	6ml	7.5ml
20% Sodium dodecyl Sulfate (SDS)	150µl				
H_2O	9.5ml	8.5ml	7.5ml	6.5ml	5ml
10% Ammonium Persulfate (APS)	100µl				
Tetramethylethylenediamine (TEMED)	60µl				
Total	20ml				

b) Isopropanol was washed off and the stacking layer was prepared as shown in. Gel was poured immediately on top of the resolving layer, and combs were inserted. Gels were left to set for at least 10 minutes at room temperature.

Acrylamide percentage	**4%**
Number of mini gels	4
1M Tris-HCl pH-6.8	1.5ml
40% acrylamide and bis-acrylamide solution, 37.5:1	1ml
20% Sodium dodecyl Sulfate (SDS)	50µl
H_2O	7.5ml
10% Ammonium Persulfate (APS)	100µl
Tetramethylethylenediamine (TEMED)	20µl
Total	10µl

c) Combs were removed and plates were placed in the electrophoresis tank, which contains 1x SDS running buffer. Samples were loaded in parallel to a standard proteins ladder (Thermo Scientific Page Ruler Pre-stained Protein Ladder, cat.no.26616). Gels were run for 1:30-2 hours on 120V. Thereafter, gels were taken out of the tank and prepared for transferring to the nitrocellulose membranes.

d) Western Blot sandwiches were set up by placing the sandwich's components in a tray filled with 1x Transfer buffer (100ml of 10x Transfer buffer, 150ml Methanol and 750ml dH2O). Transfer sandwiches were placed in the transfer tank filled with 1x transfer buffer, and proteins were

transferred for 2 hours at 70V.

e) Nitrocellulose membranes were taken off from the sandwiches and blocked with Blocking buffer (5% Milk buffer: 5g Milk powder (fat-free), 10ml of 10x PBS, 0.05% Tween-20 and dH_2O up to 100ml) for 1 hour at room temperature on rocking platform. Membranes were incubated with the primary antibody (**Table 2-4**) diluted in the blocking buffer for overnight at 4°C on a rocking platform.

f) Membranes were washed for 10 minutes, 3 times with 1x washing buffer (200ml of 10x PBS, 0.05% tween-20 and dH_2O up to 2 liters). Membranes were incubated with secondary antibody (**Table 2-5**) diluted in blocking buffer, for 1 hour at room temperature on a rocking platform.

g) Membranes were washed 3 times. Membranes were developed with Western lightning® Plus-Enhanced Chemiluminescence (PerkinElmer-NEL105001EA) substrate and placed in the developing cassette. Membranes were exposed to the X-ray films for the specific time and developed in the X-ray film processor (MI-5, JENCONS-PLS).

2.11.2 Two-dimensional polyacrylamide gel electrophoresis (2D-PAGE).

Total proteins extracted (10-30μg) were diluted in isoelectric focusing (IEF) rehydration buffer and mixed with 2μl of ampholytes (pH 3-10) to a total volume of 125 μl. The sample was then vortexed and centrifuged at 16,000xg for 2 minutes at room temperature. Dry polyacrylamide immobilized pH gradient (IPG) strips that are 7 cm in length with a pH gradient of 4-7 were used (BioRad 1632001). Carefully, IPG strip protecting cover foil was removed, a strip was gently placed gel side down in rehydration tray; the "+" marked on the IPG strip should be positioned at the end of the tray marked "+". The rehydration buffer (125μl) containing the protein sample was loaded onto rehydration tray, avoiding trapping air bubbles. Each strip was covered with 1ml mineral oil to prevent dehydration and allowed to passively rehydrate to their original thickness. Strips were rehydrated and focused in the BioRad PROTEAN IEF cell at 50V for 12 hours followed by the rapid focusing program at 10,000Vh (linear).

Strips were placed in an IPG tray, and washed with 2ml of equilibration buffer (I) (6M urea 0.375M Tris-HCl (pH8.8), 2% SDS, 20% glycerol, 2% DTT) for 10 minutes at room temperature on a rocking platform. Then, strips were washed for 10 minutes with 2ml of equilibration buffer II (6M urea, 0.375M Tris-HCl (pH8.8), 2% SDS, 20% Glycerol, and 2.5% (w/v) Iodoacetamide). Strips were applied to a 10% SDS-PAGE gel composed of the resolving layer only. Proteins were run normally according to the SDS-PAGE and Western blot steps that mentioned previously.

2.12 Antibodies.

The following antibodies were used during the project:

Table 2-4: The Primary antibodies used in this study.

Antibody	Source	Cat. No.	Host	Clonality	Dilution
NPAS2	GeneTex	GTX105741	Rabbit	Polyclonal	WB =1:1000 IF = 1:200
P21WAF1/CIP1	Cell signaling	2947	Rabbit	Polyclonal	WB =1:2000
GAPDH	Abcam	AB128915	Rabbit	Polyclonal	WB =1:10000
Phospho-Chk1 pSer345	ThermoFisher	MA5-15145	Rabbit	Monoclonal	WB =1:1000

Table 2-5: The Secondary antibodies used in this study.

Antibody	Source	Cat. No.	Dilution
Anti-rabbit secondary AB- HRP anti-light chain	Calbiochem	401315	WB =1:10000
Alexa Fluor® 488 Goat Anti-Rabbit IgG (H+L) Antibody	Invitrogen	A11008	IF =1:500

2.13 Indirect Immunofluorescence (IF) of culture cells.

Cells were grown for 24 hours on sterile 12mm round Poly-D-Lysine pre-coated coverslips glasses (Poly-D- Lysine, #1, VitroCam-1245-P01) in 24-well plates at a density of (5-10x10^5) cells per well. Subsequent, the medium was removed and the cells were washed with 1x PBS. Subsequent, the cells were preserves the morphology and antigenicity of the cells using fixing solution (4% paraformaldehyde in 1x PBS) for 10 minutes at room temperature. The cells were then incubated for 10 minutes at room temperature with 0.5ml permeabilisation solution (0.2% Triton X-100 in 1x PBS) for detection of intracellular proteins. Latter, Cells were washed 3 times for 10 minutes on rocking platform, Then, Cells were incubated in blocking solution (5%FBS in 1x PBS) for 1 hour on rocking platform. Primary antibodies were diluted in a total of 200µl blocking buffer, aspirate blocking solution and add the primary antibody mixer to wells. Incubate the plates in 4°C on the rocking platform overnight.

The cells were then washed for 10 minutes 3 times with 1x PBS, followed by incubation with the appropriate secondary antibody for 2 hours on the rocking platform at room temperature. Secondary antibodies were labelled with one of the Alexa Fluor® fluorescent probes. All antibodies were diluted in 300µl of blocking solution at different concentrations according to the manufacturer's guide; the plates were covered with foil. Then, the cells were washed 3 times for 10 minutes with 1x PBS. Plates were kept in foil till a mounting solution was added to stain the nucleus. In light off hood one drop of Antifade Mounting Medium with DAPI (Vector-H1200) was added to each of the places on slides where coverslips glasses will be eventually fixed. Coverslips glasses were moved face off on DAPI drop; Coverslips were sealed to the slide with nail polish. Negative control samples were prepared by omitting the addition of the primary antibody to test the specificity of the immunostaining reactions. Sample can keep in fridge for a week.

Images were acquired with an AxioCam HR microscope camera using Zeiss Axioskop2 Microscope filters for DAPI, FITC and Rhodamine. The camera was controlled by Zeiss Axiovision software that facilitates image processing and analysis.

2.14 Cloning into the pcDNA5/FRT/TO-Flag-EGFP vector.

2.14.1 Plasmids.

The NPAS2 cDNA clone was obtained from ThermoScientific (MHS1011-202833321). The 5' end and the 3' end of the cDNA were inserted at the EcoRI and XhoI site of the vector. Plasmid DNA was extracted from the transformed cells using GenElute™ plasmid Midiprep Kit (SIGMA, PLD35) for higher concentrations as Manufacturer's instructions. The basic digestion protocol from New England BioLabs (NEB) was used to digest the plasmid by EcoRI and XhoI to test it (**Table 2-6**). The digestion reaction was incubated at 37°C for 1-1:30 hours.

Table 2-6: Digestion components.

Component	25µl Reaction	50µl Reaction
DNA	0.5µg	1µg
10x NEB buffer	2.5µl	5µl
100x BSA (if needed)	0.25 µl	0.5 µl
Restriction Enzyme 1	5 units	10 units (=1µl is used)
Restriction Enzyme 2	5 units	10 units (=1µl is used)
Nuclease-free water	Up to 25 µl	Up to 50 µl

2.15 Cell Cycle Analysis.

Upon cell harvest, the culture medium was aspirated and cells were washed with PBS. 1ml of Trypsin was then pipetted into each plate then placed into the 37°C incubator until the cells were thoroughly trypsinised and would detach from the plate upon tapping. 1ml of culture medium was then added to each plate and mixed thoroughly with the cells before being transferred into a 10ml glass Falcon® tubes (Scientific Laboratory Supplies, UK). Samples were then centrifuged for 5 minutes at 2000rpm. The trypsin/culture media supernatant was aspirated from the pellet of cells. 1ml Ice cold 70% ethanol was then added drop-wise to the sample will vortexing, to fix the sample and prevent cell clumping. These samples were then stored at - 20°C until ready for processing.

Propidium Iodide is a fluorescent molecule, which intercalates stoichiometrically into nucleic acid sequences. When excited with 488nm wavelength light with fluoresces red, and upon binding with nucleic acid this fluorescent signal increases 20 to 30 fold. It can therefore be used to quantitatively assess the amount of DNA within a cell (Krishan 1975). Owing to its ability to bind to RNA, use of an RNase is necessary. Propidium Iodide is also impermeable to the cell membrane so samples must be fixed prior to staining.

To stain with Propidium Iodide (Sigma-Aldrich Company Ltd.) the samples were first centrifuged for 5 minutes at 12000g/4°C. 1ml of ethanol was dropped slowly on cells with vortex, then the cells washed with 1ml PBS, vortexed gently and the spun again for 5 minutes 16000g/4°C. This PBS wash was repeated another two times. Following this, to ensure that only DNA was stained by the Propidium Iodide 50µl of 100µg/ml of the ribonucleas RNase (Sigma-Aldrich Company Ltd, Dorset UK) was added to the cells. 200µl of 50µg/ml Propidium Iodide in PBS was then added to each sample, and left to incubate in the dark from at least 30 minutes.

The levels of fluorescence emitted by these samples were then measured using flow cytometery on a CyFlow® Cube 8 from sysmex. The flow cytometery software, FlowJo® (v10.1r5) was used to analyse the fluorescence data. Firstly parameters were set so that only the fluorescent output of singlet cells was processed. This was done by manual exclusion, defining the singlet population by size on a bivariate graph of the cell population. DNA histograms were then produced for each sample. The exact percentage of cell within each phase can be calculated by Watson Pragmatic Model. This model is a mathematical curve-fitting algorithm, which de-convolutes the DNA histogram into three mathematics distributions each representing a population of cells in each phase (Watson, Chambers & Smith 1987). The Watson Pragmatic Model was applied through the FlowJo® software.

CHAPTER 3

CLONING OF THE HUMAN NPAS2 GENE

Chapter 3: Cloning of the human *NPAS2* gene

This chapter summarizes the attempt to clone the full-length cDNA of human NPAS2. The aim was to insert the cDNA into the mammalian expression vector pcDNA5/FRT/TO (Figure 3-1) to generate a stable HEK-293 cell line which would allow the induction of an N-terminally EGFP-tagged NPAS2 protein. Although the NPAS2 cDNA was successfully cloned, no stable cell line could be obtained.

3.1 Introduction.

The flip-in Flp-In™ T-Rex™-293 cell line from Invitrogen was chosen to establish the stable cell line for two reasons. First, HEK-293 embryonic kidney cells have a standard cell cycle and are easy to transfect by different methods with faithful cellular mechanisms of translation and protein expression (Thomas, Smart 2005). Second, the cells have one, defined integrated copy of the Flp-In™ T-Rex™ cassette which allows for targeted gene integration. The integration is mediated by Flp recombinase at one single FRT site. As shown in Figure 3-1, co-transfection of the HEK-293 cell line with the plasmid pOG44, which expresses the FLP recombinase, and the plasmid pcDNA5/FRT/TO, which carries the EGFP fusion gene of interest, results in the stable integration of the EGFP fusion gene at the single FRT site. In theory, positive clones can be selected based on the change in antibiotic resistance from Zeocin (no integration) to Hygromycin (integration).

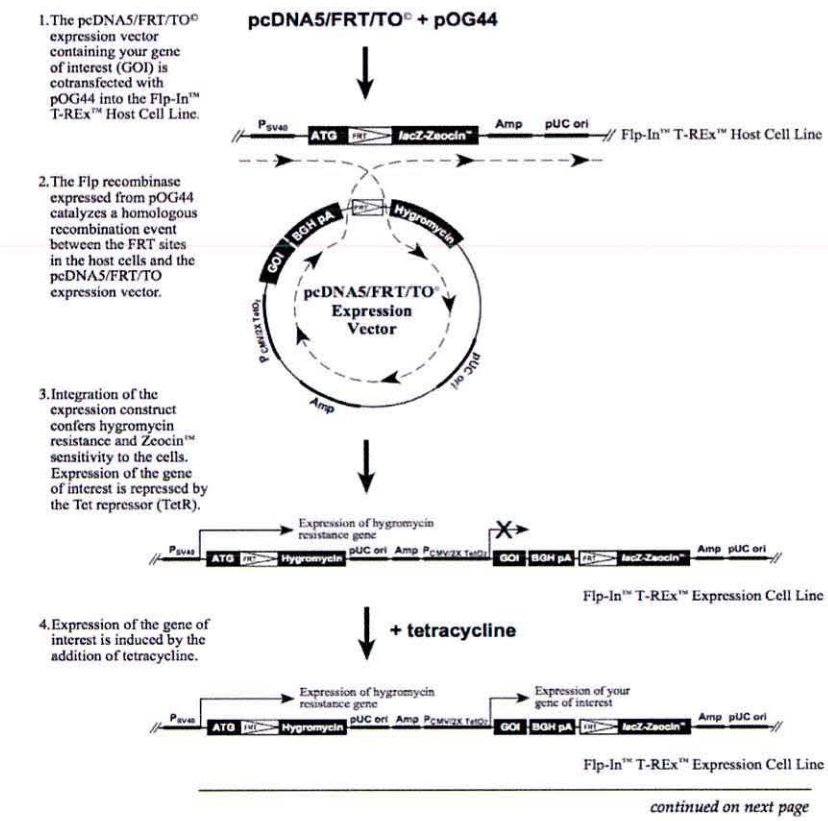

Figure 3-1: Illustrated diagram of the Flp-In™ T-REx™ System.

The steps of transfection and the expression of gene of interest are explained in details. (Adapted from Flp-In™ T- REx™ Core Kit for Generating Stable, Inducible Mammalian Expression Cell Lines by Flp Recombinase-Mediated Integration, Invitrogen. (life technologies).

3.2 Results

3.2.1 Cloning of *NPAS2* cDNA into the pcDNA5/FRT/TO vector for over expression.

The 2475nt long *NPAS2* cDNA was inserted into the pOTB7::NPAS2 vector, which purchased from Thermo Scientific (MHS1011-202833321, Entrez Gene ID: 4862). The pOTB7::NPAS2 vector was digested by EcoRI and XhoI to confirm the size of the fragment as manufacturer's instruction (**Table 2-6**). To evaluate vector digestion, gel electrophoresis was performed for both the undigested and digested pOTB7::NPAS2 vectors (Figure 3-2). To clone the *NPAS2* cDNA into pcDNA5 Flag-EGFP, the 2.5kb cDNA was amplified by PCR using the primers *hNPAS2-001-pcDNA5-XhoI-F* and *hNPAS2-001-pcDNA5-XhoI-R* (**Table 2-2**). The plasmid pcDNA5/FRT/TO was digested with the XhoI restriction enzyme and was dephosphorylated to avoid re-ligation using Alkaline Phosphatase (TSAP) (Promega, M9910) following the manufacturer's instruction. The insert fragment was ligated into the XhoI site of the mammalian expression vector pcDNA5/FRT/TO plasmid using quick T4 DNA ligase. The recombinant plasmids were transformed into competent *E.coli* Top10. To analyze the clones, PCR screening was performed on 30 randomly selected bacterial colonies. The primers FRT-F, CMV-F and EGFP-F bind all in the N-terminal section of the expression plasmid (RFT-F in the upstream repeat sequence, CMV-F in the promotor and EGFP-F in the N-terminal fusion gene) while the primer hNPAS2-001-pcDNA5-XhoI-R binds at the C-terminal end of the NPAS2 cDNA. The PCR results indicated that all the *E.coli* colonies had not the gene of interest (Figure 3-3). All PCR sample had less than the expected fragment size as shown in (Figure 3-4, Figure 3-5).

The size of PCR fragment was shows in agarose gel (Figure 3-3) were less than the expected for FRT, CMV, EGFP primers binding to hNPAS2-001-pcDNA5-XhoI-R primers. The expected fragment size of FRT-F, hNPAS2-001-pcDNA5-XhoI-R primers was 3547bp (Figure 3-4); After PCR the fragment size (≈1200bp) was smaller than the expected size (3547bp) (Figure 3-3). In other internally orientation primers (CMV, EGFP) the result of PCR fragment was (≈1200bp, ≈550bp) (Figure 3-3) and that was less than was expected to MCV-F, hNPAS2-001-pcDNA5-XhoI-R (3504bp), EGFP-F + hNPAS2-001-pcDNA5-XhoI-R (2763bp) (Figure 3-4). The size of internal orientation PCR fragment should be greater than NPAS2 PCR fragment (2513bp) (Figure 3-5) and that lead to the *E.coli* colonies had not the NPAS2 gene.

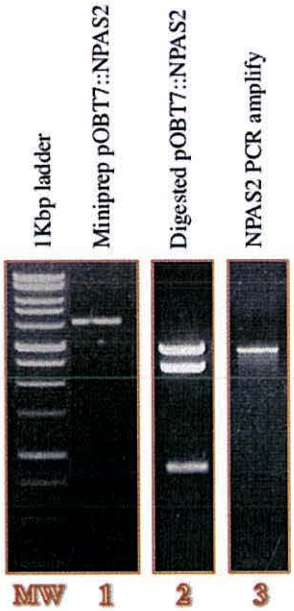

Figure 3-2: Agarose gel picture showing amplified NPAS2 from pOBT7::NPAS2 mammalian vector.

MW: 1 Kb DNA Ladder. Lane1: undigested miniprep pOBT7::NPAS2 plasmid, as a control to compare to the digestion vector. Lane2: pOTB7::NPAS2 digested by XhoI, EcoRI to check NPAS2 cDNA. Lane3: NPAS2 cDNA amplified from pOTB7::NPAS2 vector using hNPAS2-001-pcDNA5-XhoI-F, hNPAS2-001-pcDNA5-XhoI-R primers (2.5kbp).

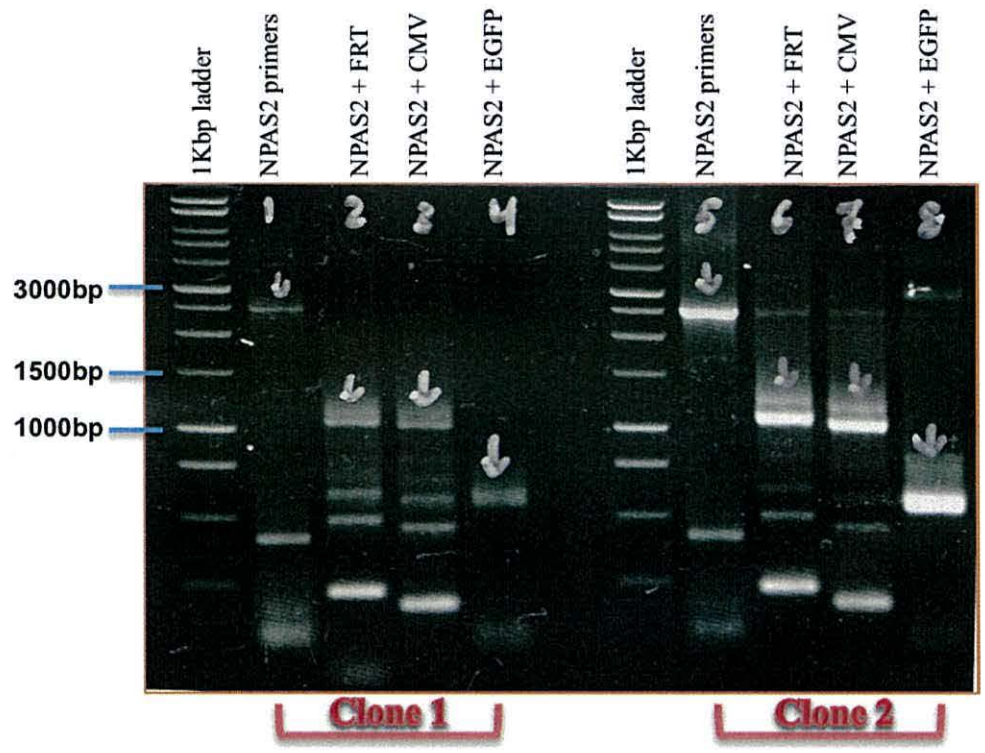

Figure 3-3: Agarose gel showing pcDNA5/FRT/TO GFP::NPAS2 vector orientation.

The PCR was performed to check the *NPAS2* cDNA orientation that was cloned into pcDNA5/FRT/TO GFP.

1/5: hNPAS2-001-pcDNA5-XhoI-F + hNPAS2-001-pcDNA5-XhoI-R (≈2500bp).

2/6: FRT-F + hNPAS2-001-pcDNA5-XhoI-R (≈ 1200bp).

3/7: MCV-F + hNPAS2-001-pcDNA5-XhoI-R (≈ 1200bp).

4/8: EGFP-F + hNPAS2-001-pcDNA5-XhoI-R (≈ 550bp).

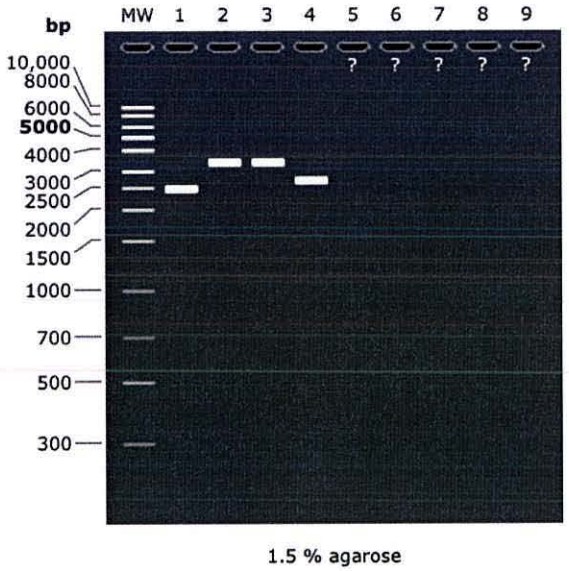

Figure 3-4: Agarose gel shows the expected size of internally orientation using software simulation PCR by creates simulation primers.

MW: 1 kb DNA Ladder

1: hNPAS2-001-pcDNA5-XhoI-F + hNPAS2-001-pcDNA5-XhoI-R (2513bp).

2: FRT-F + hNPAS2-001-pcDNA5-XhoI-R (3547bp).

3: MCV-F + hNPAS2-001-pcDNA5-XhoI-R (3504bp).

4: EGFP-F + hNPAS2-001-pcDNA5-XhoI-R (2763bp).

Figure was created with the SnapGene Software.

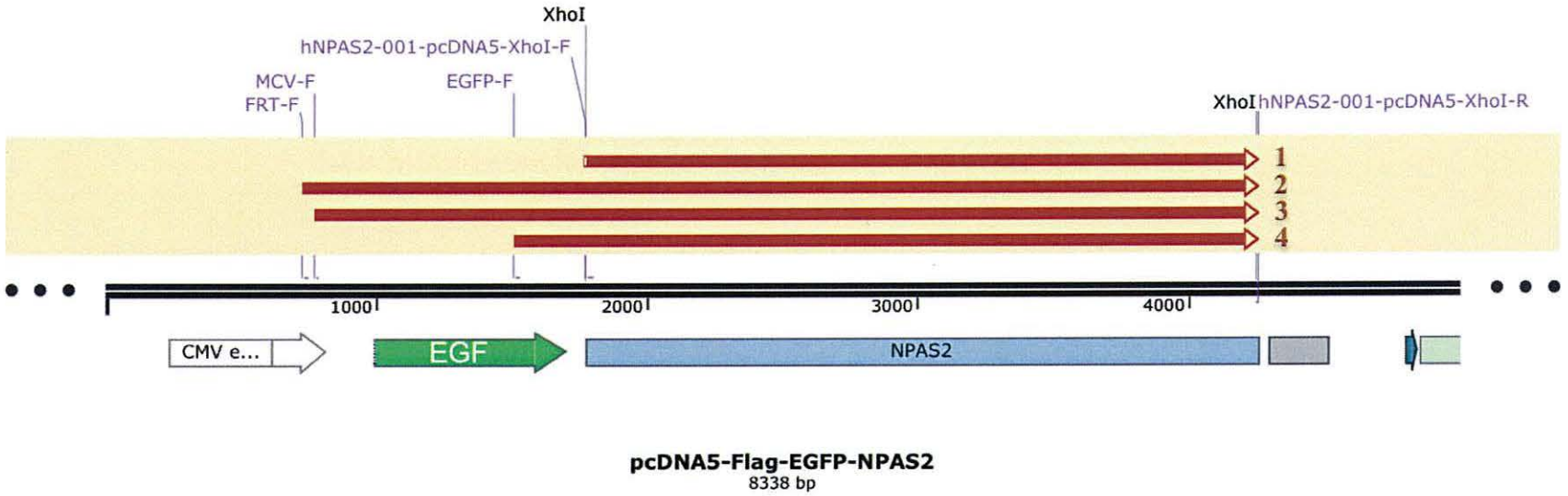

Figure 3-5: Location of the PCR primers and different sizes of the expected PCR fragments.

1: hNPAS2-001-pcDNA5-XhoI-F + hNPAS2-001-pcDNA5-XhoI-R (2513bp).

2: FRT-F + hNPAS2-001-pcDNA5-XhoI-R (3547bp).

3: MCV-F + hNPAS2-001-pcDNA5-XhoI-R (3504bp).

4: EGFP-F + hNPAS2-001-pcDNA5-XhoI-R (2763bp).

Figure was created with the SnapGene Software.

3.3 Discussion

It found that there are several reasons to fail molecular colon. The most important reasons that could relate to this result are long genes trouble with the template was used and repeated sequences.

On account of NPAS2 size is 2.5kbp. The longer DNA sequence, the more troublesome to amplify full-length fragments from PCR, get the quality embedded into a plasmid vector. Amplify the plasmid in bacterial cells which resist the burden of replicating so much foreign DNA. To check the effectively cloned a long gene requires many time-consuming steps of gel purification, transformation, miniprep and sequencing and it may attempt a few rounds of this without achievement.

While the pOTB7::NPAS2 vector purchased from Thermo Scientific and stored in lab's freezer. Starting with plasmid DNA shared by another researcher, or perhaps stored in lab's freezer for months or years, it's best to verify the sequence before setting up your PCR before starting the experiments. But ordering sequencing primers and waiting for results adds more time to your experiments. But if the sequence comes back different it will be acquiring a new template.

Many long genes like NPAS2 contains repeated sequences and that end up with a mixture of many different amplicons resulting from improper annealing during successive rounds of PCR. Even close similarity can cause improper annealing or ligation (http://www.genscript.com/reasons_cloning_fails_solutions.html [accessed 16 March 2017]).

CHAPTER 4

INVESTIGATION OF THE EXPRESSION OF THE NPAS2 PROTEIN IN HUMAN CELL LINES IN RESPONSE TO OXIDATIVE STRESS, UV, HEAT STRESS AND CPT

Chapter 4: Investigation of the expression levels of the NPAS2 protein in human cell lines in response to oxidative stress, UV, heat stress and CPT.

4.1 Introduction

The human *NPAS2* gene encodes 6 protein coding variants as curated in the Ensemble data base (accessed 29 June 2016). Figure 4-1 shows the domain organization of the 6 proteins and (Table 4-1) lists the details of the corresponding cDNAs.

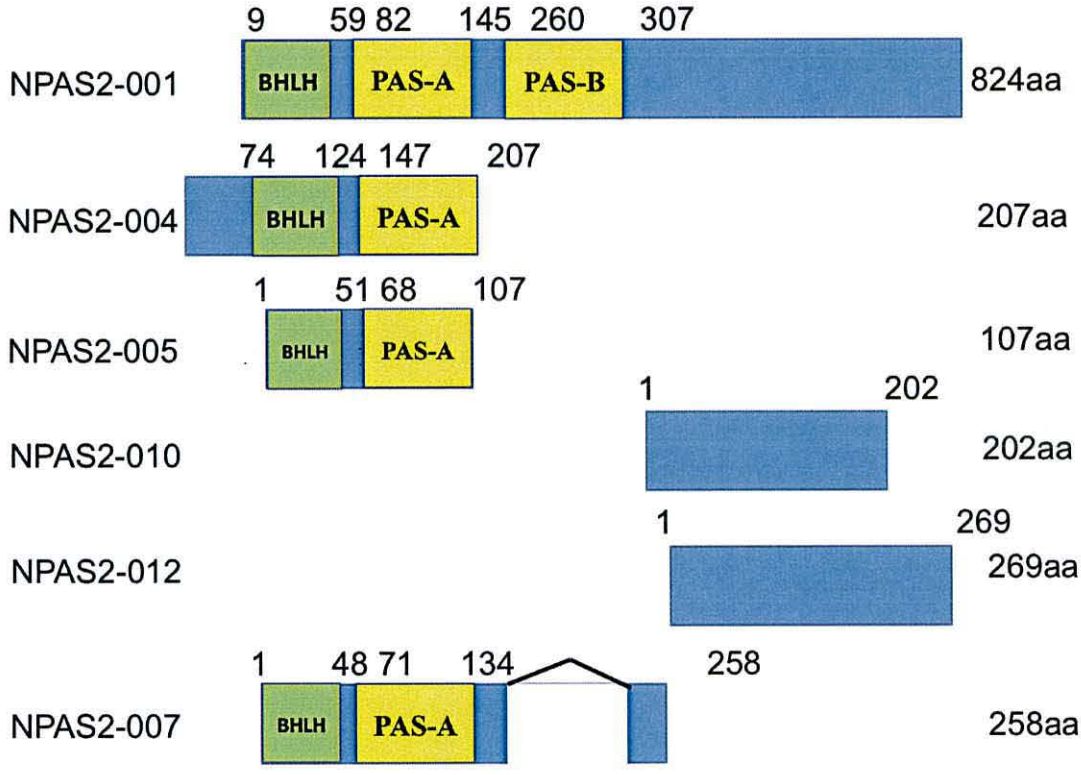

Figure 4-1: Protein coding splices variants of human NPAS2.

NPAS2-001 is the full-length protein with one N-terminal Basic-Helix-Loop-Helix (BHLH) and two PAS domains. All other variants are truncated versions. NPAS2-004 has an extra 65aa at its N-terminus. NPAS2-012 has a deletion of the second PAS domain.

Only one variant (NPAS2-001) is full-length containing the Basic-Helix-Loop-Helix (BHLH) domain and both PAS domains. All other forms are truncated and one form, NPAS2-004 has 65 additional amino acids at its N-terminus (Appendix 1). NPAS2 this far only indirectly been linked with the response to DNA damage and cell cycle regulation. Down-regulation of NPAS2 expression by siRNA in MCF-7 breast adenocarcinoma cells resulted in the repression of 7 genes (*FANCG, DMC1*, *DDB1*, *MSH2*, *PRKDC*, *MAPK12* and *EXO1*) linked with DNA repair and cell cycle arrest. As a result NPAS2 depleted cells have a DNA break repair defect as detected by the DNA damage checkpoint defect (Hoffman et al. 2008).

To find out whether the levels of the NPAS2 protein change or whether NPAS2 becomes modified, MCF-7, HeLa and HEK-293 cells were exposed to with oxidative stress (hydrogen peroxide), UV light, heat stress and the topoisomerase 1 inhibitor camptothecin (CPT). While MCF-7 (breast adenocarcinoma) and HeLa (cervical carcinoma) are cancer cell lines, HEK-293 is embryonic kidney cells with strong neuronal characteristics. NPAS2 was detected with a polyclonal rabbit antibody against a domain (not disclosed) within the C-terminus of the protein (Genetex, GTX105741). It recognizes a band of approximately 80kDa.

Table 4-1: Human *NPAS2* splice variants.

Variant	Transcript ID	cDNA length (nt)	Amino Acids	UniProt Number
NPAS2-001	ENST00000335681	4007	824aa	Q99743
NPAS2-012	ENST00000433408	1047	269aa	H7BZA3
NPAS2-007	ENST00000448812	774	258aa	H7BZA3
NPAS2-004	ENST00000427413	625	207aa	H7C0Z2
NPAS2-010	ENST00000450763	607	202aa	H7BZY5
NPAS2-005	ENST00000451740	321	107aa	H7C0J4

{Investigation of the expression levels of the NPAS2 protein in human cell lines in response to oxidative stress, UV, heat stress and CPT.}

4.2 Results

4.2.1 NPAS2 protein expression in the response to different DNA damaging agents.

4.2.1.1 Oxidative Stress

Cells were treated with 500μM H_2O_2 in complete medium for 0.5 hour, 1 hour, 2 hours, 4 hours and 24 hours at 37°C (Figure 4-2). Total protein extracts were prepared to assay the expression levels of NPAS2. An anti-GAPDH antibody (Glyceraldehyde-3-phosphate dehydrogenase) was used as a loading control and anti-p21/WAF1/CIP1 antibody was used as p21 levels were reported to increase with increasing hydrogen peroxide concentrations (Lee, Lee & Han 2006).

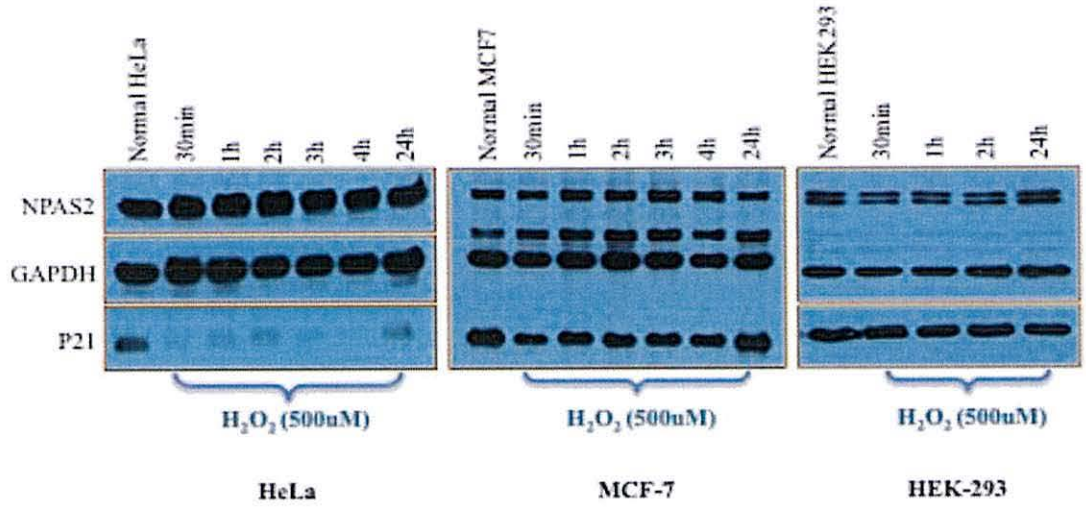

Figure 4-2: Hydrogen peroxide (H_2O_2) treatment of HeLa, MCF-7 and HEK-293 cells.

Cells were treated with 500μM H_2O_2 in complete medium for the indicated times. Total protein extracts were prepared and analyzed using anti-NPAS2, anti-p21 and anti-GAPDH antibodies. NPAS2 (80kDa), GAPDH (37kDa0, p21 (21kDa). The acrylamide percentage was (10%). The additional band above the GAPDH signal is specific to the latter protein and was only observed in MCF-7 cells.

In all three cell lines the levels of NPAS2 were not affected by osmotic stress. In embryonic HEK-293 cells NPAS2 did run as a double band that was much less obvious in the two cancer cell lines (HeLa, MCF-7). Unexpectedly, p21 was strongly down-regulated by oxidative stress only in the cervical carcinoma HeLa cell line. A similar down-regulation was so far only reported for the GM00637 fibroblast cell line where p21 degradation is dependent on the proteasome (Xie et al. 2002).

4.2.1.2 Heat stress

To test whether heat stress affects NPAS2 protein levels in HeLa, HEK-293 or MCF-7 cells, cells in complete medium were exposed for 1 hour to 43°C and allowed to recover at 37°C for 0.5 hour, 1 hour, 2 hours and 24 hours (Figure 4-3). Total protein samples were prepared at the indicated time points and analysed for the expression of NPAS2, p21 and GAPDH. Interestingly, heat stress triggered the down-regulation of NPAS2, which has not yet been reported, and this decline was restricted to the two cancer cell lines (HeLa and MCF-7). In both cell lines, this correlated with a down-regulation of p21. The latter was very clear in the cervical carcinoma HeLa cells and to a lesser extend in the breast adenocarcinoma MCF-7 cells as p21 levels recovered at the 2 hours and 24 hours time points (Figure 4-3).

The impact of heat stress on p21 protein levels has so far only been studied in a few cell lines. While its levels do not change in liver and liver cancer cells (Han et al. 2013), p21 increases throughout the first 3 hours of recovery after a 15 minute heat shock at 44°C in A172 glioma cells (Fuse et al. 1996).

{Investigation of the expression levels of the NPAS2 protein in human cell lines in response to oxidative stress, UV, heat stress and CPT.}

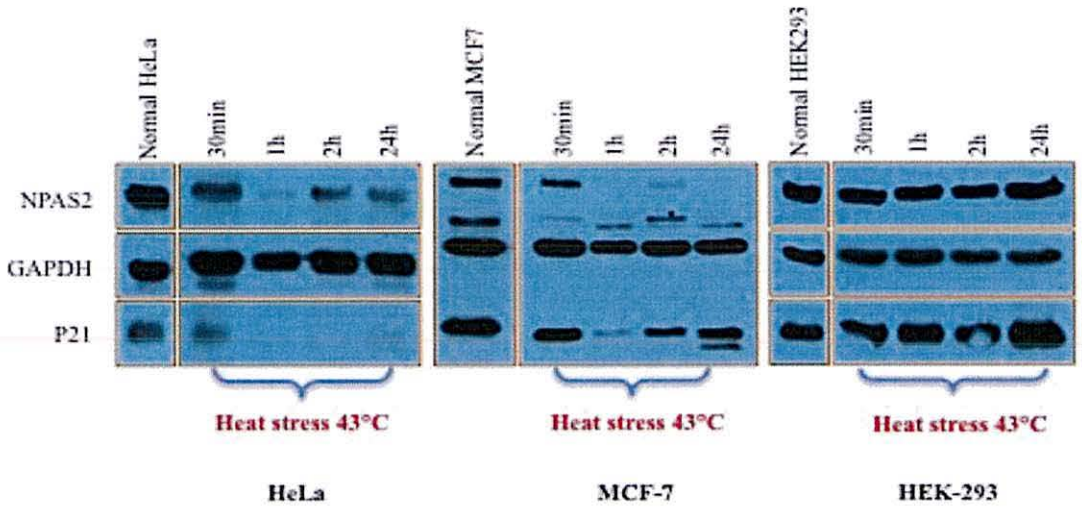

Figure 4-3: Heat shock treatment of HeLa, MCF-7 and HEK-293 cells.

The indicated cell lines were heat shocked at 43°C for 1 hour in complete medium. Protein samples were prepared at the indicated time points during the recovery period at 37°C after the heat shock. Extracts were analyzed using anti-NPAS2, anti-p21 and anti-GAPDH antibodies. NPAS2 (80kDa), GAPDH (37kDa), p21 (21kDa). The acrylamide percentage was (10%). Please note that NPAS2 and p21 levels decline in HeLa and MCF-7 cells, but not in HEK-293 cells.

4.2.1.3 Pyrimidine dimer formation through exposure to ultraviolet light (UV).

UV light induces pyrimidine dimers in the DNA structure which interfere with transcription and DNA replication. A dose of 40J/m^2 was used. This dose has very effective on cell lines as it triggered the rapid degradation of p21 WAF1/CIP1 as reported previously (Bendjennat et al. 2003) (Figure 4-4). An NPAS2 level was down-regulation in MCF-7 but was no change in HEK-293 and HeLa cells. While UV treatment had no effect on NPAS2 levels in MCF-7 and HEK-293 cells, its levels declined in HeLa cells at the 30 minute and 1 hour time points. This cell line specific decline in cervical cancer cells implies a unique change in HeLa cells which affects the turnover of NPAS2. Cell line specific effects are also obvious for p21 as its levels only decline in HeLa and HEK-293 cells within 2 hours post-UV but not in MCF-7 cells. The latter cell line showed a decline at the 24 hours time point.

{Investigation of the expression levels of the NPAS2 protein in human cell lines in response to oxidative stress, UV, heat stress and CPT.}

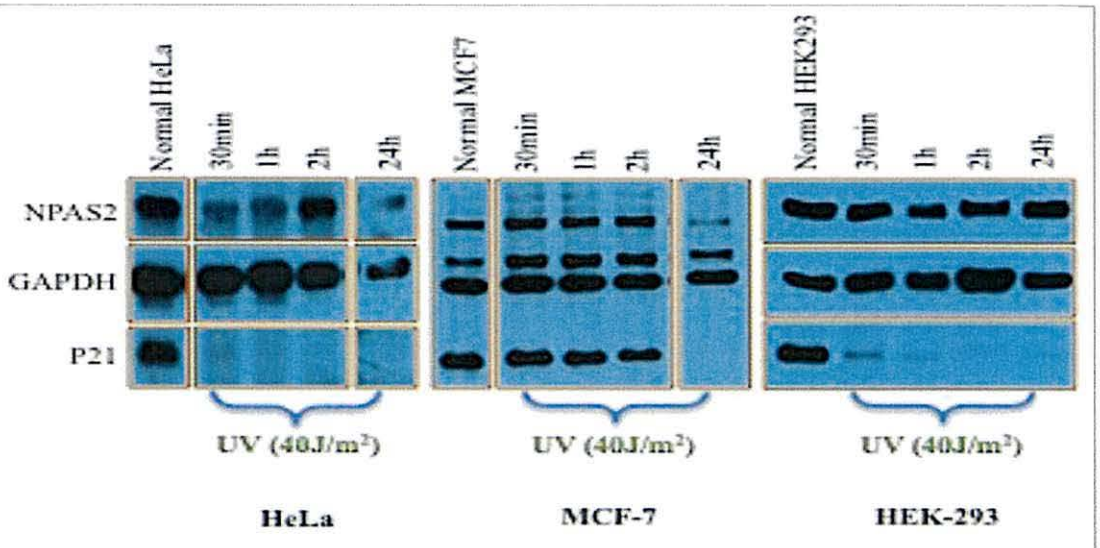

Figure 4-4: Pyrimidine dimer formation through exposure to ultraviolet light (UV) in HeLa, MCF-7 and HEK-293 cells.

Cells were exposed to 40J/m^2 of UV light and allowed to recover in fresh medium for the indicated periods of time. Total protein extracts were prepared and analysed using the anti-NPAS2, anti- GAPDH and anti-p21 antibodies. NPAS2 (80kDa), GAPDH (37kDa), p21 (21kDa). The acrylamide percentage was (10%). Please note that NPAS2 and p21 levels decline in HeLa cells, whereas only p21 levels drop in HEK-293 cells. NPAS2 doesn't change in MCF-7 and HEK-293 cells. P21 levels remain high within the first 2 hours in MCF-7 cells.

4.2.1.4 Replication fork damage by camptothecin (CPT) treatment.

It is well known that the DNA enzyme topoisomerase I (topo I) or known as camptothecin (CPT) arrests cells in S-phase when replication forks break upon their collision with the immobilized Topoisomerase1 enzyme (Ryan et al. 1991). As in the case of hydrogen peroxide (Figure 4-2), CPT treatment had no immediate impact on NPAS2 protein levels in all three cell lines. Neither did p21 levels drop within the first 2 hours (Figure 4-5). Only when cells were exposed for 24 hours to 1μM CPT a decline in NPAS2 was detected in the two cancer cell lines (HeLa, MCF-7). The latter could be linked with CPT-induced cell death as also the GAPDH loading control indicated a decrease in the amount of protein.

{Investigation of the expression levels of the NPAS2 protein in human cell lines in response to oxidative stress, UV, heat stress and CPT.}

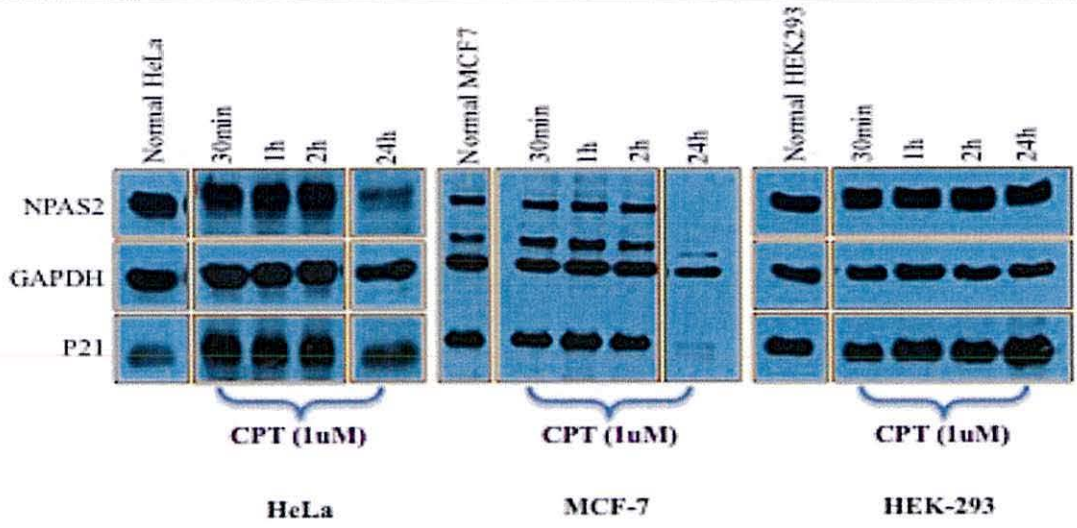

Figure 4-5: Camptothecin (CPT) treatment of HeLa, MCF-7 and HEK-293 cells.

Cells were treated with 1μM of CPT for up to 24 hours. Total protein extracts were prepared at the indicated time points prepared and analysed using the anti-NPAS2, anti-GAPDH and anti-p21 antibodies. NPAS2 (80kDa), GAPDH (37kDa), p21 (21kDa). The acrylamide percentage was (10%). The decline in NPAS2 at the 24 hours time point in the cancer lines HeLa and MCF-7 could be linked with cell death. A similar decline was not detected in the non-cancerous HEK-293 cell line.

To ensure that the DNA damaging treatment activated the DNA damage checkpoint. HCT-116 colon carcinoma cell and HEK-293 cells were treated with 1μM of CPT for up to 24 hours, exposed to 40J/m^2 UV light and allowed to recover for up to 24 hours or exposed to 43°C for 1 hour and allowed to recover for up to 24 hours. Total cell extracts were then probed for NPAS2 and for the phosphorylation of Chk1 kinase at serine-345 by ATR kinase which is an established marker for the activation of the DNA damage checkpoint (Jiang et al. 2003). As expected, heat stress did not activate Chk1-S345 phosphorylation, but CPT and UV treatment did. The electrophoretic mobility of NPAS2 did not change under any conditions (Figure 4-6).

{Investigation of the expression levels of the NPAS2 protein in human cell lines in response to oxidative stress, UV, heat stress and CPT.}

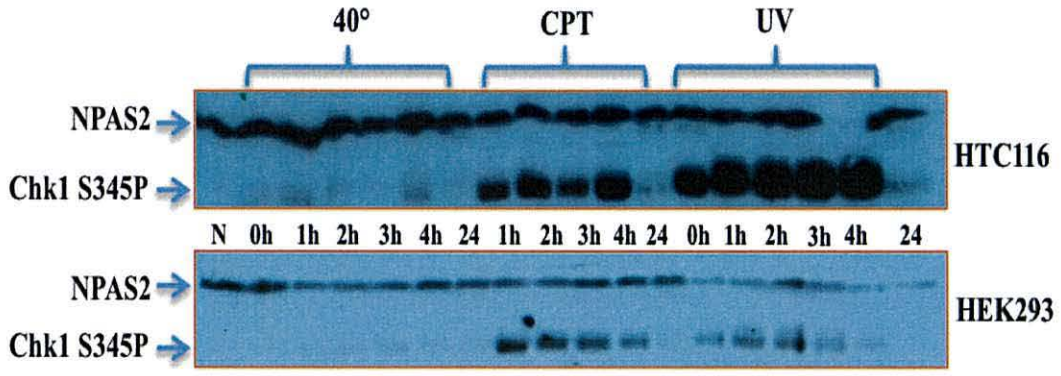

Figure 4-6: Chk1 serine-345 phosphorylation in heat, camptothecin (CPT) and UV treated HTC-116 and HEK-293 cells.

Cells were treated with 1μM of CPT for the indicated time points, exposed to 40J/m^2 UV or to 43°C for 1 hour and allowed to recover for up to 24 hours. Total protein extracts were prepared at the indicated time points prepared and analysed using the anti-NPAS2 and a phospho-specific Chk1 S345P antibody.

{Investigation of the expression levels of the NPAS2 protein in human cell lines in response to oxidative stress, UV, heat stress and CPT.}

Summarizes the changes in NPAS2 and p21 protein levels in the three tested cell lines. NPAS2 levels did not change in the non-cancerous HEK-293 cell line, while NPAS2 was down-regulated in the two cancer cell lines (HeLa, MCF-7) especially by heat stress. The CDK inhibitor p21 was down-regulated in HeLa cells in the response to hydrogen peroxide, heat and UV light but not in the presence of CPT. A decline in p21 was also observed in MCF-7 cells at elevated temperatures and in HEK-293 cells after UV treatment.

Table 4-2: Summary of the changes in NPAS2 and p21 protein levels in the three cell lines.

(↓) = decrease, (→) no change.

Treatment	HeLa	MCF-7	HEK-293
H_2O_2	NPAS2 → P21↓	NPAS2→ P21→	NPAS2→ P21→
Heat shock	NPAS2 ↓ P21↓	NPAS2 ↓ P21↓	NPAS2→ P21→
UV light	NPAS2 ↓ P21↓	NPAS2→ P21→	NPAS2 → P21↓
CPT	NPAS2→ P21→	NPAS2→ P21→	NPAS2→ P21→

4.2.2 Isoelectric focusing (IEF) of NPAS2 reveals different protein variants.

Although the full-length form of NPAS2 appears as one band in most experiments, it could well be that this band contains more than one form of the protein. To detect differently modified forms of NPAS2 total protein extracts were analysed on linear pH 3-10 isoelectric focusing strips. Small amounts of the protein extracts were loaded on a Bio-Rad dry-strip (linear) with a pH range from 3 to 10. The theoretical isoelectric value of NPAS2 is pH6.35. After the separation of the protein by overall charge, the strips were placed on a 10% SDS page to separate the protein by size. The experiment was performed with protein harvested from HEK-293 and HeLa cells. As shown in (Figure 4-7), most of NPAS2 displayed a very alkaline isoelectric point at around 10 (Form 1 in Figure 4-7) with a smaller amount at pH 3 (form 2 in Figure 4-7). Moreover, form 1 is a double signal containing a larger protein species (5-10kDa larger). This was very clear when protein extracts obtained from HeLa cells were analysed (Figure 4-7 B). Interestingly, both UV light and oxidative stress resulted in the appearance of more negatively charged forms which were however different dependent on the type of stress. While UV light resulted in one more negatively charged form (in the pH range of 4-5), oxidative stress produced three forms at around a pH of 8 when HEK-293 cells were exposed to 500μM hydrogen peroxide for 24 hours (Figure 4-7 A). Both events could be caused by different phosphorylation events of NPAS2.

{Investigation of the expression levels of the NPAS2 protein in human cell lines in response to oxidative stress, UV, heat stress and CPT.}

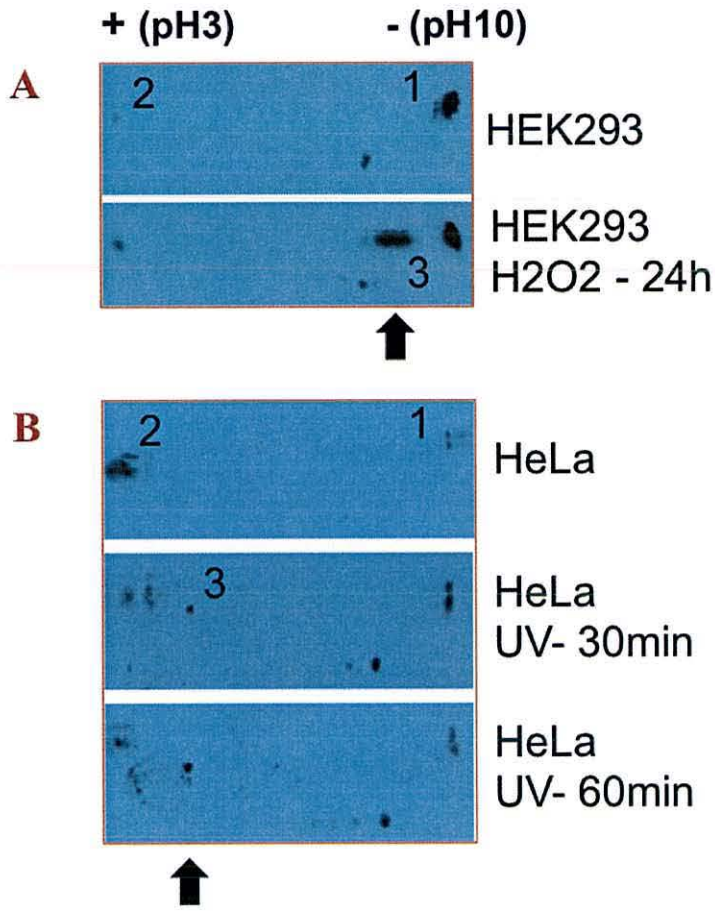

Figure 4-7: Isoelectric focusing of NPAS2 reveals different protein variants

A: HEK-293 cells were either untreated or exposed to 500μM hydrogen peroxide for 24 hours. Protein was loaded onto a Bio-Rad dry-strip pH3-10 (linear) to separate NPAS2 by charge. After the run (10,000Vh, rapid), the strip was placed on top of a 10% acrylamide gel to separate NPAS2 by size. Form 1: main NPAS2 signal at a pH of 10, form 2: minor NPAS2 signal at a pH of 3, form 3: stress induced forms of NPAS2 (indicated by the arrow).

B: HeLa cells were exposed to 40J/m^2 and proteins were extracted after 30 minute and 60 minute post-treatment.

Given that NPAS2 associates with ARNTL/BMAL1 in a larger complex (Kondratov et al. 2006), soluble protein extracts of HEK-293 cells obtained from untreated cells or cells exposed to 500μM H_2O_2 for 24 hours were separated on a Superdex 200 size fractionation column. The column separates protein complexes between 50kDa and 700kDa. In untreated cells NPAS2 eluted with an apparent molecular weight of 100-150kDa (fraction 16 in Figure 4-8) which is close to its monomeric size of 92kDa. ARNTL/BMAL1 is with 69kDa smaller than NPAS2 and the dimeric complex could elute at around 150kDa which correlates well with the elution peak in fraction 16.

Interestingly after treatment of cells with hydrogen peroxide a significant amount of NPAS2 eluted at around 500-700kDa which implies the formation of higher molecular weight complexes. A low amount of these larger complexes can also be seen in untreated cells (Figure 4-8). Similar large NPAS2 complexes have not yet been reported.

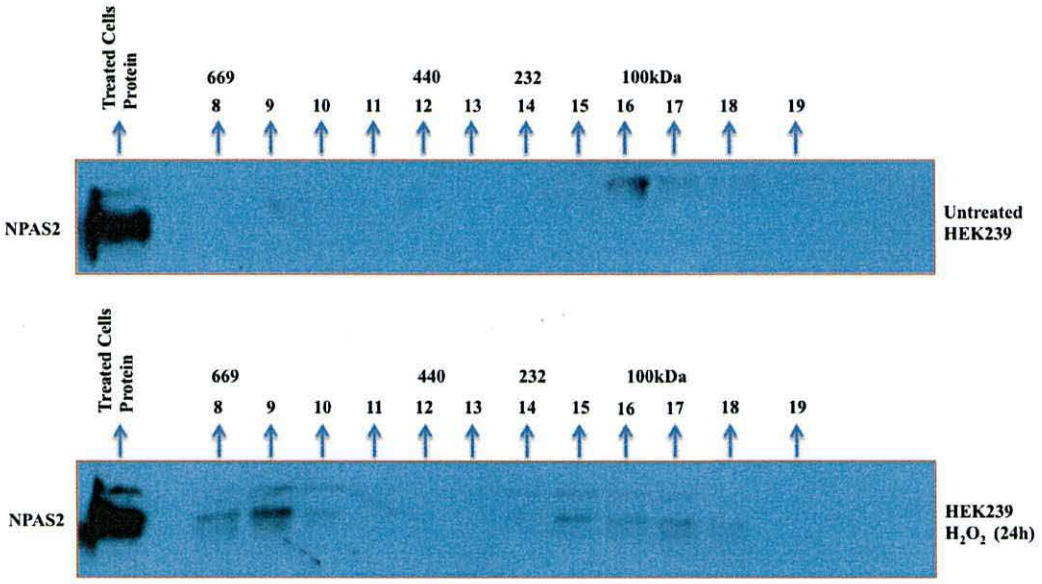

Figure 4-8: NPAS2 forms high molecular weight complexes in the response to oxidative stress in HEK-293 cells

HEK-293 cells were left untreated or exposed to 500μM H_2O_2 for 24 hours. Soluble protein extracts were separated on a Superdex 200 size exclusion column (bed volume = 24ml). Twenty-four 1ml fractions were collected and the protein was precipitated with trichloroacetic acid. Protein from fractions 8 to 19 were analysed after electrophoresis on an 8% acrylamide gel. NPAS2 was visualized with the anti-NPAS2 antibody.

{Investigation of the expression levels of the NPAS2 protein in human cell lines in response to oxidative stress, UV, heat stress and CPT.}

4.2.3 Cell fractionation and cellular localization of NPAS2 in MCF-7 and HEK-293 cells.

Given that NPAS2 associates with CLOCK in a hetero-dimeric transcription factor (Gorbacheva et al. 2005), it is to be expected that NPAS2 localizes to the nucleus. To explore the cellular localization MCF-7 and HEK-293 cells were fractionated in a membrane fraction, a cytosolic and a nuclear fraction.

Cells were left untreated or they were incubated with 500μM hydrogen peroxide for 0.5 hour, 1 hour, 2 hours or 24 hours. As shown in (Figure 4-9), NPAS2 was enriched in the soluble nuclear fraction in untreated HEK-293 cell with only a small amount in the cytoplasm. Hydrogen peroxide did not significantly affect the nuclear localization of NPAS2, although a transient increase in the cytoplasmic fraction was observed when cells were incubated for 30 minutes with hydrogen peroxide. It was also noticed that NPAS did run as a double band in these experiments.

NPAS2 was also predominantly nuclear in MCF-7 cells independently of the exposure to oxidative stress. In contrast to the HEK-293 cells, less NPAS2 was detected in the cytoplasm and more in the membrane fraction which increased over time when cells were incubated for longer in the presence of hydrogen peroxide (Figure 4-10).

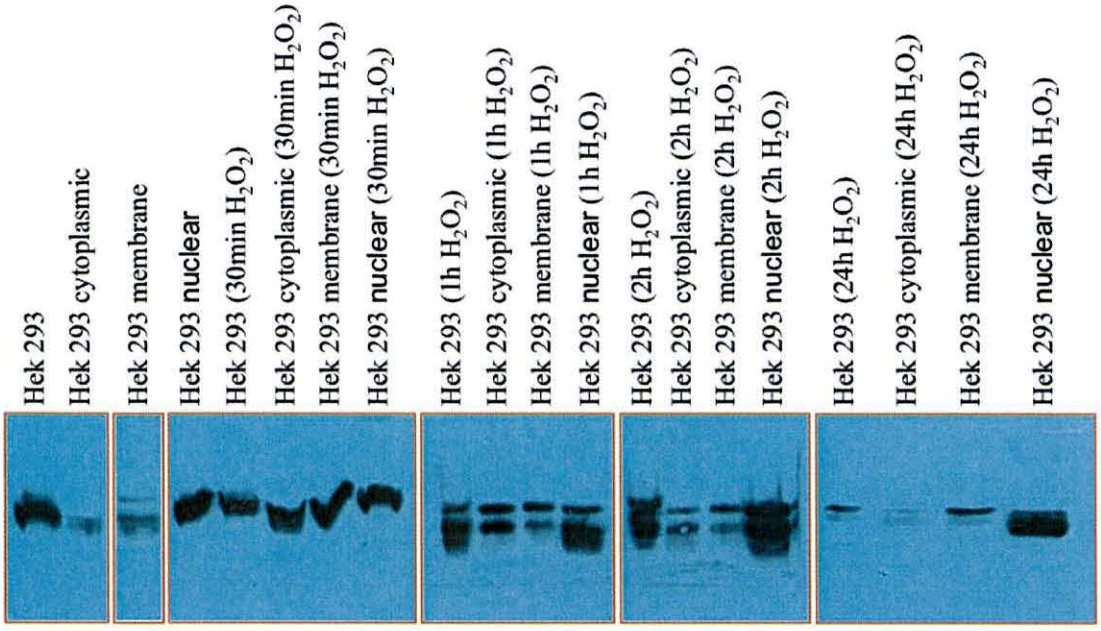

Figure 4-9: Cell fractionation of NPAS2 of untreated HEK-293 cells and cells treated with H_2O_2.

Cells was treated with 500μM H_2O_2, for the indicated times. Protein samples were subjected to the cell fractionation protocol which provided a cytoplasmic fraction, a membrane fraction and a soluble nuclear fraction.

{Investigation of the expression levels of the NPAS2 protein in human cell lines in response to oxidative stress, UV, heat stress and CPT.}

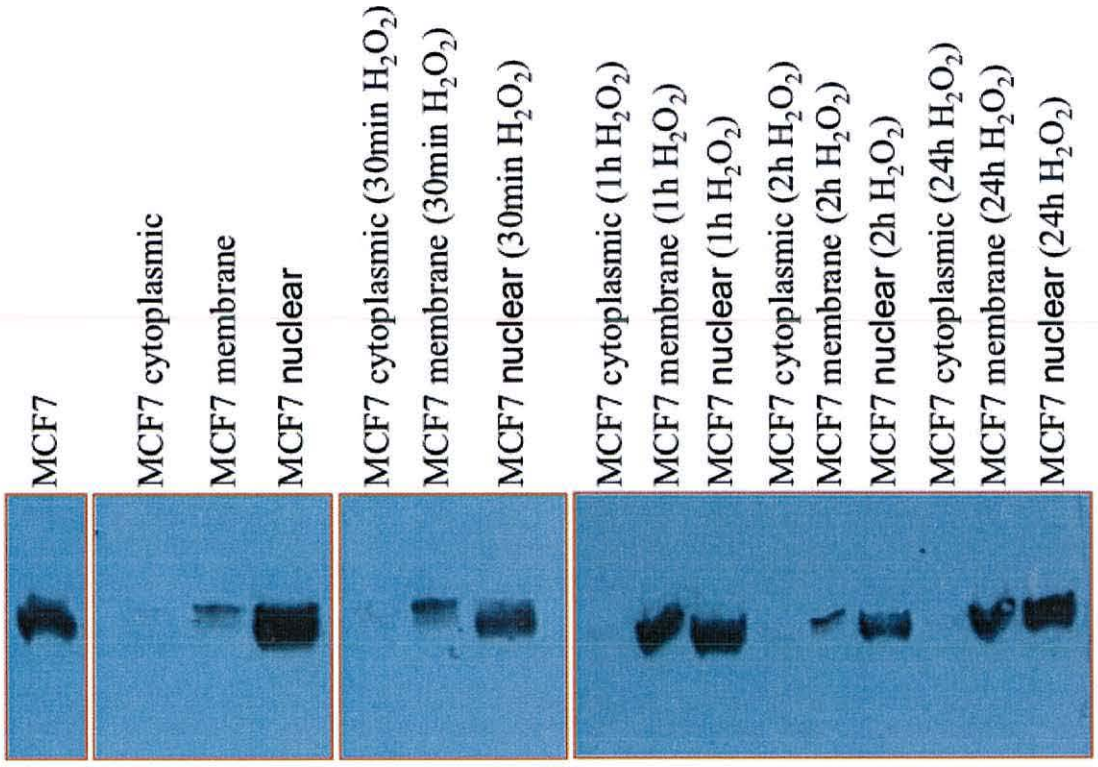

Figure 4-10: Cell fractionation of NPAS2 of untreated MCF-7 cells and cells treated with H_2O_2.

Cells were treated with 500µM H_2O_2 for the indicated periods of time. Protein samples were subjected to the cell fractionation protocol which provided a cytoplasmic fraction, a membrane fraction and a soluble nuclear fraction.

To obtain independent confirmation for these results, NPAS2 was stained in fixed HEK-293 and MCF-7 cells which were either untreated or grown in the presence of 500µM hydrogen peroxide for 2 hours. In line with the cell fractionation experiments, NPAS2 was predominantly in the nucleus of treated and untreated MCF-7 and HEK-293 cells (Figure 4-11). Also consistent with the fractionation results, there was no cytoplasmic signal of NPAS2 in MCF-7 cells. This implies that NPAS2 is nuclear in the breast adenocarcinoma cell line, whereas the protein localizes to the nucleus and the cytoplasm in the non-cancerous HEK-293 cell line. Images were quantified using ZEN Software from Carl ZEISS.

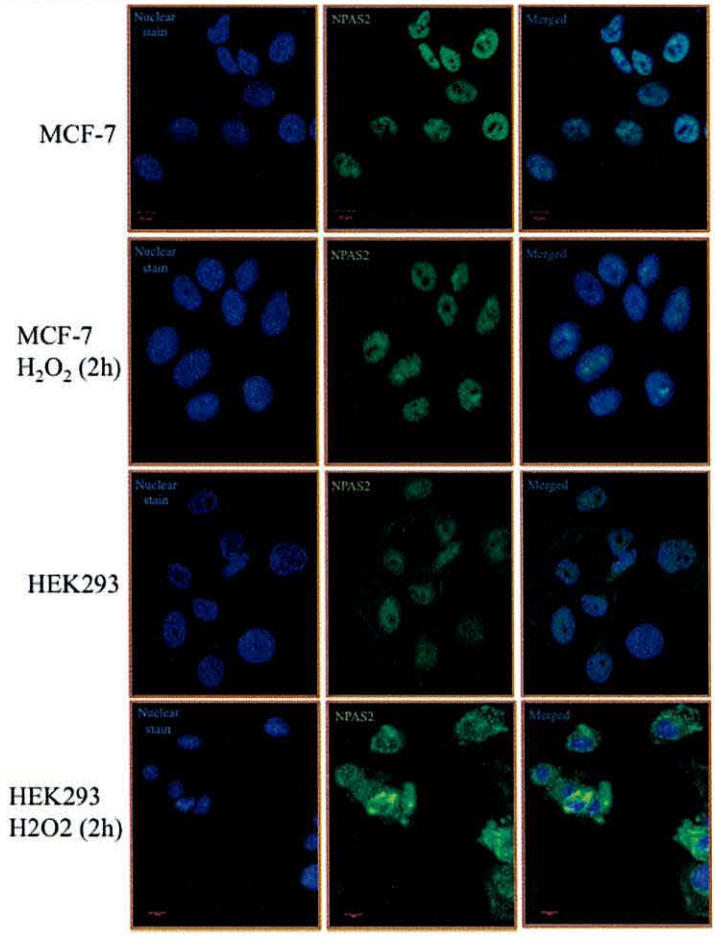

Figure 4-11: Cellular localization of NPAS2 in MCF-7 and HEK-293.

Cells were grown on circular glass plates and left untreated or in the presence of 500μM hydrogen peroxide for 2 hours. Cells were fixed and stained with a polyclonal anti-NPAS2 antibody (green) and with the DNA stain DAPI (blue). Scale bar 10μm. Images were taken and analysed using ZEN Software from Carl ZEISS.

{Investigation of the expression levels of the NPAS2 protein in human cell lines in response to oxidative stress, UV, heat stress and CPT.}

4.3 Discussion

4.3.1 Key Findings.

The key findings of this chapter are: **(1)** the down-regulation of NPAS2 in response to a heat shock in the two cancer cell lines MCF-7 and HeLa; **(2)** the presence of three forms of NPAS2 with distinct isoelectric points in untreated HEK-293 and MCF-7 cells, **(3)** the appearance of more negative forms in the response to UV irradiation and oxidative stress, **(4)** the formation of large NPAS2 protein complexes in the response to oxidative stress in HEK-293 cells and **(5)** the exclusively nuclear localization of NPAS2 in MCF-7 and HEK-293 cells.

4.3.2 Down-regulation of NPAS2 in the response to heat stress.

The decline in NPAS2 protein levels after a heat shock at 43°C for 1 hour (Figure 4-3) occurred only in the two cancer cell lines (HeLa and MCF-7) but not in the non-cancerous cell line HEK-293. This implies that this effect may be limited to malignant cells. There is however one important point to consider here. While both cancer lines are of epithelial origin, the HEK-293 cell line may be of neuronal origin (Stepanenko, Dmitrenko 2015). Since the NPAS2-BMAL transcription factor may have different functions in neuronal cells compared to epithelial cells, heat may not reduce NPAS2 levels in neurons. This idea is supported by the intriguing observation that the circadian clock is very resistant to temperature changes. In *Drosophila*, an increase in temperature results in elevated expression levels of the circadian clock protein Timeless (Kidd, Young & Siggia 2015). In mouse fibroblasts a 30 minutes heat shock at 43°C triggers the cyclic expression of BMAL and Period 2, and heat shock factor 1 (HSF1) associates with the CLOCK (NPAS2)-BMAL complex (Tamaru et al. 2011). HSF1 itself is a circadian protein and one theory on the origins of the circadian clock is based on the idea that it evolved from a temperature sensitive system (Reinke et al. 2008). Why cancer cell lines need to reduce NPAS2 protein levels at elevated temperatures is not so clear. The heat sensitivity peaks during S phase in human cells (Fox, Read & Bedford 1985) and because cancer cells divide quickly, the down-regulation of NPAS2 could be linked with DNA replication. May be NPAS2 or a gene product controlled by the transcription factor has a negative impact on DNA replication at higher temperatures.

4.3.3 Three protein forms of NPAS2 with distinct isoelectric points.

Although the theoretical isoelectric point of NPAS2 is 6.3, isoelectric focusing revealed three forms of the 80kDa protein, two with a very alkaline IP (isoelectric point) of around 10, and one form with a very acidic IP of around 3 (Figure 4-7). This implies extensive post-translational modifications which either add negative charges (more acidic form which runs closer to the positive end of the strip) or increase the number of positive charges (more alkaline form running closer to the negative end of the strip). Phosphorylation is of course a well known modification that increases the number of negative charges. An increase in positive charges is however more difficult to explain. One possibility is the amidation of carboxy groups, as this would remove the negative charge from glutamate or aspartate. Transcription factors like NPAS2 may benefit from being more positively charged as their target, the DNA is negatively charged. Amidation is however a rare modification (Duan, Walther 2015). What is however interesting is the observation that the two positively charged forms of NPAS2 do have different molecular weights as they appear on top of each other (Figure 4-7). The molecular weight difference is small and could be in the range of 10kDa that is characteristic for ubiquitin, SUMO or Nedd8 modifications. These small proteins are related to each other and become covalently attached to lysine residues (Kerscher, Felberbaum & Hochstrasser 2006). Human NPAS2 has one predicted SUMO (11.5kDa) attachment motif 160-LKSD-163 between the first and second PAS domain (Figure 4-12) (http://www.abgent.com/sumoplot [accessed 01 July 2016]). SUMO has however an acidic IP at around 5.3. Nedd8 (9kDa) is closely related to ubiquitin and has a more alkaline IP of 8.0, while ubiquitin (8.5kDa) has an IP of 6.8. NPAS2 has 4 potential neddylation sites at lysine residues 16, 19, 58 and 704 (http://neddypreddy.sabanciuniv.edu [accessed 01 July 2016]). The three N-terminal sites are all in the BHLH DNA binding domain of the protein (Figure 4-12). The ubiquitinylation site prediction tool UbiProber identified 4 lysine residues (K6, K30, K45, K51), all in the BHLH domain, which could be modified with ubiquitin (http://bioinfo.ncu.edu.cn [accessed 01 July 2016]). In summary, it is quite likely that the more positively charged, alkaline form of NPAS2 is modified by the attachment of one of these small proteins as this would explain the two signals with different molecular weights. A likely candidate is Nedd8 as its IP is alkaline (IP = 8.0), whereas SUMO and ubiquitin have more acidic isoelectric points.

4.3.4 Phosphorylation of NPAS2.

UV light results in the appearance of one NPAS2 form with a more negative IP, whereas oxidative stress leads to the appearance of three more negatively charged forms although they are not as negative as the UV-form (Figure 4-4). This implies that NPAS2 is phosphorylated under stress conditions. Previous

work has shown that the CLOCK (NPAS2)-BMAL1 transcription factor complex becomes phosphorylated in a manner that requires cryptochrome so that the complex can enter the nucleus (Kondratov et al. 2006). In these experiments NPAS2 expressed from a plasmid did run as a single band that was converted into a double-band in the presence of a second plasmid which expressed BMAL1. This is similar to the NPAS2 double band observed in HEK-293 cells (Figure 4-2). This also implies that the very negative form of NPAS2 (form 2) which is present in untreated cells represents the phosphorylated and active transcription factor. So far no kinase has been identified which phosphorylates NPAS2. Its partner human BMAL1 is phosphorylated at serine-90 by Casein kinase 2 in a manner dependent on cryptochrome (Tamaru et al. 2015).

The potential phosphorylation of NPAS2 in the presence of oxidative damage points towards a role of the three human MAP kinase pathways as they are all activated by hydrogen peroxides (Son et al. 2013). The three MAP kinase pathways in human cells are: the extracellular signal-regulated kinases (ERK1, ERK2), the c-Jun N-terminal kinase (JNK), and the p38 MAP kinase. Interestingly, *Drosophila* p38 was identified as a circadian kinase which targets the Period proteins (Dusik et al. 2014) and *Neurospora* MAK1 MAP kinase is required for the circadian gene expression rhythm (Bennett et al. 2013). In mouse cells the c-Jun N-terminal kinase (JNK) is involved in the phosphorylation of BMAL1 at Serine-520, Threonine-527 and Serine-592 (Yoshitane et al. 2012). Mouse JNK was also reported to modify Period 2 (Uchida et al. 2012). MAP kinase dependent phosphorylation was also reported for mouse cryptochrome 1 and 2 at Serine-247 (Cry1) and Serine-265 and Serine-557 (CRY2) (Sanada et al. 2004). Interesting very little is known about the role of the MAP kinase pathways in the human circadian clock and phosphorylation of NPAS2 under oxidative stress condition has not yet been reported.

4.3.5 The exclusively nuclear localization of NPAS2 in MCF-7 cells.

As shown in Figure 4-9, NPAS2 is in the cytoplasm and nucleus of HEK-293 cells but only in the nucleus of MCF-7 cells. This difference between the cell lines is supported by the cell fractionation experiments (Figure 4-10). These findings are in line with the published cytoplasmic and nuclear localization of NPAS2 in HEK-293 cells (Itoh et al. 2013). A nuclear localization of NPAS2 is consistent with its activity as a transcription factor jointly with BMAL1. The latter protein associates with nuclear bodies in monkey kidney COS-7 cells in a manner regulated by its attachment to SUMO and Ubiquitin (Lee et al. 2008). Why NPAS2 is enriched inside the nuclei of breast cancer MCF-7 cells is not clear. This could be an indirect consequence of changes to its partner protein BMAL1 as its nuclear localization is regulated by the post-translational attachment of SUMO and Ubiquitin. As in the case of the MCF-7 cell line, CLOCK and BMAL1 are both exclusively localized to the nucleus in cervical carcinoma (HeLa)

cells. Association of BMAL1 with CLOCK, or maybe NPAS2, promotes its nuclear localization, transcriptional activity and subsequent degradation in a manner dependent on cryptochrome (Kwon et al. 2006). The nuclear enrichment of NPAS2 and BMAL1 may be beneficial for malignant cells although the true reasons behind this are not yet clear.

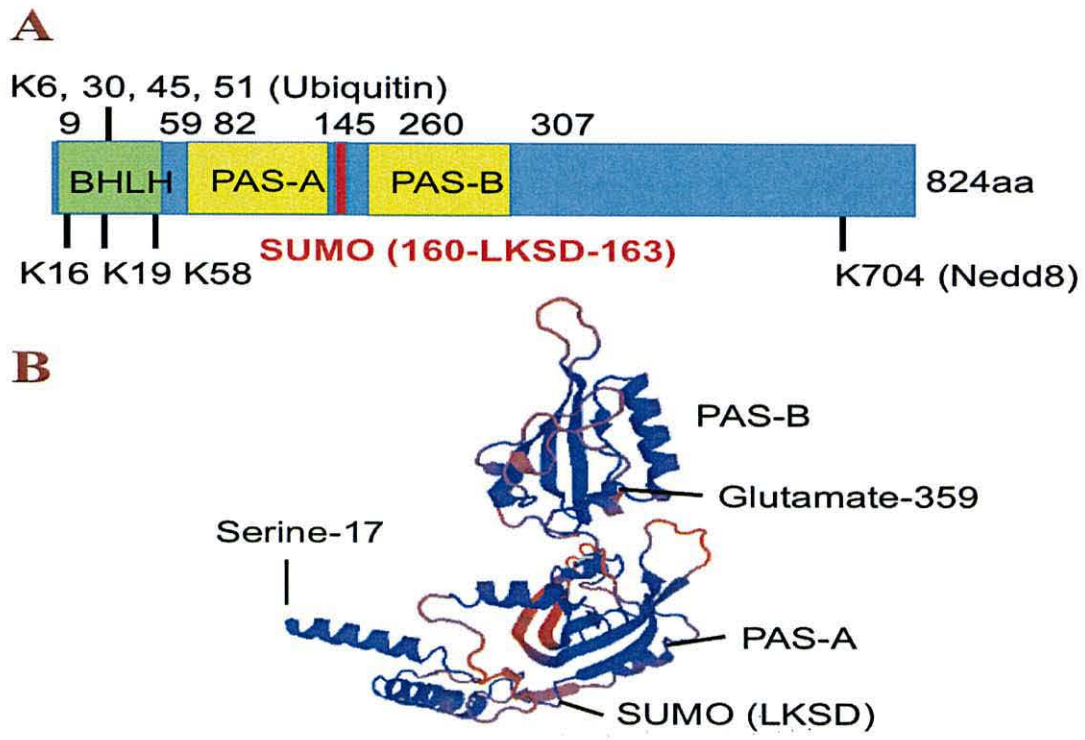

Figure 4-12: Location of modification sites (lysine residues) for Ubiquitin, Nedd8 and SUMO in human NPAS2.

A: domain organization of human NPAS2. The lysine residues which may be modified with ubiquitin are indicated at the top, whereas the lysine residues which may be modified with Nedd8 are shown below. The single SUMO attachment site at K161 is shown in red.

B: Model of the N-terminal section of human NPAS2. The model is based on the mouse heterodimeric Clock-BMAL1 complex (ID number: 4f3l.1) (Huang et al. 2012). The model was generated with Swiss Model.

{Investigation of the expression levels of the NPAS2 protein in human cell lines in response to oxidative stress, UV, heat stress and CPT.}

4.3.6 Formation of large protein complexes by NPAS2.

The size exclusion experiment (Figure 4-8) revealed two interesting findings. In untreated cells NPAS elutes at around 150kDa which would be consistent with the size of the hetero-dimeric NPAS2-ARNTL/BMAL complex (92kDa + 69kDa = 161kDa). The presence of oxidative stress induces an increase in larger NPAS2 protein complexes of between 500kDa and 700kDa. Period 2 and Cryptochrome 2 are known to bind to the CLOCK-ARNTL complex. While Cry2 binds preferentially to the DNA bound complex, Per2 and a Per2-Cry2 complex bind with higher affinity to the CLOCK-ARNTL complex away from the DNA (Kepsutlu, Kizilel & Kizilel 2014). If Per2 (137kDa) and Cry2 (67kDa) were to bind to the NPAS2-ARNTL complex (161kDa), the resulting complex would have a size of approximately 365kDa which is below the observed size range. The Biogrid database lists 26 physical interaction partners of human NPAS2 (Table 4-3) (accessed 20 July 2016).

The fact that oxidative stress activates the formation of these large complexes indicates a link between the MAP kinase pathways and NPAS2. Although no link has yet been reported, the MAP kinase p38, which is activated by oxidative stress, regulates the circadian clock in *Drosophila* (Dusik et al. 2014). More work is however required to investigate this interesting relationship in greater detail. It is also noteworthy that oxidative stress results in the appearance of post-translationally modified forms which may be phosphorylated forms of the more alkaline form of NPAS2 as revealed in the isoelectric focusing experiment (Figure 4-7). Taken together, it is possible that oxidative stress activates one of the three MAP kinase pathways (JNK, ERK1/2, p38), maybe the p38 pathway, which then results in the phosphorylation of NPAS2 and the formation of higher molecular weight complexes.

Table 4-3: Physical interaction partners of human NPAS2 as listed in the Biogrid data base.

(http://thebiogrid.org/110923/summary/homo-sapiens/npas2.html) accessed 20 July 2016.

Protein	Function
ARNTL	aryl hydrocarbon receptor nuclear translocator-like
RARA/NR1B1	retinoic acid receptor, alpha
RXRA/NR2B1	retinoid X receptor, alpha
ARNTL2	aryl hydrocarbon receptor nuclear translocator-like 2
RASSF7	Ras association (RalGDS/AF-6) domain family (N-terminal) member 7
SHMT2	serine hydroxymethyltransferase 2 (mitochondrial)
EFS	embryonal Fyn-associated substrate
CLOCK	clock circadian regulator
HGS	hepatocyte growth factor-regulated tyrosine kinase substrate
CSNK2B	casein kinase 2, beta polypeptide
CRY2	cryptochrome circadian clock 2
RORC	RAR-related orphan receptor C
DEC1	deleted in esophageal cancer 1
CRX	cone-rod homeobox
CRY1	cryptochrome circadian clock 1
RPL6	ribosomal protein L6
HSP90AA1	heat shock protein 90kDa alpha (cytosolic), class A member 1

{Investigation of the expression levels of the NPAS2 protein in human cell lines in response to oxidative stress, UV, heat stress and CPT.}

CREBBP	CREB binding protein
KAT2B	K (lysine) acetyltransferase 2B
NCOA3	nuclear receptor coactivator 3
HESX1	HESX homeobox 1
RHOXF1	Rhox homeobox family, member 1
EP300	E1A binding protein p300
TRAF4	TNF receptor-associated factor 4
ZSCAN1	zinc finger and SCAN domain containing 1
ARNT2	aryl-hydrocarbon receptor nuclear translocator 2

CHAPTER 5

INVESTIGATION INTO THE EXPRESSION LEVELS OF NPAS2 AND BMAL1 MRNAS IN HUMAN CELL LINES

Chapter 5: Investigation of the expression levels of *NPAS2* and *ARNT/Bmal1* mRNAs in human cell lines.

5.1 Introduction.

The hallmark of the circadian clock is the oscillating mRNA levels of *NPAS2* (*CLOCK*), *BMAL1* and the other clock proteins (Tei et al. 1997). Since down-regulation of NPAS2 was reported in the majority of colon cancer patients as being important to promote cell growth and migration (Xue et al. 2014) the *NPAS2* and *BMAL1* mRNA levels were analysed in normal tissues and cancer cell lines. A similar correlation between low *NPAS2* mRNA levels and poor prognosis extends to breast cancer (Yi et al. 2010).

Expression levels of NPAS2 and BMAL1 were analysed using qRT-PCR with the following primer sets from Qiagen: NPAS2 (amplicon length 91bp, QT00032480) and BMAL1 (amplicon length 91bp, QT00011844).

Although the precise sequence of the Qiagen primers in the RT-PCR kit is not disclosed, the position on the mRNA is given. Figure 5-1 shows the position of the 91bp amplicon in the four *NPAS2* cDNAs that encode the N-terminal splice variants and the full-length protein (*NPAS2-001, 004, 005, 007*). The amplicon covers the boundary between exons 3 and 4, which encodes a section of the first PAS domain that is present in all N-terminal NPAS2 variants, and the full-length protein. The *BMAL1* amplicon covers the boundary between exons 9 and 10 in the N-terminal part of the coding region.

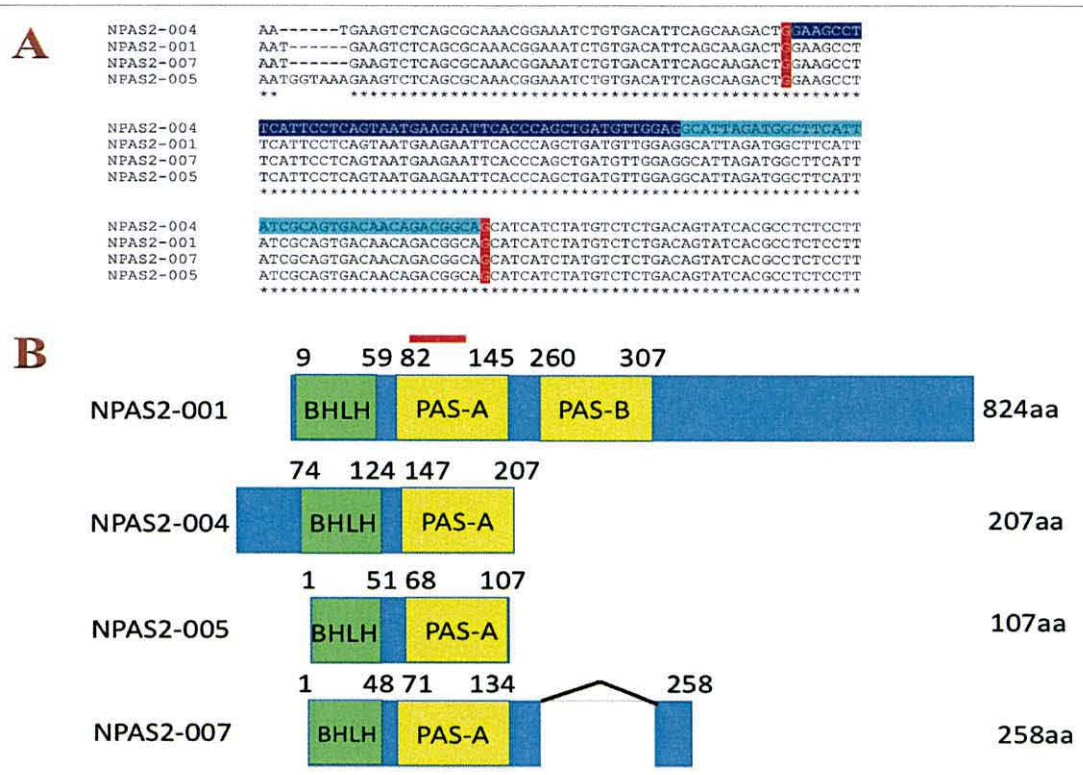

Figure 5-1: Location of the NPAS2 RT-PCR amplicon.

A: The primers amplify a section of 91 base pairs across the exon 3 – exon 4 boundary. The approximate location of the amplicon is between the two highlighted guanine bases. Exon 3 is shown in dark blue and exon 4 in light blue. The cDNA sequence of the full-length NPAS2 protein (NPAS2-001) and the three splice variants which encode the N-terminal NPAS2 proteins are aligned with Clustal Omega.

B: the amplicon locates to the PAS-A domain. The red bar indicates the exon 3-4 boundary at amino acid 91.

5.2 Results

5.2.1 *NPAS2* is expressed in normal human tissues.

To analyse *NPAS2* expression levels in normal human tissues, total RNA from 20 human tissues (Human Total RNA Master Panel II – Code: 636643) was purchased from Clontech. Reverse transcription coupled with PCR (RT-PCR) was performed using the *NPAS2* primers QT00032480, which amplify the full-length mRNA and three potential splice variants of *NPAS2* (Figure 5-1). Primers specific for *β-Actin* were used as an internal standard. As shown in (Figure 5-2), *NPAS2* expression was detected in all 20 tissues at comparable levels.

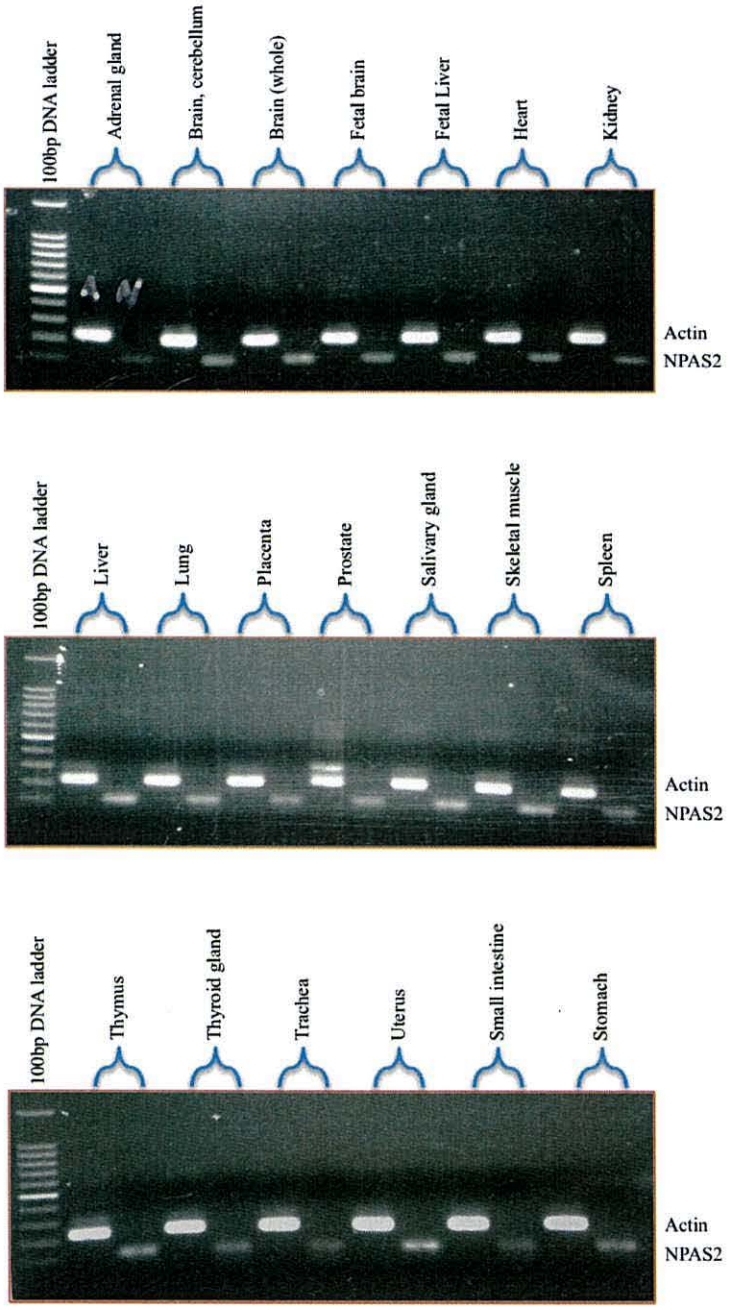

Figure 5-2: PCR screening of *NPAS2* gene expression in normal human tissues RNAs.

Twenty human tissues RNAs were tested for the expression of NPAS2 using the Qiagen RT-PCR primers QT00032480. The expected amplicon of 91bp was detected in all tissues at comparable levels. Primers specific for β-Actin were used as a positive control for the cDNAs quality. The size of the actin amplicon is (200bp) The experiment was performed three-times yielding very similar results.

5.2.2 Effect of carbon monoxide on the mRNA levels of NPAS2 and BMAL1 in HEK293.

To test whether an increase in carbon monoxide in the cells would have an impact on the mRNA levels of NPAS2 or BMAL1 (Figure 5-3), cells were incubated with Tricarbonyldichlororuthenium (II) dimer (CORM-2). This chemical releases carbon monoxide when added to cells (Megias, Busserolles & Alcaraz 2007). HEK-293 cells were treated with 300μM of this chemical for 3 hour and total RNA was isolated. Result has show significant down-regulation in BMAL expression (P value: 0.0128), and significant up-regulation in NPAS2 expression (P value: 0.0175).

The experiment was repeated and protein extracts were analysed. As shown in (Figure 5-4), the total amount of NPAS2 appeared to be decreased after the treatment with the carbon monoxide releasing chemical although no loading control is available for this experiment. While this result is preliminary, it would be in line with the reduction of NPAS2 protein levels in the response to heat stress in HeLa and MCF-7 cells.

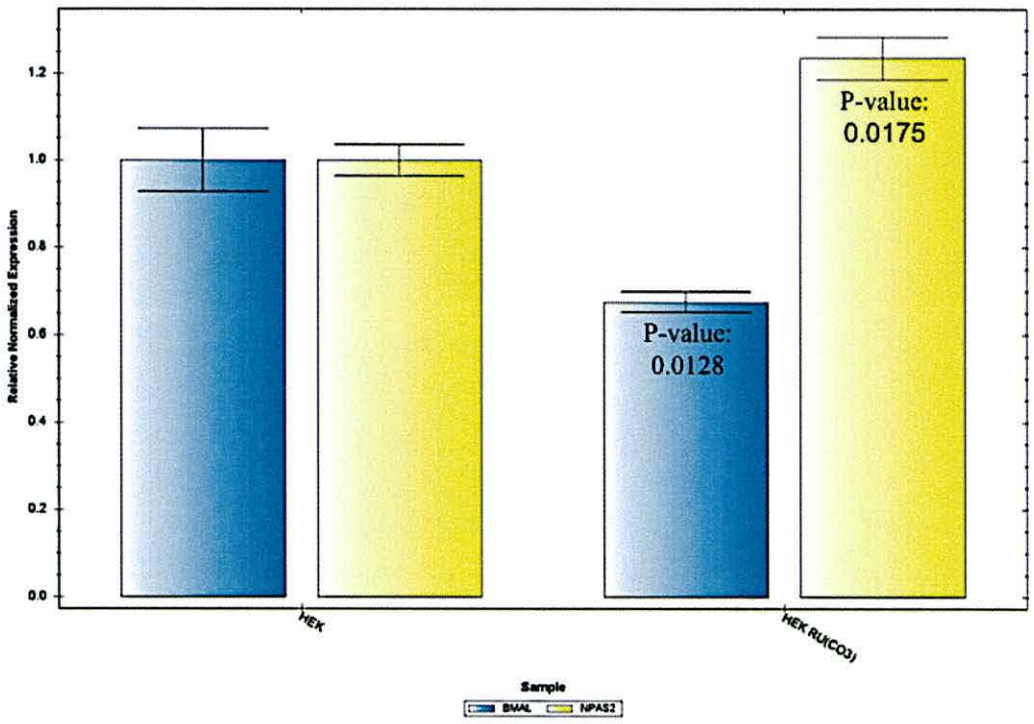

Figure 5-3: qRT-PCR analysis of *NPAS2* and *Bmal1* expression levels in HEK-293 treated with carbon monoxide-releasing Tricarbonyldichlororuthenium (II) dimer (CORM-2) $[RuCl_2(CO)_3]_2$.

Data was generated by SYBR® Green-based real time qRT-PCR is used to assess quantitatively the expression of a target gene. The bar chart displays the gene expression results for NPAS2, Bmal in treated HEK-293 cells with CORM-2; cells were incubated with 300μM of Tricarbonyldichlororuthenium (II) dimer for 3 hour. Compared to the HEK-293 cells (control) the treated sample has show significant down-regulation in BMAL expression (P value: 0.0128), and significant up-regulation in NPAS2 expression (P value: 0.0175). Expression data were normalised to the GAPDH and TUBULIN reference genes. The error bars represent the standard error of the mean (SEM) for three repeats.

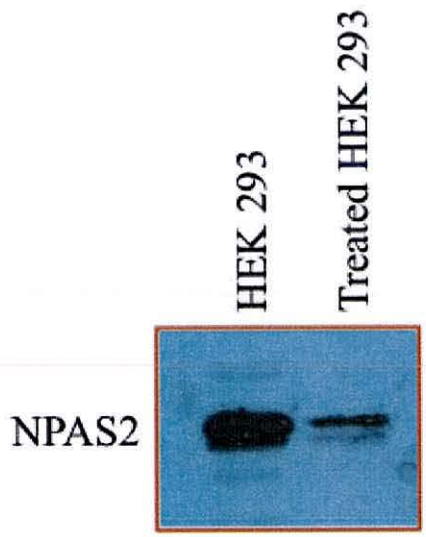

Figure 5-4: NPAS2 protein expression in HEK-293 treated with Tricarbonyldichlororuthenium (II) dimer (CORM-2) $[RuCl_2(CO)_3]_2$.

HEK-293 cells were incubated with 300μM of Tricarbonyldichlororuthenium (II) dimer (CORM-2) for 3 hour and total protein extracts were prepared.

5.2.3 Effect of different stress treatments on *NPAS2* and *BMAL1* RNA levels in HeLa and HEK-293 cells.

A similar experiment was performed with HeLa and HEK-293 cells that were treated with 40J/m^2 UV light or exposed to heat shock at 43°C for 1 hour. RNA was isolated 0.5 hour, 2 hours and 4 hours post-treatment. Cells were also grown in the presence of 500μM hydrogen peroxide (H_2O_2) for 0.5 hour and 4 hours prior to RNA extraction. HEK-293 cells were also exposed to 1μM CPT for 30 minutes, 2 hours and 4 hours. There were three interesting observations in HEK-293 cells. First, CPT treatment which breaks DNA in S phase upon inhibition of topoisomerase 1 resulted significant down-regulation in NPAS2 expression (P value: 0.0001), and significant down-regulation in BMAL expression (P value: 0.0014) but only after prolonged exposure for 4 hours (Figure 5-5). Second, both mRNA pools significant increased after 30 minutes UV treatment (NPAS2 P-value: 0.0001, BMAL P-value: 0.0002). on other hand NPAS2 has significant declined after 4 hours post-UV irradiation (P-value: 0.0004). Finally, only *NPAS2* mRNA levels significant declined after the heat shock treatment (P-value: <.0001) while *BMAL1* levels significant increased (0 hour P-value: 0.0214, 30min P-value: 0.0087, 4 hour: 0.0173) (Figure 5-5).

As shown in (Figure 5-6), neither UV nor heat had a similar impact on NPAS2 and BMAL1 mRNA levels as observed in HEK-293 cells. Exposures of HeLa cells to oxidative stress significant increased in both mRNA levels of NPAS2 (30 min P-value: 0.0002, 4 hour P-value: 0.0003) and BMAL1 (30 min P-value: 0.0001, 4 hour P-value: 0.0025). This is interesting since NPAS2 undergoes significant post-translational changes in the response to oxidative damage. As shown in (Figure 4-7, Figure 4-8), NPAS2 is modified when exposed to hydrogen peroxide for 24 hours as evident in the isoelectric focusing experiment and NPAS2 appears to form larger molecular weight complexes as shown by size exclusion chromatography.

Given that the protein levels of NPAS2 decline after a heat shock in HeLa cells (Figure 4-3) but its mRNA levels do not significantly change, it possible that heat triggers the degradation of NPAS2 in this cell line. Although the protein levels remained unchanged in HEK-293 cells (Figure 4-3), the mRNA levels of NPAS2 specifically declines in this cell line (Figure 5-5). This implies that heat stress has a negative impact on NPAS2 in a cell line specific manner.

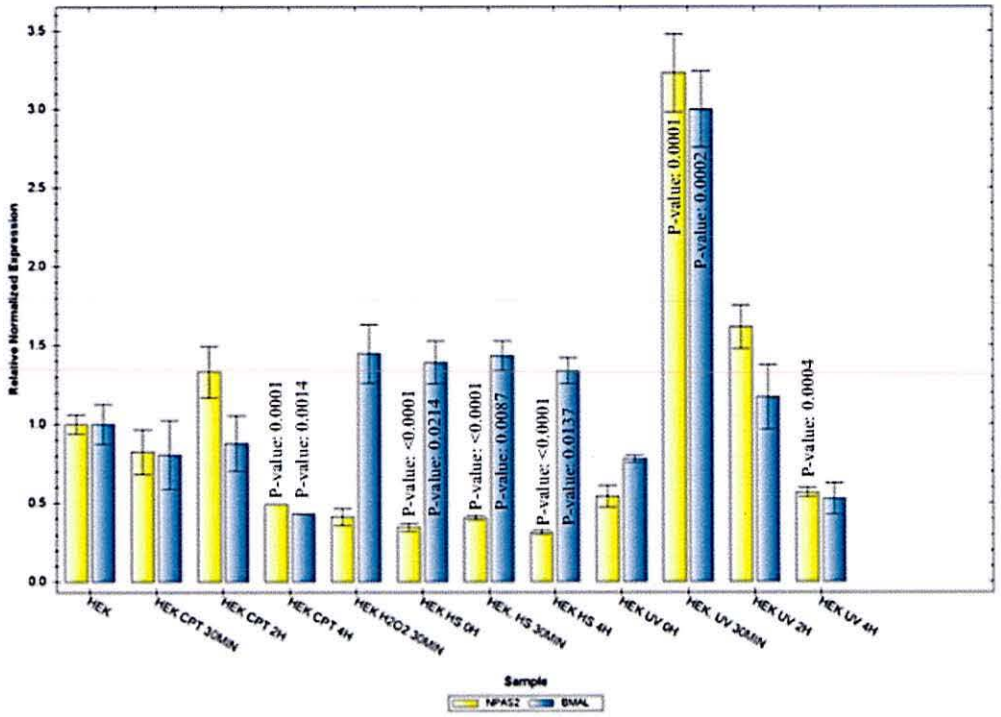

Figure 5-5: qRT-PCR analysis of *NPAS2* and *Bmal1* expression in DNA Damage Responses of HEK-293 cells.

Data was generated by SYBR® Green-based real time qRT-PCR is used to assess quantitatively the expression of a target gene. The gene expression results for *NPAS2* and *Bmal1* in HEK-293 cells treated with 1μM CPT for (30 minutes, 2 hours, 4 hours), 500μM H_2O_2 for (30 minutes), Heat stress 43°C for (oh, 30 minutes, 4 hours), or 40 J/m^2 UV for (oh, 30 minutes, 2 hours, 4 hours) light or left untreated are shown. Expression data were normalised to the GAPDH and TUBULIN reference genes. The error bars represent the standard error of the mean (SEM) for three repeat experiments. The expression levels of *NPAS2* and *BMAL1* in untreated cells were set to 1 (base line).

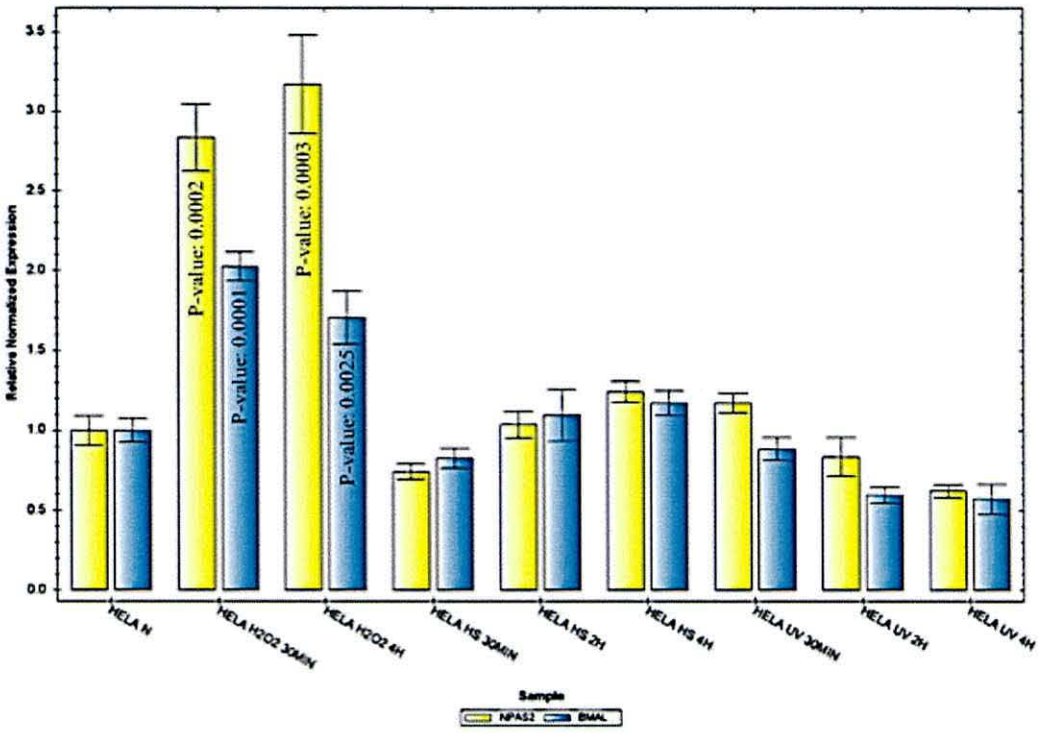

Figure 5-6: qRT-PCR analysis of *NPAS2* and *Bmal1* expression in stressed HeLa cells.

Data was generated by SYBR® Green-based real time qRT-PCR is used to assess quantitatively the expression of a target gene. The gene expression results for *NPAS2* and *Bmal1* in HeLa cells treated with 500μM H_2O_2 for (30 minutes, 4 hours), Heat stress 43°C for (30 minutes, 2 hours, 4 hours), or 40 J/m^2 UV for (30 minutes, 2 hours, 4 hours) light or left untreated are shown. Expression data were normalised to the GAPDH and TUBULIN reference genes. The error bars represent the standard error of the mean (SEM) for three repeat experiments. The expression levels of *NPAS2* and *BMAL1* in untreated cells were set to 1 (base line).

5.2.4 Effects of stress on *NPAS2* and *BMAL1* RNA levels in MCF-7 cells.

RNA was isolated from MCF-7 for 0 hour, 0.5 hour, 1 hour and 4 hours after having exposed the cells to 40J/m^2 of UV light or to a heat shock at 43°C for 1 hour hours. MCF-7 cells were also grown in the presence of 1μM CPT for 0.5 hour, 2 hours and 4 hours, and in the presence of 500μM hydrogen peroxide for 2 hours. Unlike in the other cell lines, all treatment decreased the mRNA levels of *NPAS2* and *BMAL1* to different degrees (Figure 5-7). Although heat caused a general reduction in the NPAS2 mRNA levels (0 hour P-value: 0.0001, 30 min P-value: 0.0002, 1 hour P-value: 0.0011, 2 hour P-value: 0.0002, 4 hour P-value: 0.0002), it unlikely that the 2-fold decline accounts for the down-regulation of the protein in MCF-7 cells (Figure 4-3). Again it may be more likely that NPAS2 is degraded in the response to elevated temperatures in this cell line.

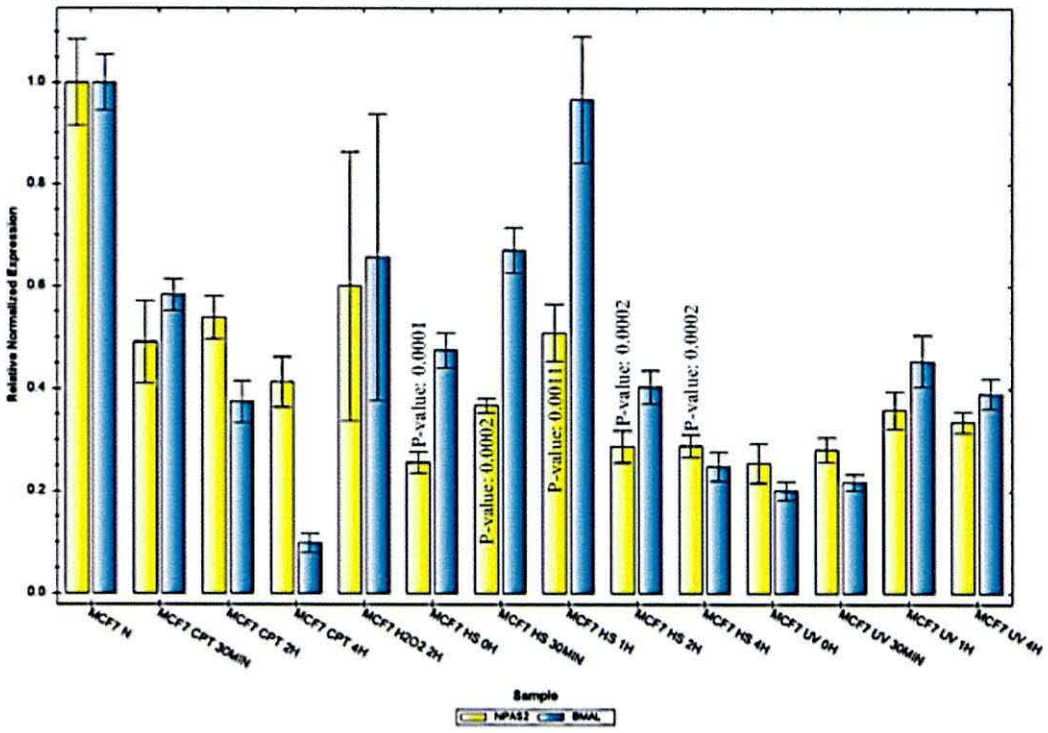

Figure 5-7: qRT-PCR analysis of NPAS2 and Bmal1 expression in stressed MCF-7 cells.

Data was generated by SYBR® Green-based real time qRT-PCR is used to assess quantitatively the expression of a target gene. The gene expression results for *NPAS2* and *Bmal1* in MCF-7 cells treated with 1μM CPT for (30 minutes, 2 hours, 4 hours), 500μM H_2O_2 for (2 hours), Heat stress 43°C for (0 hour, 30 minutes, 1 hour, 2 hours, 4 hours), or 40J/m^2 UV for (0 hour, 30 minutes, 1 hour, 4 hours) light or left untreated are shown. Expression data were normalised to the GAPDH and TUBULIN reference genes. The error bars represent the standard error of the mean (SEM) for three repeat experiments. The expression levels of *NPAS2* and *BMAL1* in untreated cells were set to 1 (base line).

5.2.5 Comparison of the basal expression level of NPAS2 and BMAl1 in untreated HEK-293, HeLa and MCF-7 cells.

Since the protein levels of NPAS2 are different in untreated HEK-293, HeLa and MCF-7 cells (Figure 5-8), the basal mRNA levels of *NPAS2* and *BMAL1* were compared in untreated cells. The levels of HELA mRNA pool (P-value: 0.0006) was increase more than in HEK-293 cells, but not in MCF-7 cells which had a 2-fold increase in *NPAS2* (P-value: <0.0001) mRNA levels compared to *BMAL1* (P-value: <0.0001) (Figure 5-8). MCF-7 are breast carcinoma cells and a down-regulation of BMAL1 due to hyper-methylation in its promotor was reported in a study in which 37 of the 53 breast cancer tissues were positive for the promotor methylation (Kuo et al. 2009) showed hypermethylation on the promoters of *PER1, PER2, CRY1,* or *BMAL1*. This implies that the unbalanced expression of BMAL1 and NPAS2 could contribute to the development of this cancer type.

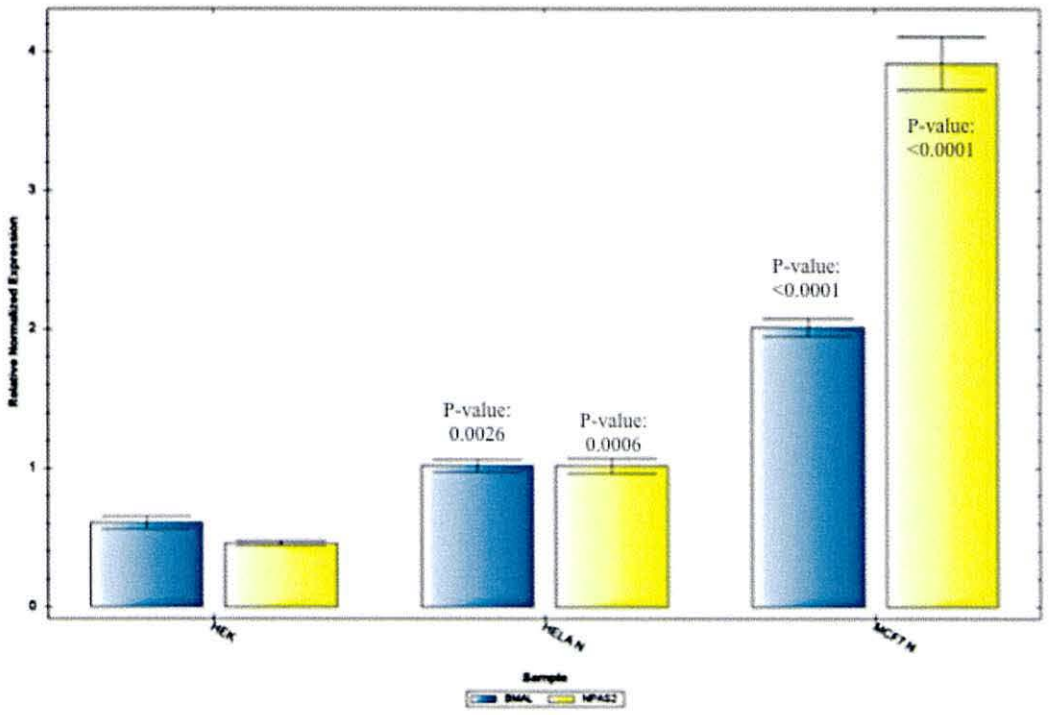

Figure 5-8: Comparison of the basal expression levels of *NPAS2* and *Bmal1* in untreated HEK-293, HeLa and MCF-7 cells.

Data was generated by SYBR® Green-based real time qRT-PCR is used to assess quantitatively the expression of a target gene. The basal expression results from the different q-RT-PCR experiments were compared. The values for the untreated samples are shown. Expression data were normalised to the GAPDH and TUBULIN reference genes. The error bars represent the standard error of the mean (SEM) for three repeats.

5.2.6 Neuroblastoma (KELLY) cells express very low amounts of *NPAS2* mRNA

KELLY cells derived from a human neuroblastoma and are characterized by over-expression of the c-myc oncogene (Shwab, Alitalo & Klemphauer 1983). Since NPAS2 is expressed in the mammalian fore brain (Garcia et al. 2000), mRNA levels of *NPAS2*, *BMAL1*, *CLOCK* and *GAPDH* were analyzed in total RNA samples obtained from untreated KELLY cells. As shown in Figure 5-9, mRNA levels are very low for NPAS2 but not for CLOCK, suggesting that the neuroblastoma developed from a brain region with low NPAS2 levels. The experiment was repeated with total RNA from HeLa cells, KELLY cells and from the brain tissue sample from the human tissue panel. Again, *NPAS2* expression levels were very low

in KELLY cells (Figure 5-10).

To test whether BMAL1 mRNA levels respond to UV treatment, KELLY cells were irradiated with a dose of 40J/m^2 and total RNA was isolated after 0.5 hour, 2 hours and 4 hours. UV induced DNA damage reduced BMAL1 mRNA levels in a time dependent manner down to 50% after 4 hours (P-value: <0.0001) (Figure 5-11).

In summary, these findings show that NPAS2 is not highly expressed in this cell line and that the CLOCK-BMAL1 complex is the dominant circadian transcription system in this neuroblastoma cell line.

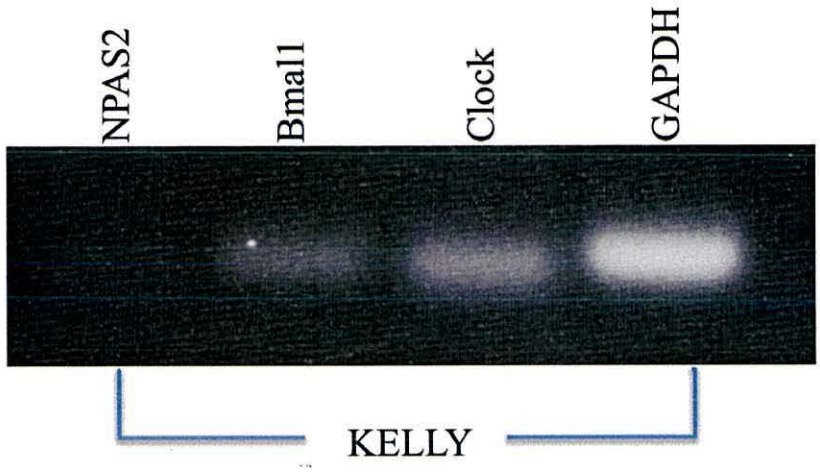

Figure 5-9: RT-PCR analysis of *NPAS2*, *Bmal1*, *and CLOCK* in KELLY neuroblastoma cells.

Agarose gels showing the expression of *NPAS2*, *Bmal1* and *CLOCK* in KELLY cell line. GAPDH used as a reference (positive control).

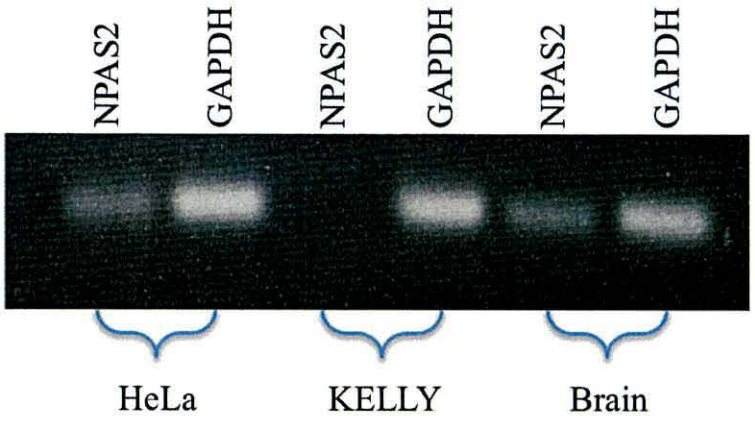

Figure 5-10: PCR analysis of NPAS2 expression in HeLa, KELLY and Brain RNAs.

Agarose gels showing the expression of *NPAS2* in HeLa, KELLY, Brain RNAs. GAPDH used as a reference (positive control).

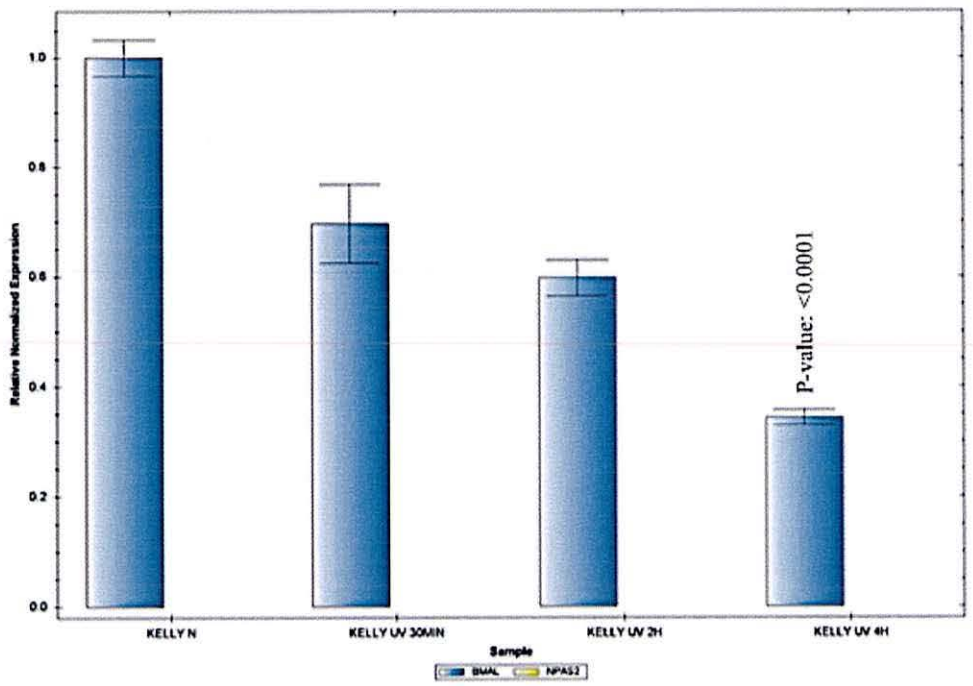

Figure 5-11: qRT-PCR analysis of NPAS2, Bmal expression in DNA Damage Responses of KELLY cells.

Data was generated by SYBR® Green-based real time qRT-PCR used to assess quantitatively the expression of a target gene. The bar chart displays the gene expression results for NPAS2, Bmal in treated KELLY cells with UV; compared to the KELLY cells (control). Expression data were normalised to the GAPDH and TUBULIN reference genes. The error bars represent the standard error of the mean (SEM) for three repeats.

5.2.7 Expression of *NPAS2* and *BMAL1* in G1 synchronized cells.

5.2.7.1 Serum Starvation (G1 cell cycle block).

The circadian clock and the cell cycle are two key systems that coordinate cell growth. Recent work revealed that over-expression of the oncogene c-Myc down-regulates the circadian rhythm by reducing expression of *NPAS2*, *BMAL1/ARNTL* and *CLOCK* (Shostak et al. 2016). To test whether NPAS2 expression is cell cycle dependent, serum starvation of cell cultures was used to halt the cell cycle in G1 (Shin et al. 2008). To find out whether *NPAS2* mRNA and protein levels are cell cycle regulated, HeLa and MCF-7 cell lines were grown in 10cm plates until they reached ~70% confluency within 2 days. The culture medium was then removed and the cells were washed with 10ml PBS and the standard cell culture medium was replaced with DMEM medium without fetal bovine serum or antibiotics. Cells were cultured at 37°C for another 24 hour period to arrest cells in G1. Cells were than released from the G1 block by the addition of complete medium with serum and samples were harvested at 0 hour, 6 hours and 12h. Cell cycle progression was analysed by Flow Cytometery.

As shown in (Figure 5-12), both HeLa and MCF-7 cells have already a large population of cells in G1 even when they grow in complete medium. The shoulders to the right of the high G1 peak are S phase and G2 cells. The large amount of G1 cells has been reported previously for MCF-7 and HeLa cells (Mao et al. 2012). In the case of the MCF-7 cell line, serum starvation increased the amplitude of the G1 peak from 250 counts in complete medium to around 400 counts and decreased the number of S phase and G2 cells. Since this pattern did not change 6 hours and 12h post-starvation, MCF-7 cells may not have re-entered the cell cycle from the G1 arrest. In the case of the HeLa cells, the starvation experiment may not have worked well as the number of S phase and G2 cells did not decrease (Figure 5-12).

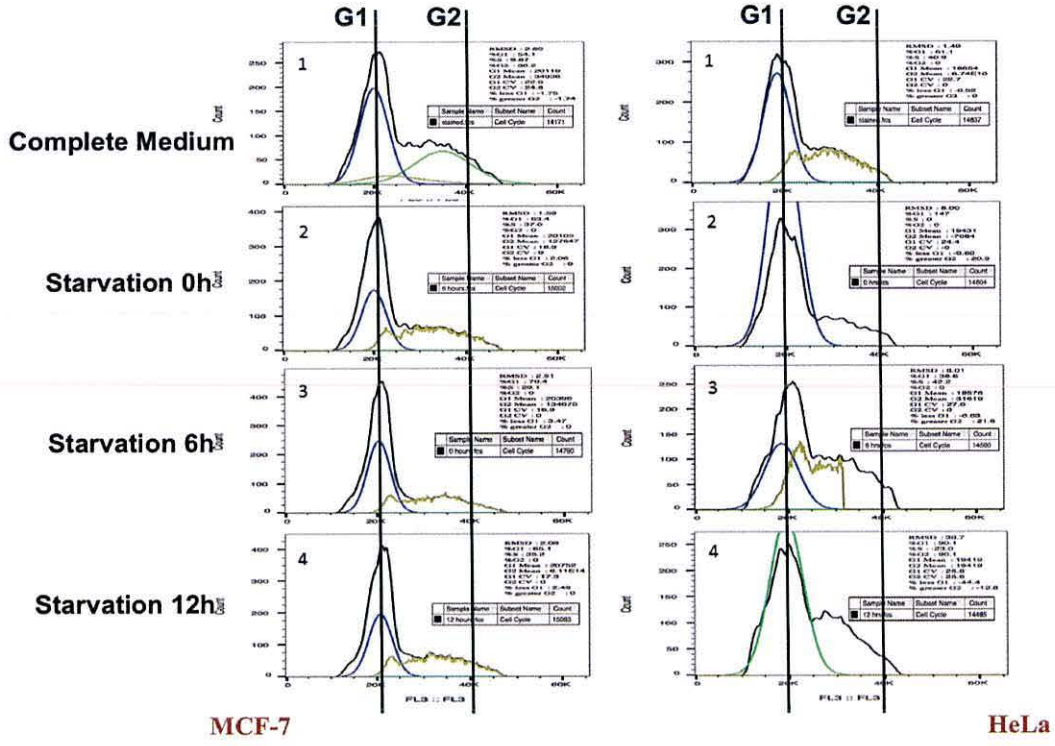

Figure 5-12: Serum starvation of MCF-7 and HeLa cells.

Cells were grown to ~70% confluency and the complete medium were replaced with medium lacking fetal bovine serum for 24 hours. This serum starvation increases the number of cells in the G1/G0 phase of the cell cycle. After the 24 hours starvation period, medium with serum was added again (release 0 hour) and samples were taken after 6 hours and 12h post-starvation. The DNA content of each sample was measured using flow cytometery. The black line shows the DNA content. The position of G1 and G2 cells are indicated. Cells between the two lines are in S phase.

Interestingly, serum withdrawal triggered a clear decline in the mRNA levels of *NPAS2* and *BMAL1* in both experiments. In HeLa cells the levels of *NPAS2* dropped to a higher degree (0 hour P-value: <0.0001, 6 hour and 12 hour P-value: 0.0001) when compared to *BMAL1* mRNA levels (6 hour and 12 hour P-value: 0.0008) (Figure 5-13). In MCF-7 cells the drop was more balanced (Figure 5-14). Since this decrease in mRNA levels was observed in both experiments in which the G1 arrest may have worked only to a certain degree, it is more likely that this decline is linked with the activation of the MAP kinase pathway under starvation conditions rather than a G1 arrest.

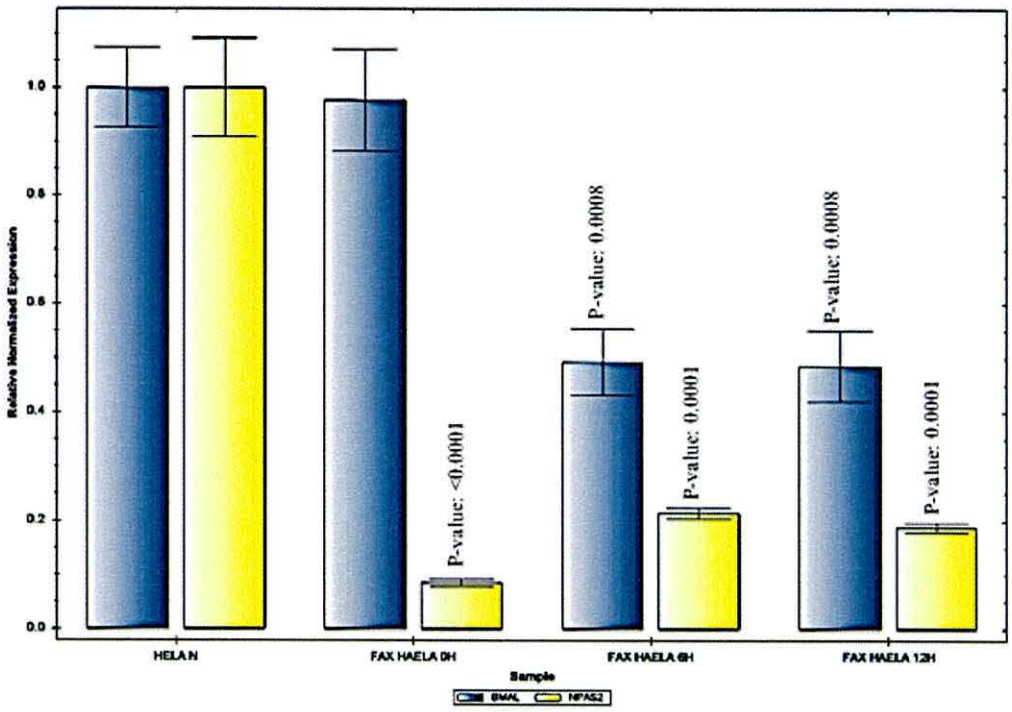

Figure 5-13: qRT-PCR analysis of *NPAS2* and *Bmal1* expression in HeLa cells after synchronized by serum starvation.

Data was generated by SYBR® Green-based real time qRT-PCR to assess quantitatively the expression of a target gene. The bar chart displays the gene expression results for NPAS2, Bmal in HeLa cells were synchronized by serum withdrawal at the G0-G1 transition point; compared to the HeLa cells (control). Expression data were normalised to the GAPDH and TUBULIN reference genes. The error bars represent the standard error of the mean (SEM) for three repeats.

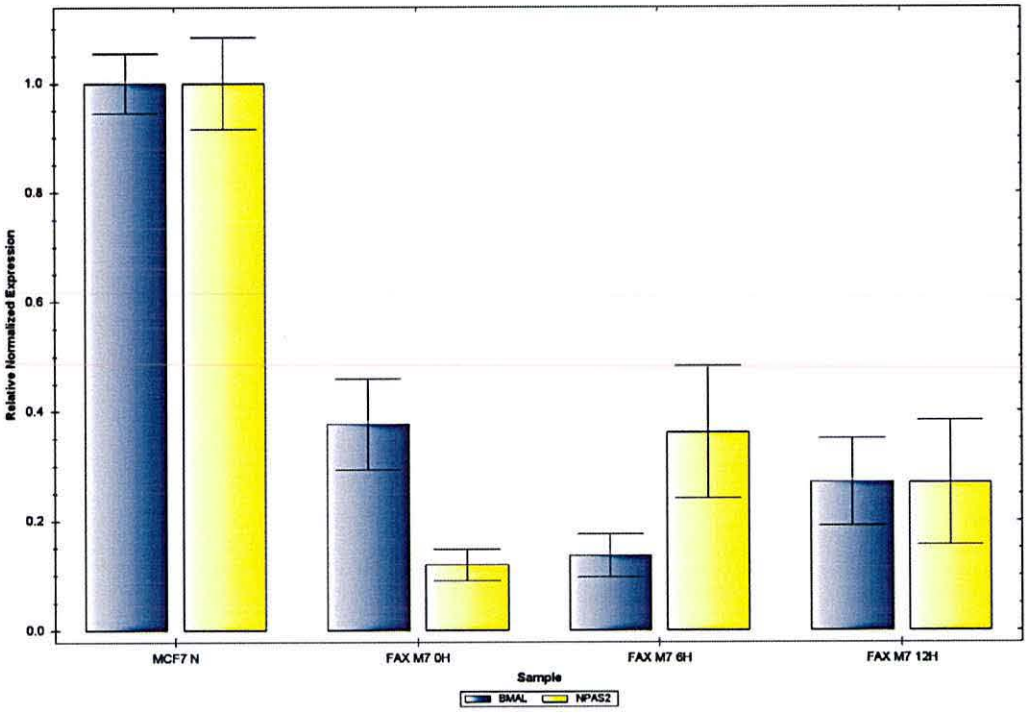

Figure 5-14: qRT-PCR analysis of *NPAS2* and *Bmal1* expression in MCF-7 cells after synchronized by serum starvation.

Data was generated by SYBR® Green-based real time qRT-PCR to assess quantitatively the expression of a target gene. The bar chart displays the gene expression results for NPAS2, Bmal in MCF-7 cells were synchronized by serum withdrawal at the G0-G1 transition point; compared to the MCF-7 cells (control). Expression data were normalised to the GAPDH and TUBULIN reference genes. The error bars represent the standard error of the mean (SEM) for three repeats.

5.3 Discussion

The key findings of this chapter are **(1)** the down-regulation of NPAS2 mRNA levels against an increase in BMAL1 mRNA levels in the response to heat stress in HEK-293 cells, **(2)** the three-fold increase in *NPAS2* mRNA levels in the response to oxidative stress in HeLa cells, **(3)** the very low *NPAS2* expression levels in KELLY neuroblastoma cells and **(4)** a decrease in *NPAS2* and *BMAL1* mRNA levels in the response to serum starvation. It should be taken into account that the primers used to quantify *NPAS2* mRNA levels amplify the four N-terminal splice variants of *NPAS2*. Hence any biological consequences of the observed changes could affect either of the 4 forms of the NPAS2 protein.

Table 5-1: Summary of the changes in mRNA levels of NPAS2 and BMAL1 in the response to different types of stress

Treatment	NPAS2 mRNA levels	BMAL1 mRNA levels
Heat	*NPAS2* ↓	*BMAL1* ↑
Oxidative Stress	*NPAS2* ↑	*BMAL1* ↑
Serum Starvation	*NPAS2* ↓	*BMAL1* ↓

5.3.1 Down-regulation of *NPAS2* mRNA levels in the response to heat stress.

As shown in Figure 5-5, *NPAS2* mRNA levels decline after the exposure of cells to 43°C for 1 hour despite an increase in *BMAL1* mRNA levels. This implies a shift from an NPAS2-BMAL1 hetero-dimer to a BMAL1-BMAL1 homodimer. While heat stress did not reduce the protein amounts of NPAS2 in HEK-293 cells, it did so in HeLa and MCF-7 cells (Chapter 4). Since a similar shift from the active hetero-dimers to inactive BMAL1 homo-dimers occurs in the response to the binding of carbon monoxide to the heme groups at the PAS domains of NPAS2 (Dioum et al. 2002) it is possible that heat stress results in an increase in this gas. Indeed, heat induces the expression of the human heat shock protein 32 (Hsp32) which is a heme oxygenase-1 (HO-1). Upon its induction, the enzyme produces carbon monoxide to protect cells against apoptosis (Liu et al. 2003, Al-Owais et al. 2012). It is therefore a possibility that heat stress regulates NPAS2 indirectly by increasing the cellular levels of carbon monoxide. It seems that heat-stressed cells need to down-regulate NPAS2 to increase their survival

changes. Treating HEK-293 cells with the carbon monoxide releasing chemical Tricarbonyldichlororuthenium (II) dimer did however not change the mRNA levels to the same extend as heat stress (Figure 5-3) which argues against the idea that carbon monoxide is the main effector of heat stress on the mRNA levels of *NPAS2*.

5.3.2 Up-regulation of *NPAS2* mRNA levels in the response to oxidative stress.

Oxidative stress increased *NPAS2* mRNA levels by three-fold (Figure 5-6) in HeLa cells. Although the overall protein levels do not change in this cell line in the presence of hydrogen peroxide (Figure 4-2), NPAS2 becomes post-translationally modified as shown by the appearance of additional forms in the isoelectric focusing experiment (Figure 4-7) and forms larger molecular weight complexes as seen in the size exclusion experiment (Figure 4-8). Taken together, these findings imply a novel role of NPAS2 in the response to oxidative stress. This idea is in line with the requirement of BMAL1/ARNTL to increase survival of mouse fibroblasts in the presence of hydrogen peroxide (Khapre et al. 2011). Similar observations extend to *Drosophila* where the response to oxidative stress is regulated by the circadian clock (Krishnan, Davis & Giebultowicz 2008) and the MAP kinase p38, which is activated by oxidative stress, acts as a circadian protein (Dusik et al. 2014).

5.3.3 Down-regulation of NPAS2 after serum starvation.

Removal of serum induces a starvation response which is dependent on the MAP kinase ERK1/2 and the AKT kinase in HEK-293 cells (Pirkmajer, Chibalin 2011). It was also shown that members of the p38 MAP kinase family are involved in starvation responses in human cells (Wei et al. 2015). Given that three types of stress (heat, oxidative and starvation) which activate the MAP kinase pathways affect the levels of NPAS2 as well as the post-translational modifications of the protein (oxidative stress) and its protein levels (heat stress), it is likely that there is a close link between the MAP kinase pathways and NPAS2 which has not yet been reported. The responses are stress-dependent and cell line-specific. While heat stress and starvation results in a decline in *NPAS2* mRNA levels, oxidative stress increases the levels (**Table 5-1**). This is very interesting since feeding and fasting cycles are the primary time trigger for clocks in peripheral tissues (Potter et al. 2016). Hence, the down-regulation of *NPAS2* may synchronise the peripheral clocks under starvation conditions.

CHAPTER 6

AN ANALYSIS OF MISSENSE SINGLE NUCLEOTIDE POLYMORPHISMS (SNP) IN NPAS2

Chapter 6: An analysis of missense Single Nucleotide Polymorphisms (SNPs) in NPAS2.

6.1 Introduction.

Some studies have suggested that night workers may suffer from a slightly increased risk of breast cancer. A study analyzing breast cancer frequencies in nurses found a positive correlation between an increase in the disorder and single nucleotide polymorphisms (SNPs) in the circadian genes *AANAT* (rs3760138, rs4238989), *BMAL1* (rs2290035, rs2278749, rs969485) and *ROR-b* (rs3750420), whereas a decreased risk was associated with SNPs in the genes *CLOCK* (rs3749474), *BMAL1* (rs2278749), *BMAL2* (rs2306074), *CSNK1E* (rs5757037), *NPAS2* (rs17024926, intron variant mutation), *ROR-b* (rs3903529, rs3750420), MTNR1A (rs131113549) and PER3 (rs1012477) (Zienolddiny et al. 2013). The *AANAT* gene encodes the enzyme aralkylamine N-acetyltransferase which is involved in the circadian production of melatonin (Coon et al. 2001). The *ROR-b* encodes one of the retinoic acid-related orphan receptors which may bind melatonin, and the *MTNR1A* gene produces the high affinity melatonin receptor (Slominski et al. 2012). While these findings are in line with the finding that shift work may cause cancer by interfering with the circadian hormone melatonin (Stevens 2005) they also show that the impact may dependent on the type of SNP in any of these genes.

To investigate the possible impact of SNPs on the biological functions of NPAS2, the missense mutations listed in the Ensembl database for the human *NPAS2* gene were analysed in this chapter. The analysis focuses on the N-terminal section of NPAS2 encompassing the BHLH domain and the two PAS domains (serine-17 to glutamate-359), as a structural model is available for this part of NPAS2. The model was generated using the SwissModel tool (https://swissmodel.expasy.org/) and the template 4f3l.1 which is the crystal structure of the N-terminal section of the mouse heterodimeric CLOCK-BMAL1 transcription complex (Huang et al. 2012).

6.2 Missense mutations in the Basic-Helix-Loop-Helix Domain of human NPAS2.

The Ensembl data base lists currently 251 missense mutations for the human NPAS2 gene (accessed 08 July 2016) (Appendix 2) of which 66 SNPs fall within amino acids 17 and 359 and of which 49 are classified as damaging or possibly damaging and 17 as benign. This analysis focuses on the missense SNPs which are classified as damaging or possibly damaging affecting an N-terminal amino acid between S17 and E359.

The first 11 N-terminal SNPs are within the Basic-Helix-Loop-Helix (BHLH) DNA binding domain of NPAS2 (Figure 6-1).

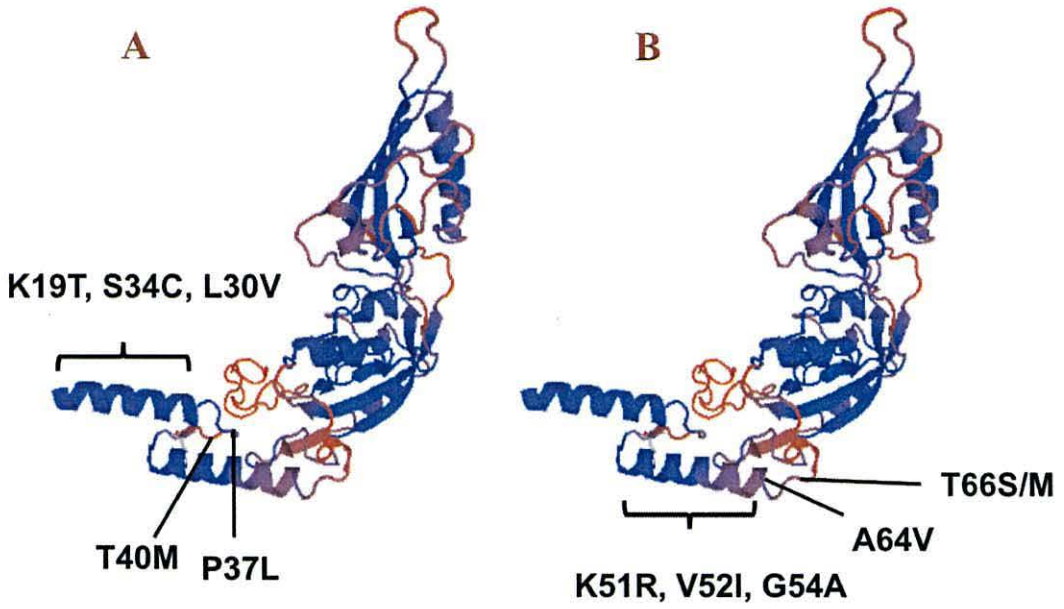

Figure 6-1: Model of the N-terminal domain of human NPAS2 with the missense SNPs in the Basic-Helix-Loop-Helix (BHLH) DNA binding domain.

A: first N-terminal alpha-helix, possibly involved in DNA binding.

B: second alpha-helix, possibly involved in dimerization. All SNPs are listed in **Table 6-1**.

Table 6-1: Missense SNPs affecting the Basic-Helix-Loop-Helix (BHLH) DNA binding domain of human NPAS2.

SNP ID Number	Amino Acid Change
rs752546267	K19T
rs140186927	S34C
rs746714721	L36V
rs200029671	P37L
rs749697021	T40M
rs772478314	K51R
rs773279753	V52I
rs138995271	G54A
rs183671025	A64V
rs770032871	T66S
rs775528411	T66M

Transcription factors which contain a BHLH domain form dimers through one of the two alpha helices in the domain while the second, more positively charged alpha helix, binds to the E box motif (CANNTG) in the DNA (Chaudhary, Skinner 1999). Given that the first helix of the BHLH domain of NPAS2 contains more positively charged lysine (K) and arginine (R) residues (17-SEKKRRDQFNVLIKELS-33), it may be this helix which binds to the DNA. The only SNPs in the first helix affect lysine 19 (rs752546267 (K19T)) which could interfere with DNA binding of the NPAS2-BMAL1 complex. Replacement of leucine 57 by a negatively charged glutamate in CLOCK, which corresponds to leucine 32 in NPAS2, was shown to strongly reduce binding to the E box motive in a reporter assay (Huang et al. 2012).

Interestingly, the other N-terminal SNPs are in the loop connecting the two helices (serine-34 (rs140186927 (S34C)), leucine 36 (rs746714721 (L36V)) and proline 37 (rs200029671) (Figure 6-1-A). Using the NetPhos 2.0 Server (accessed 08 July 2016), the phosphorylation probability of S34 (rs140186927), T40 (rs749697021) and T66 (rs770032871, rs775528411) were analysed, but none of these potential phosphorylation sites returned a high phosphorylation probability.

6.3 Missense mutations in the two PAS Domains of human NPAS2.

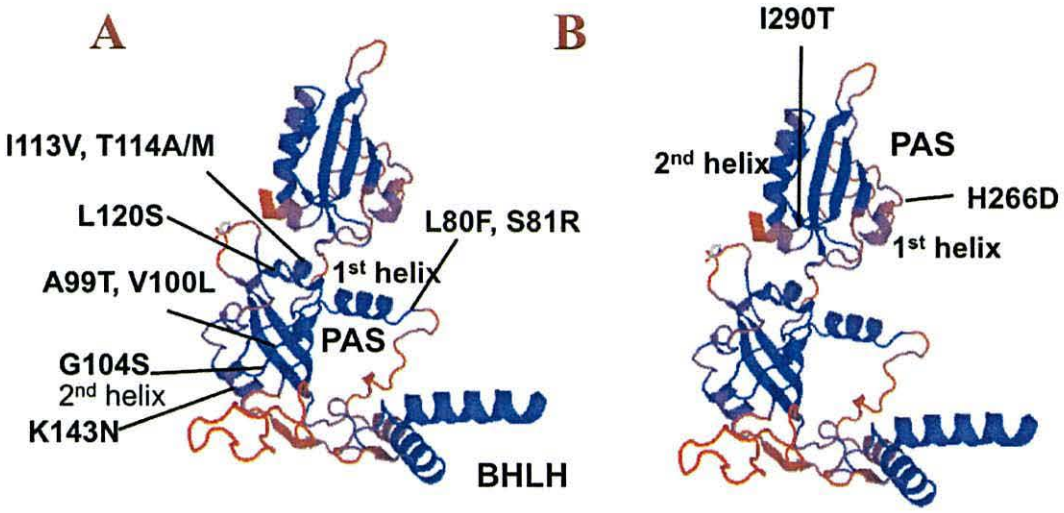

Figure 6-2: Missense SNPs in the PAS domains of human NPAS2.

A: first PAS domain (82-145aa). The mutations affect the loop leading into the first alpha helix, the loop leading down to the second alpha helix and the second alpha helix.

B: second PAS domain (260-307aa). The two SNPs affect a loop next to the first helix and the loop running behind the two beta sheets leading into the second helix. All SNPs are listed in **Table 6-2**.

Table 6-2: Missense SNPs affecting the PAS domains of human NPAS2.

SNP ID Number	Amino Acid Change	SNP ID Number	Amino Acid Change
rs750128945	L80F	rs373612998	I113V
rs779574673	S81R	rs756405653	T114A
rs753351516	A99T	rs780487648	T114M
rs754514291	V100L	rs774317309	L120S
rs757600072	G104S	rs766883992	K143N
rs779356852	H266D	rs541173118	I290T

There is 10 SNPs which affect the first PAS domain in NPAS2 which is involved in dimerization. They affect the two alpha helical sections and the connecting loop which adopts as well some alpha helical conformation. They do not affect the two beta sheets which are behind the helical section (Figure 6-2). The two beta sheets lead up to the second PAS domain. Interestingly serine-81 (rs779574673) which is replaced by a positively charged arginine residue has a high phosphorylation probability of 97.3% according to NetPhos 2 (accessed 08 July 2016). This implies a possible role in post-translational modification of NPAS2 which may regulate its binding to other PAS domain proteins like BMAL1. Interestingly, deletion of the PAS domain in BMAL1 did not abolish dimerization with CLOCK (NPAS2), but stopped the transcriptional activity of the CLOCK-BMAL1 complex (Dardente et al. 2007). In contrast to the first PAS domain, only two SNPs (I290T, rs541173118 & H266D rs779356852) affect the second PAS domain. This could indicate that the second PAS domain is more important as a lower number of changes can be tolerated or that the changes in the first PAS domain can lead to beneficial changes.

6.4 Missense mutations in the Loop R195-E223 opposite the BHLH domain of human NPAS2.

The model of human NPAS2 shows a large loop (arginine-195 to glutamate-233) which is located opposite the BHLH domain (Figure 6-3). There are 6 missense SNPs in this region (**Table 6-3**) of which 3 (S204P, C205R, G207A) cluster in one short are of this loop. When human CLOCK is used as a template for the SwissModel tool (UniProt ID: O15516), the software produces as expected a very similar model with one important difference, the loop opposite the BHLH domain (lysine-220 to cystein-250) which is slightly shorter in CLOCK compared to NPAS2 (Appendix 3). This indicates a high degree of plasticity of the loop which may be involved in protein-protein interactions or post-translational modifications.

Table 6-3: Missense SNPs affecting the loop R195-E223 opposite the BHLH domain of human NPAS2.

SNP ID Number	Amino Acid Change
rs763172499	R195C
rs572470679	R195H
rs750277651	S204P
rs756091688	C205R
rs766211274	G207A
rs746290665	L220V

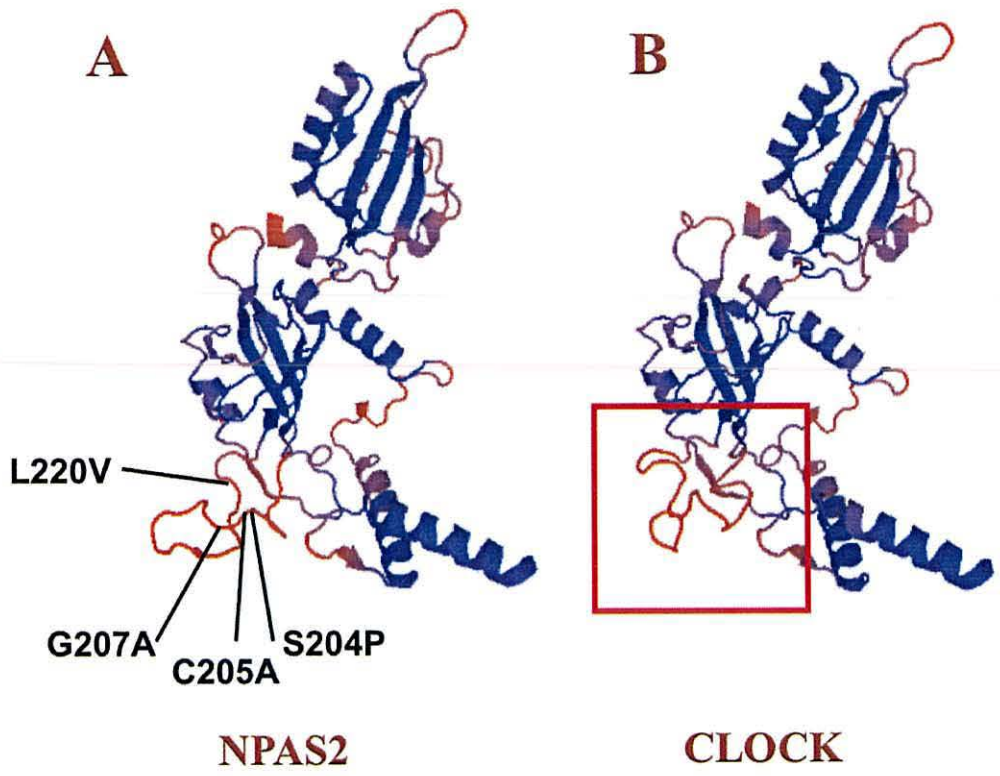

Figure 6-3: Missense SNPs affecting the loop R195-E223 opposite the BHLH domain of human NPAS2.

A: Model of human NPAS2 with the location of the SNPs indicated.

B: Model of human CLOCK (based on the mouse CLOCK protein structure 4f3l.1.B). The loop which differs from NPAS2 is highlighted. All SNPs are listed in **Table 6-3**.

To test the idea of high plasticity of this loop region, the NPAS2 protein was modeled with a proline at position 204 instead of the serine residue (rs750277651). This was done by using the NPAS2-001 protein sequence with the amino acid exchange at position 204 as a template for SwissModel (accessed 09 July 2016). As shown in (Figure 6-4), the proline at position 204 dramatically changes the structure of the loop strongly suggesting that this SNP (rs750277651) has a profound impact on the biology of NPAS2. The NetPhos 3.0 analysis did not return a high phosphorylation probability for serine-205 (5.1%) making it less likely that this is a phosphorylation site. There is however a serine at position 202 on the N-terminal site of serine-204 (200-VPSPSCNGF-208) which is located next to a proline. Such SP motives are the target site of cyclin-dependent kinases and of the MAP kinases (Roskoski 2012). Accordingly, the phosphorylation probability for serine-202 is 84.5%. It could therefore be possible that

the serine-204-to-proline exchange affects the phosphorylation of NPAS2 indirectly by changing the structure of the loop thereby preventing the phosphorylating of serine-202 or other potential phosphorylation sites in this region.

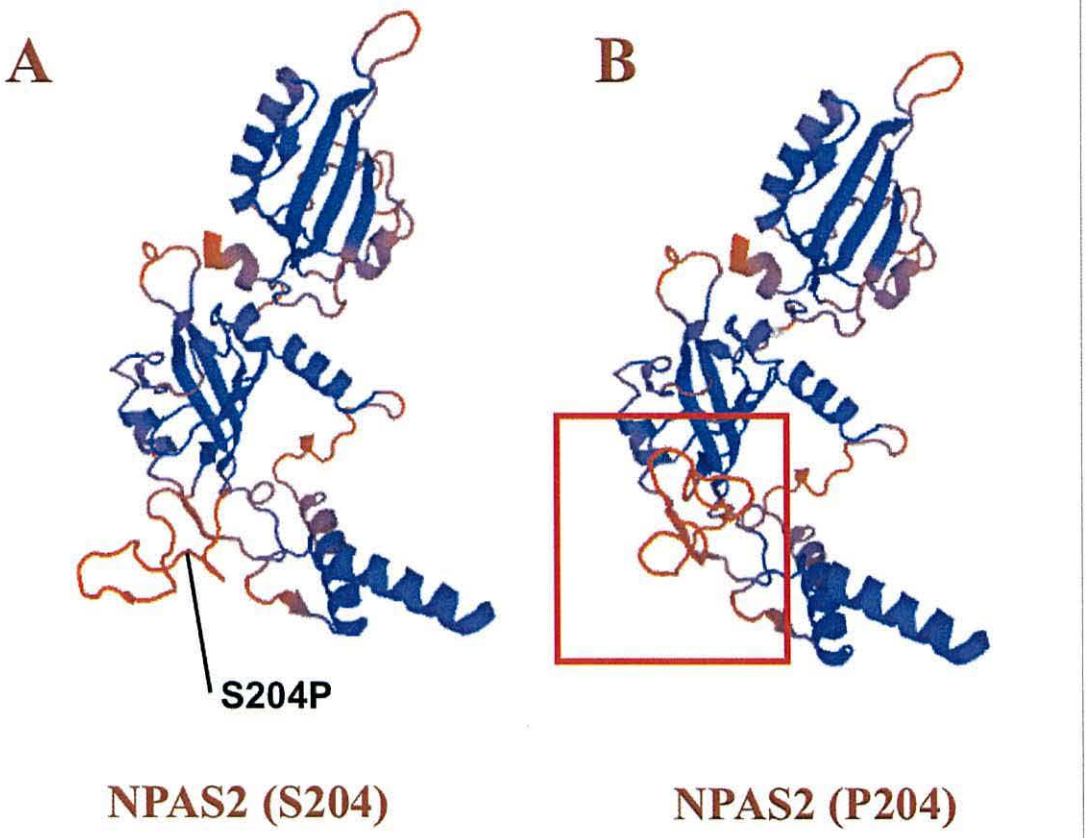

Figure 6-4: The S204P SNP (rs750277651) affects the structure of the loop opposite the BHLH domain of human NPAS2.

A: Model of human NPAS2 with a serine residue at position 204.

B: Model of human NPAS2 with a proline residue at position 204.

Please note the dramatic changes to the structure of the loop region.

6.5 Missense mutations in the beta-sheets of the two PAS domains of human NPAS2.

Part of the PAS domain structure is a beta-sheet sheet which is positioned opposite the alpha helical PAS fold (Taylor, Zhulin 1999) (Figure 6-5).

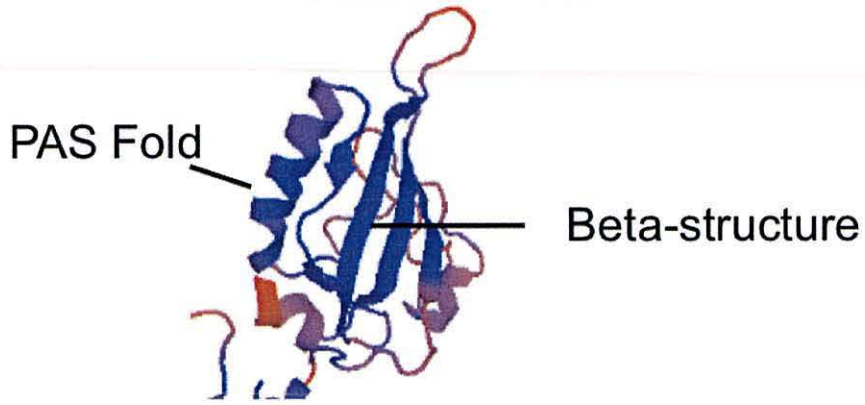

Figure 6-5: The beta-sheet structure opposite the alpha helical PAS fold in the second PAS domain of NPAS2.

While the first PAS domain of NPAS2 has two large beta-sheets, the second PAS domain has three large sheets. As shown in Figure 6-6, the missense mutations affect the ends of the beta sheets rather than amino acids in the middle of the structure. The exception is isoleucine-188 (I188V, rs372678357) which is located in the middle of beta sheet 2. The same observation applies to the three beta-sheets of the second PAS domain where threonine-252 (T252N, rs555063320) is the exception as this mutation is in the middle of the first beta-sheet (Figure 6-7) (**Table 6-4**). Interestingly T252 has a high phosphorylation probability of 83.3% according to NetPhos 3.0 (http://www.cbs.dtu.dk/services/NetPhos/; accessed 09 July 2016). The sequence 248-LEEFTSRHS-256 surrounding T252 is very hydrophilic and contains charged amino acids. The three kinases most likely to modify this threonine are DYRK1A (Q13627, dual-specificity tyrosine-regulated kinase 1A), DYRK1B (Q9Y463) and the MAP kinase MEK7 (MAP2K7, O14733) according to KinaseNet prediction tool (http://www.kinasenet.ca; accessed 09 July 2016). Interestingly, mouse DYRK1A kinase phosphorylates cryptochrome 1 at serine-557 to regulate the protein turnover of Cry1 (Kurabayashi et al. 2010). This dual specific kinase is important for the development and function of the central nervous system and its gene on chromosome 21 is within the Down syndrome critical region. The kinase is also involved in Cancer development (Fernández-Martínez,

Zahonero & Sánchez-Gómez 2015). Modeling the human NPAS2 sequence with an asparagine (N) at position 252 (T252N, rs555063320) had no impact on the structure of the beta-sheet (not shown).

The human MAP kinase, MEK7 kinase (dHep kinase in *Drosophila*) is an activator of the MAP kinase c-Jun N-terminal kinase (JNK) but not of the MAP kinase p38 in the response to heat stress, UV light and cytokine signaling (Foltz et al. 1998). The kinase has not yet been linked to proteins of the circadian clock.

Table 6-4: Missense SNPs affecting the beta-sheets in the two PAS domains of human NPAS2.

First PAS domain	Amino acid position	SNPs
Beta-sheet 1	D165-R174	rs748982724 (D165N) rs748982724 (D165Y) rs774012759 (L172I)
Beta-sheet 2	T184-R195	rs759800413 (E186Q) rs372678357 (I188V) rs775639109 (N193K) rs763172499 (R195C rs572470679 (R195H)
Second PAS domain	**Amino acid position**	**SNPs**
Beta-sheet 1	E249-R254	rs555063320 (T252N)
Beta-sheet 2	Q322 –I332	rs772815471 (I332V)
Beta-sheet 3	F343-V351	rs112562018 (I344M) rs143509936 (V345M)

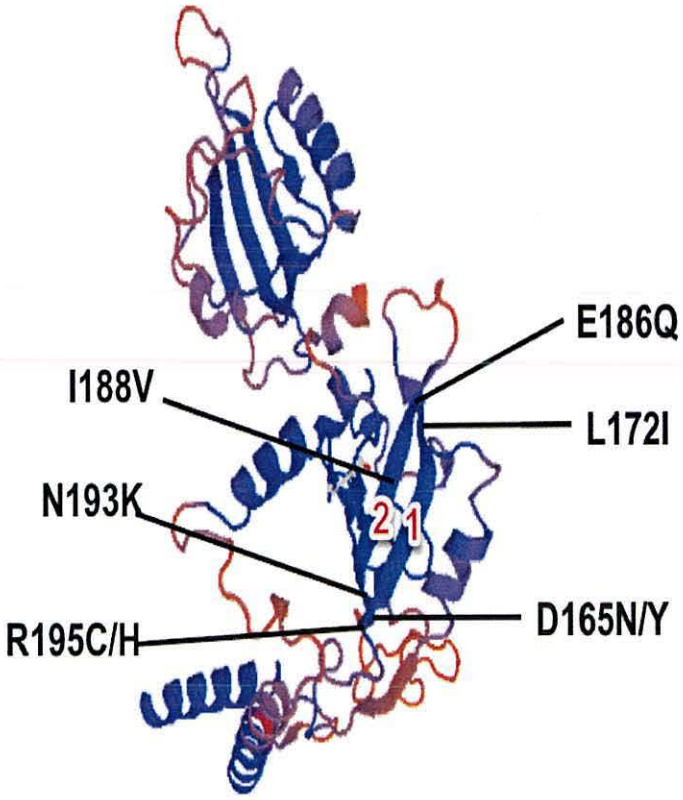

Figure 6-6: Missense SNPs in the two beta-sheets of the first PAS domain of NPAS2.

The beta-sheets are numbered. All SNPs are listed in **Table 6-4**.

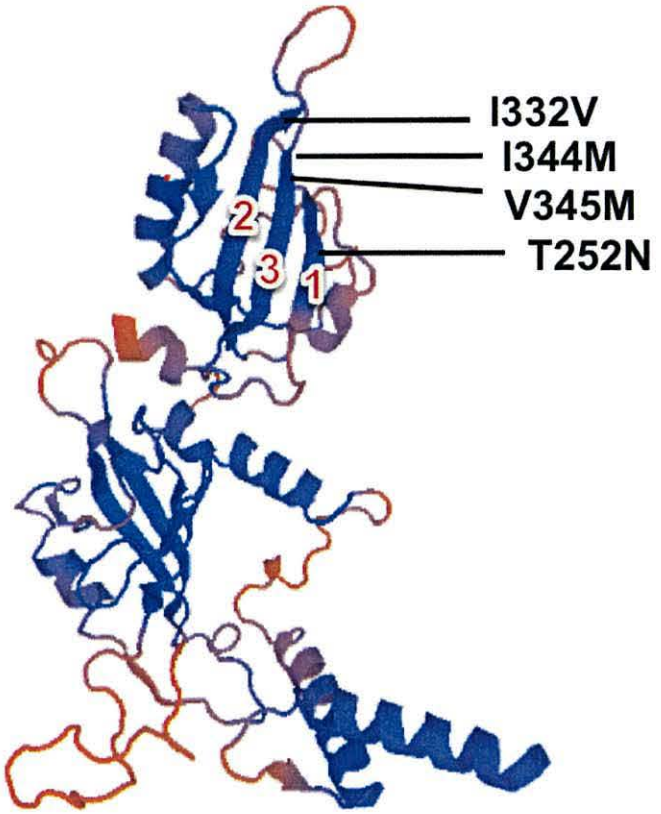

Figure 6-7: Missense SNPs in the three beta-sheets of the second PAS domain of NPAS2.

The beta-sheets are number. All SNPs are listed in **Table 6-4**.

In summary, this analysis has identified the loop between R195-E223 opposite the BHLH DNA binding domain as a very flexible part of NPAS2, the structure of which is strongly affected by the SNP rs750277651 (S204P). The mutations are located in close proximity to a potential phosphorylation site of proline-directed kinases which includes cyclin-dependent kinases and MAP kinases. The second novel finding is the presence of the SNP rs555063320 (T252N) in the first of the three beta-sheets of the second PAS domain which may be a phosphorylation site of the dual-specific kinase DYRK1A which was reported to phosphorylate mouse cryptochrome at S557 to regulate its turnover.

6.6 Models of the different N-terminal splice variants of NPAS2

To find out how the loss of protein information affects the three shorter N-terminal splice variants of NPAS2 (004, 005, 007), the corresponding protein sequences were used to model their three-dimensional structures. Please note that the N-terminal extension of NPAS2-004 is missing in the model as this sequence is not in the template crystal structure (4f3l.1.B) (Huang et al. 2012). As shown in Figure 6-8, NPAS2-004 (207aa,) and NPAS2-005 (107aa) are similar in structure with two important differences. The second helix of the NAPS2-005 BHLH domain is significantly shorter and the extra loop at its C-terminal end (present in NPAS2-004) is missing. In the longer NPAS2-007 (258aa) variant both PAS domains are incomplete which is expected to prevent binding of the heme group as well as the formation of hetero-dimers with other PAS domain proteins like BMAL1. It is therefore likely that all three splice variants act independently of the NPAS2-BMAL complex as they miss functional PAS domains which are important for complex formation.

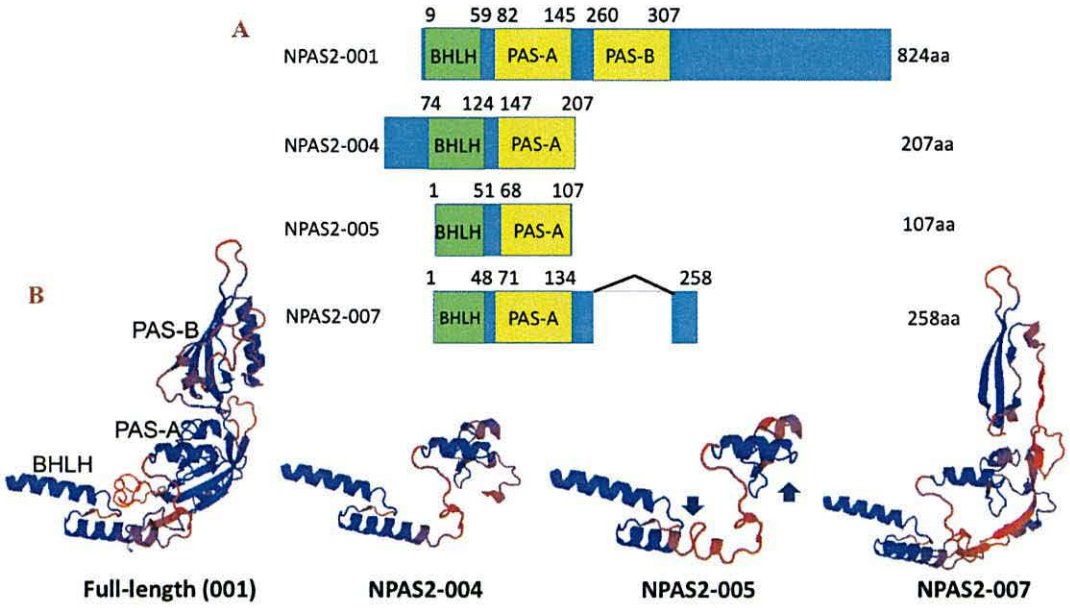

Figure 6-8: Models of the N-terminal splice variants of human NPAS2.

A: Domain organization of the full-length NPAS2 (001) protein and the three truncated splice variants (004, 005, 007).

B: Models of the four proteins (template: mouse CLOCK-BMAL1 complex 4f3l.1.B). The two arrows indicate the structural differences between NPAS2-004 and NPAS2-005.

CHAPTER 7

GENERAL DISCUSSION

Chapter 7: General Discussion

The aim of this work was to obtain a deeper insight into the biology of the circadian clock protein NPAS2. The thesis succeeded in several ways to enrich our understanding of this interesting transcription factor.

First, by revealing that full-length NPAS2 exists in three protein forms with isoelectric values which are very different from the theoretical isoelectric point of 6.35 (Chapter 4). One form is more negatively charged (Form 1 in Figure 7-1) and two forms (Form 2, Form3 in Figure 7-1) are more positively charged and differ in their molecular weight. This difference may be due to the covalent attachment of ubiquitin and/or SUMO.

Second, by identifying two post-translational modified forms of NPAS2 in the response to oxidative stress (Form 4 in Figure 7-1) and after UV irradiation (Form 5 in Figure 7-1).

Third, by observing the formation of high molecular weight complexes of NPAS2 in the response to oxidative stress. Although it is unclear which NPAS2 protein form assembles in these complexes, it could be the modified form 4 as both, complex formation and modifications are triggered by oxidative stress.

Fourth, by demonstrating that the mRNA levels of *NPAS2* (Chapter 5) increase in the response to oxidative stress, but decrease in the response to heat stress. The latter decrease is in line with the drop in NPAS2 protein levels after a heat shock in HeLa and MCF-7 cells. Interestingly serum starvation leads also to a decline in *NPAS2* mRNA levels.

Finally, NPAS2 is predominantly a nuclear protein independently of oxidative stress as confirmed by cell fractionation and immune-localization.

Taken together, these novel findings indicate a close link between NPAS2 and the cellular stress response rather than the DNA damage response. From the three main classes of human MAP kinases (Erk1, Erk2 & p38 & JNK), the most likeliest class to act on NPAS2 are the p38 related MAP kinases since they are activated by different types of stress including oxidative and heat stress (Roux, Blenis 2004). Within the p38 group are four p38 isoforms (p38α, p38β, p38γ and p38δ) (Escós et al. 2016, Jiang et al. 1996). Interestingly, p38β is highly expressed in the brain and linked with the regulation of transcription factors (Beardmore et al. 2005). Under DNA replication stress conditions, which can be triggered by oxidative damage and UV light, p38β and the JNK MAP kinases block cell cycle progression

in G2 jointly with the DNA damage checkpoint kinase Chk1 (Llopis et al. 2012). p38β is also activated in the response to nutrient limitation as triggered by serum starvation (Kalender, Selvaraj & Thomas 2011). Taken together, p38β is a possible candidate to phosphorylate NPAS2 in the response to oxidative stress. It would be interesting to specifically down-regulate this p38 isoform using the new Crispr/Cas9 technology and to analyse the modification and complex formation of NPAS2 in the presence of hydrogen peroxide.

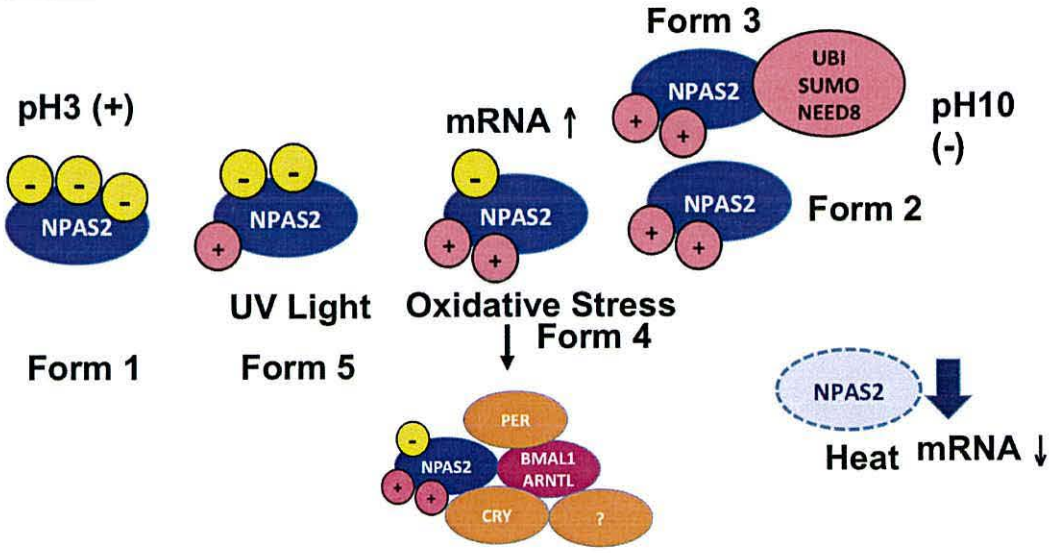

Figure 7-1: Summary Model of the key findings.

Isoelectric focusing revealed the existence of three main protein forms of NPAS2 in untreated HEK-293 cells.

Form 1 is more negatively charged as expected from the theoretical isoelectric value of 6.35 of NPAS2 and forms 2 and 3 are more positively charged. Form 3 has a higher molecular weight which is in line with the observation that NPAS2 can be ubiquitinated and sumoylated. NPAS2 has also a potential NEED8 attachment site. Form 4 appears after the treatment of cells with hydrogen peroxide (oxidative stress) and may be phosphorylated or otherwise more negatively charged and form 5 appears after UV irradiation and is more negatively charged than form 4. Form 4 may be part of a larger protein complex which was detected in cells after oxidative stress. While hydrogen peroxide increases the levels of NPAS2 mRNA, heat has the opposite effect and results in the loss of NPAS2 protein in HeLa and MCF-7 cells but not HEK-293 cells.

Jointly with the other MAP kinases Erk1/2 and JNK, p38 is involved in the regulation of the circadian clock. *Drosophila* p38 activity is highest during darkness and regulates the circadian rhythm through the phosphorylation of the Period proteins (Dusik et al. 2014). Induction of human Period 1 is dependent on p38 especially in peripheral tissues (Petrzilka et al. 2009). It is also noteworthy that the cellular production of reactive oxygen molecules is under circadian control (Wang et al. 2012). These findings may help to explain why hydrogen peroxide has a strong impact on the mRNA levels of *NPAS2* and its post-translational modifications and ability to form larger protein complexes.

Closely related to this may be the decline in *NPAS2* mRNA and protein levels after a heat shock. Elevated temperatures activate all three MAP kinases in distinct ways. Activation of the ERK kinases by heat stress requires the stimulation of the epidermal growth factor (EGF) receptor (Lin et al. 1997), while activation of the JNK kinase depends on the regulation of phosphatases which inactivate JNK (Meriin et al. 1999). Activation of p38 is dependent on the stimulation of several upstream kinases including Ask1 and MKK3 and MKK6 (Zanke et al. 1996). Any of the three MAP kinases could be involved in the down-regulation of NPAS2 after a heat shock. This rises however the question of why NPAS2 would be up-regulated in the response to oxidative stress but down-regulated under heat stress conditions?

The answer may in the ability of NPAS2 to bind with carbon monoxide through its heme groups (Dioum et al. 2002). Heat stress increases cellular carbon monoxide production by heme oxygenase HO-1 also known as heat shock factor 32 (Li et al. 2014). Heme oxygenases are essential enzyme in heme catabolism. They cleave the heme group to form biliverdin, which is subsequently converted to bilirubin and carbon monoxide. Recent work has shown that heat stress indices carbon monoxide production which in turn activates the MAP kinase p38β to stimulate the key transcription factor HSF-1 which binds to specific heat shock motifs (5`-NGAAN-3`) in heat-inducible promoters (Kim et al. 2005). Both, heat stress and oxidative stress reset the circadian clock in human cells in a manner which requires the Casein kinase 2 dependent phosphorylation of BMAL1 at serine-90 and HSF-1 at T142 cells (Tamaru et al. 2013, Tamaru, Ikeda 2016). It is therefore possible that a NPAS2-BMAL1 complex is favorable to maintain cell survival under oxidative stress conditions, whereas NPAS2 is down-regulated upon the production of carbon monoxide at high temperatures which favors a BMAL1-BMAL1 homodimeric complex (Dioum et al. 2002) (Figure 7-2).

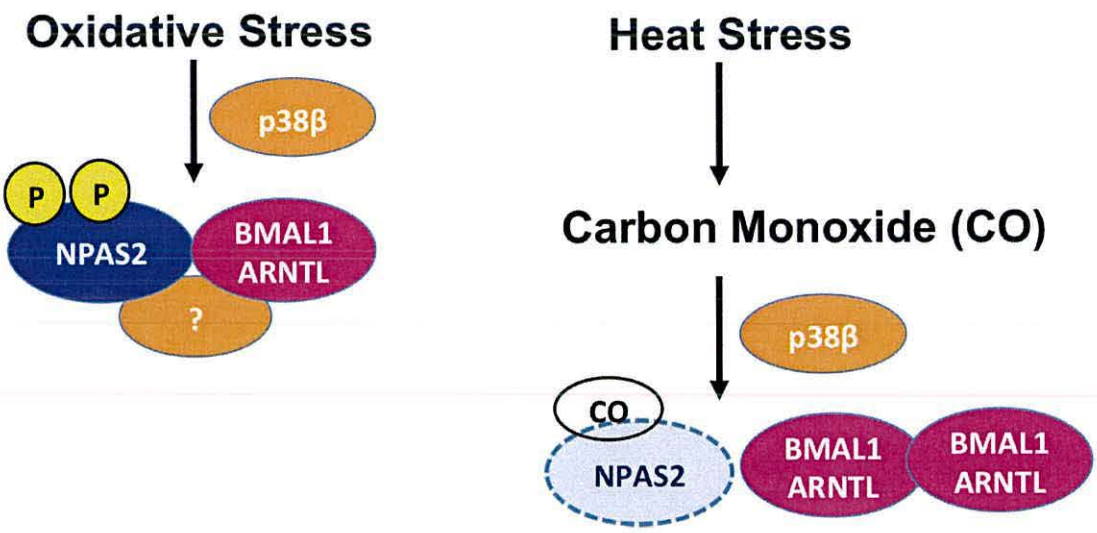

Figure 7-2: Summary model of the changes affecting NPAS2 in the response to oxidative and heat stress.

Oxidative stress leads to the phosphorylation of NPAS2 and the formation of larger protein complexes. This may be regulated by the MAP kinase p38β. It is postulated that the NPAS2-BMAL1 complex is active and contributes to cell survival. In the response to heat stress, carbon monoxide (CO) levels are rising which activates p38β and triggers the inactivation of NPAS2 when CO binds to its heme domains. It is postulated that this promotes the formation of an inactive BMAL1-BMAL1 homomeric complex.

OUTLOOK AND FUTURE WORK

Outlook and future work

The research presented in this thesis seems to have raised more questions that it has answered. There are many opportunities for extending the scope of this thesis remains. This section presents some of these directions.

Based on aim, this study set out to gather more information about the cellular activities of human NPAS2 in the context of the response to DNA damage and cellular stress and how far NPAS2 protein levels are linked with different cancers. So it is obvious that this study should link to the clinical study.

Firstly, the work on chapter 4; NPAS2 protein was down-regulation in HeLa, MCF-7 cell lines after heat shock so the question was Why cancer cell lines need to reduce NPAS2 protein levels at elevated temperatures?

While The heat sensitivity peaks during S phase in human cells (Fox, Read & Bedford 1985) and because cancer cells divide quickly, the down-regulation of NPAS2 could be linked directly or not directly with DNA replication. From that, it suggests to doing more experiment on the relation between NPAS2 protein and DNA replication at higher temperatures using DNA replication inhibitors that can use in higher temperatures.

The second line of research, which follows from chapter 5, is to investigate the link between human neuroblastoma (KELLY) cells and NPAS2. Since NPAS2 is expressed in the mammalian brain it was unclear why NPAS2 expression down-regulated in untreated cells and after UV treatment. This result makes us asking if there is a direct link between NPAS2 and human neuroblastoma.

In the following study, it recommends to clone NPAS2 sequence into human neuroblastoma cells using new technology like CRISPR/Cas9 and analysing the NPAS2 protein and RNA levels and note how that effect on KELLY cells.

Finally, The results summarized from chapter 7 in the model (Figure 7-2) suggest a close link between the MAP kinase p38, especially the splice variant p38β, and NPAS2. The analysis of the missense single nucleotide polymorphisms in the N-terminal domain (17aa-358aa) identifies a potential MAP kinase phosphorylation site (serine-202) which matches the serine-proline motive recognized by human p38 kinase (Li et al. 2015). According to the NetPhos 3.0 server (accessed on 23 July 2016), NPAS2 has 13 potential S/TP motives which could be phosphorylated by p38. Amongst them, only 6

have a phosphorylation probability of more than 50% (T234, T429, S632, T649, S663 and S747) (Figure 7-3). Interestingly, only one (T234) is located in the N-terminal section of NPAS2 while the remaining sites are in the C-terminal domain for which no structural information is available.

Figure 7-3: Potential p38 kinase phosphorylation sites in human NPAS2.

The six serine/threonine-proline motifs with an above 50% phosphorylation probability are shown in yellow. The site at serine 202 (probability 43.5%) which may be affected by the SNP S204P (rs750277651) is shown in blue. The BHLH domain is shown in dark blue, the first PAS-A domain in red and the second PAS-B domain in green.

It would be interesting to inactivate p38β activity with chemical inhibitors like PH 797804 and to test whether NPAS2 is still modified in the response top hydrogen peroxide or whether it is down-regulated in the response to heat stress. If this were to be the case, mutant versions of *NPAS2* lacking selected p38 modification sites could be integrated using the Crisp/Cas9 technology. It would also be important to enrich NPAS2 from human cells by affinity purification with anti-NPAS2 antibodies to identify phosphorylated NPAS2 peptides.

REFERENCE

Reference

Albrecht, U. & Eichele, G. 2003, "The mammalian circadian clock", *Current opinion in genetics & development,* vol. 13, no. 3, pp. 271-277.

Al-Owais, M.M., Scragg, J.L., Dallas, M.L., Boycott, H.E., Warburton, P., Chakrabarty, A., Boyle, J.P. & Peers, C. 2012, "Carbon monoxide mediates the anti-apoptotic effects of heme oxygenase-1 in medulloblastoma DAOY cells via K+ channel inhibition", *The Journal of biological chemistry,* vol. 287, no. 29, pp. 24754-24764.

Beardmore, V.A., Hinton, H.J., Eftychi, C., Apostolaki, M., Armaka, M., Darragh, J., McIlrath, J., Carr, J.M., Armit, L.J., Clacher, C., Malone, L., Kollias, G. & Arthur, J.S. 2005, "Generation and characterization of p38beta (MAPK11) gene-targeted mice", *Molecular and cellular biology,* vol. 25, no. 23, pp. 10454-10464.

Bendjennat, M., Boulaire, J., Jascur, T., Brickner, H., Barbier, V., Sarasin, A., Fotedar, A. & Fotedar, R. 2003, "UV irradiation triggers ubiquitin-dependent degradation of p21 WAF1 to promote DNA repair", *Cell,* vol. 114, no. 5, pp. 599-610.

Bennett, L.D., Beremand, P., Thomas, T.L. & Bell-Pedersen, D. 2013, "Circadian activation of the mitogen-activated protein kinase MAK-1 facilitates rhythms in clock-controlled genes in Neurospora crassa", *Eukaryotic cell,* vol. 12, no. 1, pp. 59-69.

Bhatti, P., Doody, M.M., Rajaraman, P., Alexander, B.H., Yeager, M., Hutchinson, A., Burdette, L., Thomas, G., Hunter, D.J. & Simon, S.L. 2010, "Novel breast cancer risk alleles and interaction with ionizing radiation among US radiologic technologists", *Radiation research,* vol. 173, no. 2, pp. 214-224.

Boivin, D.B. 2010, "Circadian rhythms and clock genes in psychotic disorders", *The Israel journal of psychiatry and related sciences,* vol. 47, no. 1, pp. 27.

Bunger, M.K., Wilsbacher, L.D., Moran, S.M., Clendenin, C., Radcliffe, L.A., Hogenesch, J.B., Simon, M.C., Takahashi, J.S. & Bradfield, C.A. 2000, "Mop3 is an essential component of the master circadian pacemaker in mammals", *Cell,* vol. 103, no. 7, pp. 1009-1017.

Camacho, F., Cilio, M., Guo, Y., Virshup, D., Patel, K., Khorkova, O., Styren, S., Morse, B., Yao, Z. & Keesler, G. 2001, "Human casein kinase I δ phosphorylation of human circadian clock proteins period 1 and 2", *FEBS letters,* vol. 489, no. 2, pp. 159-165.

Chaudhary, J. & Skinner, M.K. 1999, "Basic helix-loop-helix proteins can act at the E-box within the serum response element of the c-fos promoter to influence hormone-induced promoter activation in Sertoli cells", *Molecular Endocrinology,* vol. 13, no. 5, pp. 774-786.

Chiarugi, A., Dölle, C., Felici, R. & Ziegler, M. 2012, "The NAD metabolome—a key determinant of cancer cell biology", *Nature Reviews Cancer*, vol. 12, no. 11, pp. 741-752.

Cho, W.H., Kang, Y.H., An, Y.Y., Tappin, I., Hurwitz, J. & Lee, J.K. 2013, "Human Tim-Tipin complex affects the biochemical properties of the replicative DNA helicase and DNA polymerases", *Proceedings of the National Academy of Sciences of the United States of America*, vol. 110, no. 7, pp. 2523-2527.

Coon, S.L., Weller, J.L., Korf, H.W., Namboodiri, M.A., Rollag, M. & Klein, D.C. 2001, "cAmp regulation of arylalkylamine N-acetyltransferase (AANAT, EC 2.3.1.87): a new cell line (1E7) provides evidence of intracellular AANAT activation", *The Journal of biological chemistry*, vol. 276, no. 26, pp. 24097-24107.

Crumbley, C., Wang, Y., Kojetin, D.J. & Burris, T.P. 2010, "Characterization of the core mammalian clock component, NPAS2, as a REV-ERBalpha/RORalpha target gene", *The Journal of biological chemistry*, vol. 285, no. 46, pp. 35386-35392.

Dardente, H., Fortier, E.E., Martineau, V. & Cermakian, N. 2007, "Cryptochromes impair phosphorylation of transcriptional activators in the clock: a general mechanism for circadian repression", *The Biochemical journal*, vol. 402, no. 3, pp. 525-536.

Debruyne, J.P. 2008, "Oscillating perceptions: the ups and downs of the CLOCK protein in the mouse circadian system", *Journal of genetics*, vol. 87, no. 5, pp. 437-446.

DeBruyne, J.P., Noton, E., Lambert, C.M., Maywood, E.S., Weaver, D.R. & Reppert, S.M. 2006, "A clock shock: mouse CLOCK is not required for circadian oscillator function", *Neuron*, vol. 50, no. 3, pp. 465-477.

DeBruyne, J.P., Weaver, D.R. & Reppert, S.M. 2007, "CLOCK and NPAS2 have overlapping roles in the suprachiasmatic circadian clock", *Nature neuroscience*, vol. 10, no. 5, pp. 543-545.

Delerive, P., Chin, W.W. & Suen, C.S. 2002, "Identification of Reverb(alpha) as a novel ROR(alpha) target gene", *The Journal of biological chemistry*, vol. 277, no. 38, pp. 35013-35018.

Dioum, E.M., Rutter, J., Tuckerman, J.R., Gonzalez, G., Gilles-Gonzalez, M.A. & McKnight, S.L. 2002, "NPAS2: a gas-responsive transcription factor", *Science (New York, N.Y.)*, vol. 298, no. 5602, pp. 2385-2387.

Duan, G. & Walther, D. 2015, "The roles of post-translational modifications in the context of protein interaction networks", *PLoS Comput Biol*, vol. 11, no. 2, pp. e1004049.

Dubrovsky, Y.V., Samsa, W.E. & Kondratov, R.V. 2010, "Deficiency of circadian protein CLOCK reduces lifespan and increases age-related cataract development in mice", *Aging (Albany NY)*, vol. 2, no. 12, pp. 936-944.

Dusik, V., Senthilan, P.R., Mentzel, B., Hartlieb, H., Wülbeck, C., Yoshii, T., Raabe, T. & Helfrich-Förster, C. 2014, "The MAP kinase p38 is part of Drosophila melanogaster's circadian clock", *PLoS Genet*, vol. 10, no. 8, pp. e1004565.

Escós, A., Risco, A., Alsina-Beauchamp, D. & Cuenda, A. 2016, "p38 γ and p38 δ Mitogen Activated Protein Kinases (MAPKs), New Stars in the MAPK Galaxy", *Frontiers in cell and developmental biology*, vol. 4.

Fernández-Martínez, P., Zahonero, C. & Sánchez-Gómez, P. 2015, "DYRK1A: the double-edged kinase as a protagonist in cell growth and tumorigenesis", *Molecular & Cellular Oncology*, vol. 2, no. 1, pp. e970048.

Foltz, I.N., Gerl, R.E., Wieler, J.S., Luckach, M., Salmon, R.A. & Schrader, J.W. 1998, "Human mitogen-activated protein kinase kinase 7 (MKK7) is a highly conserved c-Jun N-terminal kinase/stress-activated protein kinase (JNK/SAPK) activated by environmental stresses and physiological stimuli", *Journal of Biological Chemistry*, vol. 273, no. 15, pp. 9344-9351.

Fox, M., Read, R. & Bedford, J. 1985, "The cell cycle dependence of thermotolerance: III. HeLa cells heated at 45.0° C", *Radiation research*, vol. 104, no. 3, pp. 429-442.

Fuse, T., Yamada, K., Asai, K., Kato, T. & Nakanishi, M. 1996, "Heat shock-mediated cell cycle arrest is accompanied by induction of p21 CKI", *Biochemical and biophysical research communications*, vol. 225, no. 3, pp. 759-763.

Garcia, J.A., Zhang, D., Estill, S.J., Michnoff, C., Rutter, J., Reick, M., Scott, K., Diaz-Arrastia, R. & McKnight, S.L. 2000, "Impaired cued and contextual memory in NPAS2-deficient mice", *Science (New York, N.Y.)*, vol. 288, no. 5474, pp. 2226-2230.

Gery, S., Komatsu, N., Baldjyan, L., Yu, A., Koo, D. & Koeffler, H.P. 2006, "The circadian gene per1 plays an important role in cell growth and DNA damage control in human cancer cells", *Molecular cell*, vol. 22, no. 3, pp. 375-382.

Gibson, U.E., Heid, C.A. & Williams, P.M. 1996, "A novel method for real time quantitative RT-PCR", *Genome research*, vol. 6, no. 10, pp. 995-1001.

Gorbacheva, V.Y., Kondratov, R.V., Zhang, R., Cherukuri, S., Gudkov, A.V., Takahashi, J.S. & Antoch, M.P. 2005, "Circadian sensitivity to the chemotherapeutic agent cyclophosphamide depends on the functional status of the CLOCK/BMAL1 transactivation complex", *Proceedings of the National Academy of Sciences of the United States of America*, vol. 102, no. 9, pp. 3407-3412.

Gotoh, T., Vila-Caballer, M., Santos, C.S., Liu, J., Yang, J. & Finkielstein, C.V. 2014, "The circadian factor Period 2 modulates p53 stability and transcriptional activity in unstressed cells", *Molecular biology of the cell*, vol.

25, no. 19, pp. 3081-3093.

Grechez-Cassiau, A., Rayet, B., Guillaumond, F., Teboul, M. & Delaunay, F. 2008, "The circadian clock component BMAL1 is a critical regulator of p21WAF1/CIP1 expression and hepatocyte proliferation", *The Journal of biological chemistry*, vol. 283, no. 8, pp. 4535-4542.

Han, J., Xu, X., Qin, H., Liu, A., Fan, Z., Kang, L., Fu, J., Liu, J. & Ye, Q. 2013, "The molecular mechanism and potential role of heat shock-induced p53 protein accumulation", *Molecular and cellular biochemistry*, vol. 378, no. 1-2, pp. 161-169.

Hoffman, A.E., Zheng, T., Ba, Y. & Zhu, Y. 2008, "The circadian gene NPAS2, a putative tumor suppressor, is involved in DNA damage response", *Molecular cancer research : MCR*, vol. 6, no. 9, pp. 1461-1468.

Hoffman, A.E., Zheng, T., Stevens, R.G., Ba, Y., Zhang, Y., Leaderer, D., Yi, C., Holford, T.R. & Zhu, Y. 2009, "Clock-cancer connection in non-Hodgkin's lymphoma: a genetic association study and pathway analysis of the circadian gene cryptochrome 2", *Cancer research*, vol. 69, no. 8, pp. 3605-3613.

Huang, N., Chelliah, Y., Shan, Y., Taylor, C.A., Yoo, S.H., Partch, C., Green, C.B., Zhang, H. & Takahashi, J.S. 2012, "Crystal structure of the heterodimeric CLOCK:BMAL1 transcriptional activator complex", *Science (New York, N.Y.)*, vol. 337, no. 6091, pp. 189-194.

Ishida, M., Ueha, T. & Sagami, I. 2008, "Effects of mutations in the heme domain on the transcriptional activity and DNA-binding activity of NPAS2", *Biochemical and biophysical research communications*, vol. 368, no. 2, pp. 292-297.

Itoh, R., Fujita, K., Mu, A., Kim, D.H.T., Tai, T.T., Sagami, I. & Taketani, S. 2013, "Imaging of heme/hemeproteins in nucleus of the living cells expressing heme - binding nuclear receptors", *FEBS letters*, vol. 587, no. 14, pp. 2131-2136.

Jiang, K., Pereira, E., Maxfield, M., Russell, B., Goudelock, D.M. & Sanchez, Y. 2003, "Regulation of Chk1 includes chromatin association and 14-3-3 binding following phosphorylation on Ser-345", *The Journal of biological chemistry*, vol. 278, no. 27, pp. 25207-25217.

Jiang, Y., Chen, C., Li, Z., Guo, W., Gegner, J.A., Lin, S. & Han, J. 1996, "Characterization of the structure and function of a new mitogen-activated protein kinase (p38beta)", *The Journal of biological chemistry*, vol. 271, no. 30, pp. 17920-17926.

Kaasik, K. & Lee, C.C. 2004, "Reciprocal regulation of haem biosynthesis and the circadian clock in mammals", *Nature*, vol. 430, no. 6998, pp. 467-471.

Kalender, A., Selvaraj, A. & Thomas, G. 2011, "A matter of energy stress: p38 β meets mTORC1.", *Cell research,* vol. 21, no. 6, pp. 859-861.

Kang, T. & Sancar, A. 2009, "Circadian regulation of DNA excision repair: implications for chrono-chemotherapy", *Cell Cycle,* vol. 8, no. 11, pp. 1665-1667.

Kang, T.H., Lindsey-Boltz, L.A., Reardon, J.T. & Sancar, A. 2010, "Circadian control of XPA and excision repair of cisplatin-DNA damage by cryptochrome and HERC2 ubiquitin ligase", *Proceedings of the National Academy of Sciences of the United States of America,* vol. 107, no. 11, pp. 4890-4895.

Keesler, G.A., Camacho, F., Guo, Y., Virshup, D., Mondadori, C. & Yao, Z. 2000, "Phosphorylation and destabilization of human period I clock protein by human casein kinase I ε ", *Neuroreport,* vol. 11, no. 5, pp. 951-955.

Kepsutlu, B., Kizilel, R. & Kizilel, S. 2014, "Quantification of interactions among circadian clock proteins via surface plasmon resonance", *Journal of Molecular Recognition,* vol. 27, no. 7, pp. 458-469.

Kerscher, O., Felberbaum, R. & Hochstrasser, M. 2006, "Modification of proteins by ubiquitin and ubiquitin-like proteins", *Annu.Rev.Cell Dev.Biol.,* vol. 22, pp. 159-180.

Khapre, R.V., Kondratova, A.A., Susova, O. & Kondratov, R.V. 2011, "Circadian clock protein BMAL1 regulates cellular senescence in vivo", *Cell cycle,* vol. 10, no. 23, pp. 4162-4169.

Kidd, P.B., Young, M.W. & Siggia, E.D. 2015, "Temperature compensation and temperature sensation in the circadian clock", *Proceedings of the National Academy of Sciences of the United States of America,* vol. 112, no. 46, pp. E6284-92.

Kim, H.P., Wang, X., Zhang, J., Suh, G.Y., Benjamin, I.J., Ryter, S.W. & Choi, A.M. 2005, "Heat shock protein-70 mediates the cytoprotective effect of carbon monoxide: involvement of p38 beta MAPK and heat shock factor-1", *Journal of immunology (Baltimore, Md.: 1950),* vol. 175, no. 4, pp. 2622-2629.

King, D.P., Zhao, Y., Sangoram, A.M., Wilsbacher, L.D., Tanaka, M., Antoch, M.P., Steeves, T.D., Vitaterna, M.H., Kornhauser, J.M. & Lowrey, P.L. 1997, "Positional cloning of the mouse circadian clockgene", *Cell,* vol. 89, no. 4, pp. 641-653.

Kondratov, R.V., Kondratova, A.A., Lee, C., Gorbacheva, V.Y., Chernov, M.V. & Antoch, M.P. 2006, "Posttranslational regulation of circadian transcriptional CLOCK (NPAS2)/BMAL1 complex by CRYPTOCHROMES", *Cell Cycle,* vol. 5, no. 8, pp. 890-895.

Krishan, A. 1975, "Rapid flow cytofluorometric analysis of mammalian cell cycle by propidium iodide staining",

The Journal of cell biology, vol. 66, no. 1, pp. 188-193.

Krishnan, N., Davis, A.J. & Giebultowicz, J.M. 2008, "Circadian regulation of response to oxidative stress in Drosophila melanogaster", *Biochemical and biophysical research communications*, vol. 374, no. 2, pp. 299-303.

Kuo, S., Chen, S., Yeh, K., Hou, M., Chang, Y., Hsu, N.C. & Chang, J. 2009, "Disturbance of circadian gene expression in breast cancer", *Virchows Archiv*, vol. 454, no. 4, pp. 467-474.

Kurabayashi, N., Hirota, T., Sakai, M., Sanada, K. & Fukada, Y. 2010, "DYRK1A and glycogen synthase kinase 3beta, a dual-kinase mechanism directing proteasomal degradation of CRY2 for circadian timekeeping", *Molecular and cellular biology*, vol. 30, no. 7, pp. 1757-1768.

Kwon, I., Lee, J., Chang, S.H., Jung, N.C., Lee, B.J., Son, G.H., Kim, K. & Lee, K.H. 2006, "BMAL1 shuttling controls transactivation and degradation of the CLOCK/BMAL1 heterodimer", *Molecular and cellular biology*, vol. 26, no. 19, pp. 7318-7330.

Lee, Y.J., Lee, J.H. & Han, H.J. 2006, "Extracellular adenosine triphosphate protects oxidative stress - induced increase of p21WAF1/Cip1 and p27Kip1 expression in primary cultured renal proximal tubule cells: Role of PI3K and Akt signaling", *Journal of cellular physiology*, vol. 209, no. 3, pp. 802-810.

Lee, H.M., Chen, R., Kim, H., Etchegaray, J.P., Weaver, D.R. & Lee, C. 2011, "The period of the circadian oscillator is primarily determined by the balance between casein kinase 1 and protein phosphatase 1", *Proceedings of the National Academy of Sciences of the United States of America*, vol. 108, no. 39, pp. 16451-16456.

Lee, J., Lee, Y., Lee, M.J., Park, E., Kang, S.H., Chung, C.H., Lee, K.H. & Kim, K. 2008, "Dual modification of BMAL1 by SUMO2/3 and ubiquitin promotes circadian activation of the CLOCK/BMAL1 complex", *Molecular and cellular biology*, vol. 28, no. 19, pp. 6056-6065.

Leonardi, G.C., Rapisarda, V., Marconi, A., Scalisi, A., Catalano, F., Proietti, L., Travali, S., Libra, M. & Fenga, C. 2012, "Correlation of the risk of breast cancer and disruption of the circadian rhythm (Review)", *Oncology reports*, vol. 28, no. 2, pp. 418-428.

Li, L., Li, C., Wu, J., Huang, S. & Wang, G. 2014, "Heat shock protein 32/heme oxygenase - 1 protects mouse Sertoli cells from hyperthermia - induced apoptosis by CO activation of sGC signalling pathways", *Cell biology international*, vol. 38, no. 1, pp. 64-71.

Li, L., Gao, G., Shankar, J., Joshi, B., Foster, L.J. & Nabi, I.R. 2015, "p38 MAP kinase-dependent phosphorylation of the Gp78 E3 ubiquitin ligase controls ER-mitochondria association and mitochondria motility", *Molecular*

biology of the cell, vol. 26, no. 21, pp. 3828-3840.

Lin, R.Z., Hu, Z., Chin, J.H. & Hoffman, B.B. 1997, "Heat shock activates c-Src tyrosine kinases and phosphatidylinositol 3-kinase in NIH3T3 fibroblasts", *Journal of Biological Chemistry*, vol. 272, no. 49, pp. 31196-31202.

Liu, X.M., Chapman, G.B., Peyton, K.J., Schafer, A.I. & Durante, W. 2003, "Antiapoptotic action of carbon monoxide on cultured vascular smooth muscle cells", *Experimental biology and medicine (Maywood, N.J.)*, vol. 228, no. 5, pp. 572-575.

Llopis, A., Salvador, N., Ercilla, A., Guaita-Esteruelas, S., Barrantes, I.d.B., Gupta, J., Gaestel, M., Davis, R.J., Nebreda, A.R. & Agell, N. 2012, "The stress-activated protein kinases p38 α / β and JNK1/2 cooperate with Chk1 to inhibit mitotic entry upon DNA replication arrest", *Cell Cycle*, vol. 11, no. 19, pp. 3627-3637.

Ma, P.C., Rould, M.A., Weintraub, H. & Pabo, C.O. 1994, "Crystal structure of MyoD bHLH domain-DNA complex: perspectives on DNA recognition and implications for transcriptional activation", *Cell*, vol. 77, no. 3, pp. 451-459.

Mansour, H.A., Talkowski, M.E., Wood, J., Chowdari, K.V., McClain, L., Prasad, K., Montrose, D., Fagiolini, A., Friedman, E.S. & Allen, M.H. 2009, "Association study of 21 circadian genes with bipolar I disorder, schizoaffective disorder, and schizophrenia", *Bipolar disorders*, vol. 11, no. 7, pp. 701-710.

Mao, J., Li, X., Chen, W., Xu, B., Zhang, H., Li, H., Wang, L., Jin, X., Zhu, J. & Wang, W. 2012, "Cell cycle-dependent subcellular distribution of ClC-3 in HeLa cells", *Histochemistry and cell biology*, vol. 137, no. 6, pp. 763-776.

Maris, J.M. 2010, "Recent Advances in Neuroblastoma", *N Engl J Med*, vol. 362, no. 23, pp. 2202-2211.

Matsuo, T., Yamaguchi, S., Mitsui, S., Emi, A., Shimoda, F. & Okamura, H. 2003, "Control mechanism of the circadian clock for timing of cell division in vivo", *Science (New York, N.Y.)*, vol. 302, no. 5643, pp. 255-259.

Mazzoccoli, G., De Cata, A., Piepoli, A. & Vinciguerra, M. 2014, "The circadian clock and the hypoxic response pathway in kidney cancer", *Tumor Biology*, vol. 35, no. 1, pp. 1-7.

Megias, J., Busserolles, J. & Alcaraz, M. 2007, "The carbon monoxide - releasing molecule CORM - 2 inhibits the inflammatory response induced by cytokines in Caco - 2 cells", *British journal of pharmacology*, vol. 150, no. 8, pp. 977-986.

Meriin, A.B., Yaglom, J.A., Gabai, V.L., Zon, L., Ganiatsas, S., Mosser, D.D., Zon, L. & Sherman, M.Y. 1999, "Protein-damaging stresses activate c-Jun N-terminal kinase via inhibition of its dephosphorylation: a novel

pathway controlled by HSP72", *Molecular and cellular biology*, vol. 19, no. 4, pp. 2547-2555.

Musiek, E.S., Lim, M.M., Yang, G., Bauer, A.Q., Qi, L., Lee, Y., Roh, J.H., Ortiz-Gonzalez, X., Dearborn, J.T. & Culver, J.P. 2013, "Circadian clock proteins regulate neuronal redox homeostasis and neurodegeneration", *The Journal of clinical investigation*, vol. 123, no. 12, pp. 5389-5400.

Nicholas, B., Rudrasingham, V., Nash, S., Kirov, G., Owen, M. & Wimpory, D. 2007, "Association of Per1 and Npas2 with autistic disorder: support for the clock genes/social timing hypothesis", *Molecular psychiatry*, vol. 12, no. 6, pp. 581-592.

Otterbein, L.E., Hedblom, A., Harris, C., Csizmadia, E., Gallo, D. & Wegiel, B. 2011, "Heme oxygenase-1 and carbon monoxide modulate DNA repair through ataxia-telangiectasia mutated (ATM) protein", *Proceedings of the National Academy of Sciences of the United States of America*, vol. 108, no. 35, pp. 14491-14496.

Partch, C.L., Green, C.B. & Takahashi, J.S. 2014, "Molecular architecture of the mammalian circadian clock", *Trends in cell biology*, vol. 24, no. 2, pp. 90-99.

Partonen, T., Treutlein, J., Alpman, A., Frank, J., Johansson, C., Depner, M., Aron, L., Rietschel, M., Wellek, S. & Soronen, P. 2007, "Three circadian clock genes Per2, Arntl, and Npas2 contribute to winter depression", *Annals of Medicine*, vol. 39, no. 3, pp. 229-238.

Petrzilka, S., Taraborrelli, C., Cavadini, G., Fontana, A. & Birchler, T. 2009, "Clock gene modulation by TNF-alpha depends on calcium and p38 MAP kinase signaling", *Journal of Biological Rhythms*, vol. 24, no. 4, pp. 283-294.

Pinacho, R., Villalmanzo, N., Meana, J.J., Ferrer, I., Berengueras, A., Haro, J.M., Villén, J. & Ramos, B. 2016, "Altered CSNK1E, FABP4 and NEFH protein levels in the dorsolateral prefrontal cortex in schizophrenia", *Schizophrenia research*, .

Pirkmajer, S. & Chibalin, A.V. 2011, "Serum starvation: caveat emptor", *American journal of physiology.Cell physiology*, vol. 301, no. 2, pp. C272-9.

Potter, G.D., Cade, J.E., Grant, P.J. & Hardie, L.J. 2016, "Nutrition and the circadian system", *The British journal of nutrition*, vol. 116, no. 3, pp. 434-442.

Reick, M., Garcia, J.A., Dudley, C. & McKnight, S.L. 2001, "NPAS2: an analog of clock operative in the mammalian forebrain", *Science (New York, N.Y.)*, vol. 293, no. 5529, pp. 506-509.

Reinke, H., Saini, C., Fleury-Olela, F., Dibner, C., Benjamin, I.J. & Schibler, U. 2008, "Differential display of DNA-binding proteins reveals heat-shock factor 1 as a circadian transcription factor", *Genes & development*,

vol. 22, no. 3, pp. 331-345.

Reppert, S.M. & Weaver, D.R. 2002, "Coordination of circadian timing in mammals", *Nature*, vol. 418, no. 6901, pp. 935-941.

Reppert, S.M. & Weaver, D.R. 2001, "Molecular analysis of mammalian circadian rhythms", *Annual Review of Physiology*, vol. 63, no. 1, pp. 647-676.

Roskoski, R. 2012, "ERK1/2 MAP kinases: structure, function, and regulation", *Pharmacological research*, vol. 66, no. 2, pp. 105-143.

Roux, P.P. & Blenis, J. 2004, "ERK and p38 MAPK-activated protein kinases: a family of protein kinases with diverse biological functions", *Microbiology and molecular biology reviews : MMBR*, vol. 68, no. 2, pp. 320-344.

Rutter, J., Reick, M., Wu, L.C. & McKnight, S.L. 2001, "Regulation of clock and NPAS2 DNA binding by the redox state of NAD cofactors", *Science (New York, N.Y.)*, vol. 293, no. 5529, pp. 510-514.

Ryan, A.J., Squires, S., Strutt, H.L. & Johnson, R.T. 1991, "Camptothecin cytotoxicity in mammalian cells is associated with the induction of persistent double strand breaks in replicating DNA", *Nucleic acids research*, vol. 19, no. 12, pp. 3295-3300.

Ryter, S.W. & Otterbein, L.E. 2004, "Carbon monoxide in biology and medicine", *Bioessays*, vol. 26, no. 3, pp. 270-280.

Saha, S. & Sassone-Corsi, P. 2007, "Circadian clock and breast cancer: a molecular link", *Cell Cycle*, vol. 6, no. 11, pp. 1329-1331.

Sanada, K., Harada, Y., Sakai, M., Todo, T. & Fukada, Y. 2004, "Serine phosphorylation of mCRY1 and mCRY2 by mitogen - activated protein kinase", *Genes to Cells*, vol. 9, no. 8, pp. 697-708.

Sancar, A., Lindsey-Boltz, L.A., Kang, T., Reardon, J.T., Lee, J.H. & Ozturk, N. 2010, "Circadian clock control of the cellular response to DNA damage", *FEBS letters*, vol. 584, no. 12, pp. 2618-2625.

Savvidis, C. & Koutsilieris, M. 2012, "Circadian rhythm disruption in cancer biology", *Molecular medicine (Cambridge, Mass.)*, vol. 18, pp. 1249-1260.

Schibler, U. & Sassone-Corsi, P. 2002, "A web of circadian pacemakers", *Cell*, vol. 111, no. 7, pp. 919-922.

Schibler, U., Ripperger, J.A. & Brown, S.A. 2001, "Circadian rhythms. Chronobiology--reducing time", *Science (New York, N.Y.)*, vol. 293, no. 5529, pp. 437-438.

Shin, J., Hong, S., Lee, S.O., Kim, T., Park, I., An, S., Lee, W., Lim, J., Kim, K. & Yang, Y. 2008, "Serum starvation induces G1 arrest through suppression of Skp2-CDK2 and CDK4 in SK-OV-3 cells", *International journal of oncology*, vol. 32, no. 2, pp. 435-439.

Shostak, A., Ruppert, B., Ha, N., Bruns, P., Toprak, U.H., Project, I.M., Eils, R., Schlesner, M., Diernfellner, A. & Brunner, M. 2016, "MYC/MIZ1-dependent gene repression inversely coordinates the circadian clock with cell cycle and proliferation", *Nature Communications*, vol. 7.

Shwab, M., Alitalo, K. & Klemphauer, K. 1983, "Amplified DNA with limited homology to myc cellular oncogene is shared by human neuroblastoma tumor", *Nature*, vol. 305, pp. 245-248.

Silvis, A.M., McCormick, M.L., Spitz, D.R. & Kiningham, K.K. 2016, "Redox balance influences differentiation status of neuroblastoma in the presence of all-trans retinoic acid", *Redox biology*, vol. 7, pp. 88-96.

Slominski, R.M., Reiter, R.J., Schlabritz-Loutsevitch, N., Ostrom, R.S. & Slominski, A.T. 2012, "Melatonin membrane receptors in peripheral tissues: distribution and functions", *Molecular and cellular endocrinology*, vol. 351, no. 2, pp. 152-166.

Smith, K.D., Fu, M.A. & Brown, E.J. 2009, "Tim-Tipin dysfunction creates an indispensible reliance on the ATR-Chk1 pathway for continued DNA synthesis", *The Journal of cell biology*, vol. 187, no. 1, pp. 15-23.

Solocinski, K. & Gumz, M.L. 2015, "The Circadian Clock in the Regulation of Renal Rhythms", *Journal of Biological Rhythms*, vol. 30, no. 6, pp. 470-486.

Son, Y., Kim, S., Chung, H.T. & Pae, H.O. 2013, "Reactive oxygen species in the activation of MAP kinases", *Methods in enzymology*, vol. 528, pp. 27-48.

Soria, G. & Gottifredi, V. 2010, "PCNA-coupled p21 degradation after DNA damage: The exception that confirms the rule?", *DNA repair*, vol. 9, no. 4, pp. 358-364.

Soria, V., Martínez-Amorós, È, Escaramís, G., Valero, J., Pérez-Egea, R., García, C., Gutiérrez-Zotes, A., Puigdemont, D., Bayés, M. & Crespo, J.M. 2010, "Differential association of circadian genes with mood disorders: CRY1 and NPAS2 are associated with unipolar major depression and CLOCK and VIP with bipolar disorder", *Neuropsychopharmacology*, vol. 35, no. 6, pp. 1279-1289.

Stepanenko, A. & Dmitrenko, V. 2015, "HEK293 in cell biology and cancer research: phenotype, karyotype, tumorigenicity, and stress-induced genome-phenotype evolution", *Gene*, vol. 569, no. 2, pp. 182-190.

Stevens, R.G. 2005, "Circadian disruption and breast cancer: from melatonin to clock genes", *Epidemiology*, vol. 16, no. 2, pp. 254-258.

Stokkan, K.A., Yamazaki, S., Tei, H., Sakaki, Y. & Menaker, M. 2001, "Entrainment of the circadian clock in the liver by feeding", *Science (New York, N.Y.)*, vol. 291, no. 5503, pp. 490-493.

Sun, X. & Lin, Y. 2016, "Npas4: Linking Neuronal Activity to Memory", *Trends in neurosciences*, vol. 39, no. 4, pp. 264-275.

Tamaru, T., Hattori, M., Honda, K., Benjamin, I., Ozawa, T. & Takamatsu, K. 2011, "Synchronization of circadian Per2 rhythms and HSF1-BMAL1: CLOCK interaction in mouse fibroblasts after short-term heat shock pulse", *PLoS one*, vol. 6, no. 9, pp. e24521.

Tamaru, T., Hattori, M., Honda, K., Nakahata, Y., Sassone-Corsi, P., van der Horst, Gijsbertus TJ, Ozawa, T. & Takamatsu, K. 2015, "CRY drives cyclic CK2-mediated BMAL1 phosphorylation to control the mammalian circadian clock", *PLoS Biol*, vol. 13, no. 11, pp. e1002293.

Tamaru, T., Hattori, M., Ninomiya, Y., Kawamura, G., Varès, G., Honda, K., Mishra, D.P., Wang, B., Benjamin, I. & Sassone-Corsi, P. 2013, "ROS stress resets circadian clocks to coordinate pro-survival signals", *PloS one*, vol. 8, no. 12, pp. e82006.

Tamaru, T. & Ikeda, M. 2016, "Circadian adaptation to cell injury stresses: a crucial interplay of BMAL1 and HSF1", *The Journal of Physiological Sciences*, , pp. 1-4.

Taylor, B.L. & Zhulin, I.B. 1999, "PAS domains: internal sensors of oxygen, redox potential, and light", *Microbiology and molecular biology reviews : MMBR*, vol. 63, no. 2, pp. 479-506.

Teh, C.H., Lam, K.K., Loh, C.C., Loo, J.M., Yan, T. & Lim, T.M. 2006, "Neuronal PAS domain protein 1 is a transcriptional repressor and requires arylhydrocarbon nuclear translocator for its nuclear localization", *The Journal of biological chemistry*, vol. 281, no. 45, pp. 34617-34629.

Tei, H., Okamura, H., Shigeyoshi, Y., Fukuhara, C., Ozawa, R., Hirose, M. & Sakaki, Y. 1997, "Circadian oscillation of a mammalian homologue of the Drosophila period gene", *Nature*, vol. 389, no. 6650, pp. 512-516.

Thomas, P. & Smart, T.G. 2005, "HEK293 cell line: A vehicle for the expression of recombinant proteins", *Journal of pharmacological and toxicological methods*, vol. 51, no. 3, pp. 187-200.

Uchida, Y., Hirayama, J. & Nishina, H. 2010, "A common origin: signaling similarities in the regulation of the circadian clock and DNA damage responses", *Biological and Pharmaceutical Bulletin*, vol. 33, no. 4, pp. 535-544.

Uchida, Y., Osaki, T., Yamasaki, T., Shimomura, T., Hata, S., Horikawa, K., Shibata, S., Todo, T., Hirayama, J. &

Nishina, H. 2012, "Involvement of stress kinase mitogen-activated protein kinase kinase 7 in regulation of mammalian circadian clock", *The Journal of biological chemistry*, vol. 287, no. 11, pp. 8318-8326.

Vielhaber, E., Eide, E., Rivers, A., Gao, Z.H. & Virshup, D.M. 2000, "Nuclear entry of the circadian regulator mPER1 is controlled by mammalian casein kinase I epsilon", *Molecular and cellular biology*, vol. 20, no. 13, pp. 4888-4899.

Wang, F., Hu, Z., Yang, R., Tang, J., Liu, Y., Hemminki, K., Sutter, C., Wappenschmidt, B., Niederacher, D. & Arnold, N. 2011, "A variant affecting miRNAs binding in the circadian gene Neuronal PAS domain protein 2 (NPAS2) is not associated with breast cancer risk", *Breast cancer research and treatment*, vol. 127, no. 3, pp. 769-775.

Wang, T.A., Yu, Y.V., Govindaiah, G., Ye, X., Artinian, L., Coleman, T.P., Sweedler, J.V., Cox, C.L. & Gillette, M.U. 2012, "Circadian rhythm of redox state regulates excitability in suprachiasmatic nucleus neurons", *Science (New York, N.Y.)*, vol. 337, no. 6096, pp. 839-842.

Watson, J.V., Chambers, S.H. & Smith, P.J. 1987, "A pragmatic approach to the analysis of DNA histograms with a definable G1 peak", *Cytometry*, vol. 8, no. 1, pp. 1-8.

Wei, Y., An, Z., Zou, Z., Sumpter, R., Su, M., Zang, X., Sinha, S., Gaestel, M. & Levine, B. 2015, "The stress-responsive kinases MAPKAPK2/MAPKAPK3 activate starvation-induced autophagy through Beclin 1 phosphorylation", *eLife*, vol. 4, pp. 10.7554/eLife.05289.

Wilking, M., Ndiaye, M., Mukhtar, H. & Ahmad, N. 2013, "Circadian rhythm connections to oxidative stress: implications for human health", *Antioxidants & redox signaling*, vol. 19, no. 2, pp. 192-208.

Xie, S., Wang, Q., Luo, L., Ruan, Q., Liu, T., Jhanwar-Uniyal, M., Darzynkiewicz, Z., Traganos, F. & Dai, W. 2002, "Proteasome-dependent downregulation of p21Waf1/Cip1 induced by reactive oxygen species", *Journal of interferon & cytokine research*, vol. 22, no. 9, pp. 957-963.

Xue, X., Liu, F., Han, Y., Li, P., Yuan, B., Wang, X., Chen, Y., Kuang, Y., Zhi, Q. & Zhao, H. 2014, "Silencing NPAS2 promotes cell growth and invasion in DLD-1 cells and correlated with poor prognosis of colorectal cancer", *Biochemical and biophysical research communications*, vol. 450, no. 2, pp. 1058-1062.

Yamamoto, T., Nakahata, Y., Soma, H., Akashi, M., Mamine, T. & Takumi, T. 2004, "Transcriptional oscillation of canonical clock genes in mouse peripheral tissues", *BMC molecular biology*, vol. 5, no. 1, pp. 1.

Ye, R., Selby, C.P., Chiou, Y.Y., Ozkan-Dagliyan, I., Gaddameedhi, S. & Sancar, A. 2014, "Dual modes of CLOCK:BMAL1 inhibition mediated by Cryptochrome and Period proteins in the mammalian circadian clock", *Genes & development*, vol. 28, no. 18, pp. 1989-1998.

Yi, C., Mu, L., de la Longrais, Irene A Rigault, Sochirca, O., Arisio, R., Yu, H., Hoffman, A.E., Zhu, Y. & Katsaro, D. 2010, "The circadian gene NPAS2 is a novel prognostic biomarker for breast cancer", *Breast cancer research and treatment*, vol. 120, no. 3, pp. 663-669.

Yi, C., Zheng, T., Leaderer, D., Hoffman, A. & Zhu, Y. 2009, "Cancer-related transcriptional targets of the circadian gene NPAS2 identified by genome-wide ChIP-on-chip analysis", *Cancer letters*, vol. 284, no. 2, pp. 149-156.

Yoshitane, H., Honma, S., Imamura, K., Nakajima, H., Nishide, S.Y., Ono, D., Kiyota, H., Shinozaki, N., Matsuki, H., Wada, N., Doi, H., Hamada, T., Honma, K. & Fukada, Y. 2012, "JNK regulates the photic response of the mammalian circadian clock", *EMBO reports*, vol. 13, no. 5, pp. 455-461.

Yu, E.A. & Weaver, D.R. 2011, "Disrupting the circadian clock: gene-specific effects on aging, cancer, and other phenotypes", .

Yu, L., Arbez, N., Nucifora, L.G., Sell, G.L., Delisi, L.E., Ross, C.A., Margolis, R.L. & Nucifora, F.C.,Jr 2014, "A mutation in NPAS3 segregates with mental illness in a small family", *Molecular psychiatry*, vol. 19, no. 1, pp. 7-8.

Zanke, B.W., Boudreau, K., Rubie, E., Winnett, E., Tibbles, L.A., Zon, L., Kyriakis, J., Liu, F. & Woodgett, J.R. 1996, "The stress-activated protein kinase pathway mediates cell death following injury induced by cis-platinum, UV irradiation or heat", *Current Biology*, vol. 6, no. 5, pp. 606-613.

Zhou, Y.D., Barnard, M., Tian, H., Li, X., Ring, H.Z., Francke, U., Shelton, J., Richardson, J., Russell, D.W. & McKnight, S.L. 1997, "Molecular characterization of two mammalian bHLH-PAS domain proteins selectively expressed in the central nervous system", *Proceedings of the National Academy of Sciences of the United States of America*, vol. 94, no. 2, pp. 713-718.

Zhu, Y., Leaderer, D., Guss, C., Brown, H.N., Zhang, Y., Boyle, P., Stevens, R.G., Hoffman, A., Qin, Q. & Han, X. 2007, "Ala394Thr polymorphism in the clock gene NPAS2: A circadian modifier for the risk of non - Hodgkin's lymphoma", *International journal of cancer*, vol. 120, no. 2, pp. 432-435.

Zhu, Y., Stevens, R.G., Leaderer, D., Hoffman, A., Holford, T., Zhang, Y., Brown, H.N. & Zheng, T. 2008, "Non-synonymous polymorphisms in the circadian gene NPAS2 and breast cancer risk", *Breast cancer research and treatment*, vol. 107, no. 3, pp. 421-425.

Zhu, Y., Stevens, R.G., Hoffman, A.E., Fitzgerald, L.M., Kwon, E.M., Ostrander, E.A., Davis, S., Zheng, T. & Stanford, J.L. 2009, "Testing the circadian gene hypothesis in prostate cancer: a population-based case-control study", *Cancer research*, vol. 69, no. 24, pp. 9315-9322.

Zienolddiny, S., Haugen, A., Lie, J.S., Kjuus, H., Anmarkrud, K.H. & Kjærheim, K. 2013, "Analysis of polymorphisms in the circadian-related genes and breast cancer risk in Norwegian nurses working night shifts", *Breast Cancer Research*, vol. 15, no. 4, pp. 1.

Zuber, A.M., Centeno, G., Pradervand, S., Nikolaeva, S., Maquelin, L., Cardinaux, L., Bonny, O. & Firsov, D. 2009, "Molecular clock is involved in predictive circadian adjustment of renal function", *Proceedings of the National Academy of Sciences of the United States of America*, vol. 106, no. 38, pp. 16523-16528.

APPENDIX

Appendix

Appendix 1: NPAS2 Splice Variant Alignment.

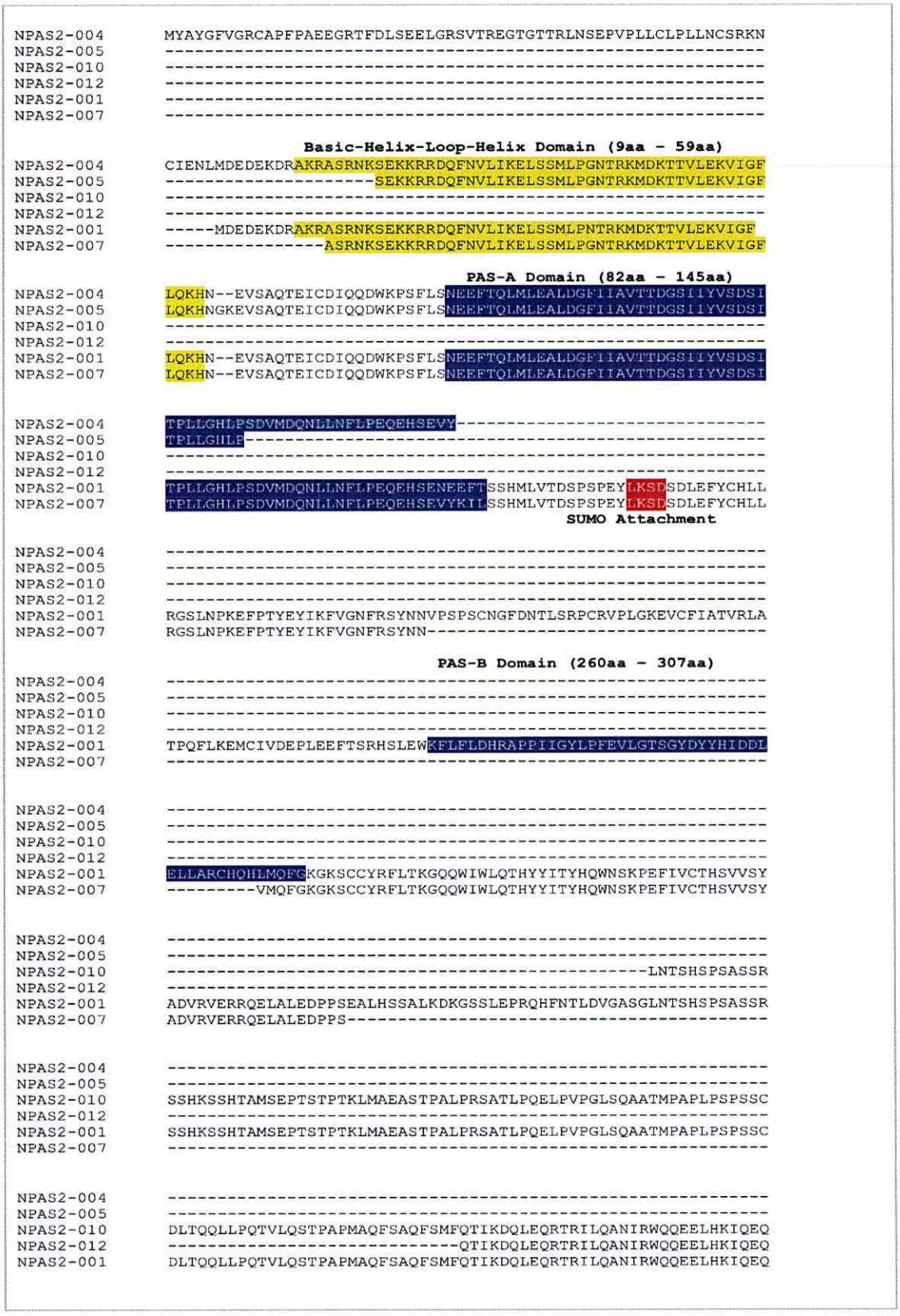

Appendix 2: SNP list.

SNP Number	Alleles	Aminoacid	Position	Consequence
rs201453714	T/A	D/E	4	possibly damaging
rs751737537	G/A	D/N	7	possibly damaging
rs377053524	C/A	A/D	12	probably damaging
rs752546267	A/C	K/T	19	probably damaging
rs140186927	C/G	S/C	34	probably damaging
rs746714721	C/G	L/V	36	probably damaging
rs200029671	C/T	P/L	37	probably damaging
rs749697021	C/T	T/M	40	possibly damaging
rs149450485	G/C	M/I	43	benign
rs772478314	A/G	K/R	51	probably damaging
rs773279753	G/A	V/I	52	possibly damaging
rs138995271	G/C	G/A	54	probably damaging
rs530619759	A/G	N/S	60	benign
rs183671025	C/T	A/V	64	possibly damaging
rs759664980	C/G	Q/E	65	benign
rs770032871	A/T	T/S	66	probably damaging
rs775528411	C/T	T/M	66	probably damaging
rs551009503	A/G	Q/R	72	benign
rs750128945	C/T	L/F	80	probably damaging
rs779574673	A/C	S/R	81	possibly damaging
rs753351516	G/A	A/T	99	probably damaging
rs754514291	G/C	V/L	100	probably damaging
rs757600072	G/A	G/S	104	probably damaging
rs184583248	A/G	I/V	106	benign
rs373612998	A/G	I/V	113	probably damaging
rs756405653	A/G	T/A	114	probably damaging
rs780487648	C/T	T/M	114	probably damaging
rs774317309	T/C	L/S	120	probably damaging
rs751013702	A/G	M/V	125	benign
rs766883992	A/C	K/N	143	possibly damaging
rs754045659	A/G	I/V	144	benign
rs267598798	C/T	L/F	145	probably damaging
rs755173202	A/G	H/R	148	benign
rs778984867	C/T	L/F	150	probably damaging
rs368195409	C/T	T/M	152	possibly damaging
rs371006593	C/T	P/L	155	benign
rs769678863	G/A	D/N	163	probably damaging
rs748982724	G/A/T	D/N	165	probably damaging
rs748982724	G/A/T	D/Y	165	probably damaging
rs774012759	C/A	L/I	172	probably damaging
rs771341508	T/C	F/L	182	benign
rs759800413	G/C	E/Q	186	probably damaging
rs372678357	A/G	I/V	188	probably damaging

rs775639109	T/G	N/K	193	possibly damaging
rs763172499	C/T	R/C	195	probably damaging
rs572470679	G/A	R/H	195	probably damaging
rs750277651	T/C	S/P	204	possibly damaging
rs756091688	T/C	C/R	205	probably damaging
rs766211274	G/C	G/A	207	possibly damaging
rs34628006	A/G	T/A	211	benign
rs201271037	C/T	T/I	211	benign
rs778690773	C/G	R/G	217	benign
rs772273032	G/A	R/Q	217	benign
rs746290665	C/G	L/V	220	possibly damaging
rs770326074	G/A	C/Y	225	benign
rs749630318	G/A	R/H	231	probably damaging
rs769048668	A/G	T/A	234	possibly damaging
rs751210882	G/A	E/K	246	benign
rs753817182	C/A	P/T	247	benign
rs141573645	C/G	P/R	247	probably damaging
rs555063320	C/A	T/N	252	probably damaging
rs779356852	C/G	H/D	266	probably damaging
rs541173118	T/C	I/T	290	possibly damaging
rs772815471	A/G	I/V	332	probably damaging
rs760347047	C/T	T/I	333	probably damaging
rs546315759	T/A	S/T	339	probably damaging
rs770419767	C/T	S/F	339	probably damaging
rs112562018	C/G/T	I/M	344	probably damaging
rs143509936	G/A	V/M	345	probably damaging
rs150464478	G/A	R/Q	357	possibly damaging
rs780664004	G/T	R/S	361	possibly damaging
rs200251302	C/T	P/L	369	benign
rs548020277	C/T	P/S	370	benign
rs571110701	T/G	S/A	371	benign
rs773819994	G/A/T	E/K	372	probably damaging
rs766798345	T/A	L/H	374	possibly damaging
rs375305010	G/A	A/T	378	benign
rs761813234	A/G	K/R	382	benign
rs750218295	T/C	S/P	384	benign
rs754613373	G/C	S/T	385	benign
rs779822835	A/T	E/D	387	benign
rs753577634	C/T	R/W	389	benign
rs77601858	G/A/C	R/Q	389	benign
rs77601858	G/A/C	R/P	389	benign
rs747410783	A/T	N/Y	393	possibly damaging
rs2305160	A/G	T/A	394	benign
rs746212435	C/G	L/V	395	benign
rs775637085	G/A	D/N	396	possibly damaging
rs768549054	G/A	V/M	397	benign

rs774483099	G/A	G/S	398	benign
rs750425809	C/T	A/V	399	benign
rs552726306	C/T	S/L	400	benign
rs753485790	G/C	G/R	401	possibly damaging
rs146893880	C/G	H/D	406	benign
rs375669635	C/T	S/L	407	benign
rs564795063	C/T	S/L	409	possibly damaging
rs200282440	C/T	A/V	410	benign
rs749718303	A/G	K/E	417	benign
rs768908216	A/T	K/N	417	possibly damaging
rs552031760	C/T	S/L	419	benign
rs773235867	C/T	T/I	421	possibly damaging
rs760704176	A/G	M/V	423	benign
rs766211324	T/C	M/T	423	benign
rs776566216	A/T	E/D	425	benign
rs371932771	C/T	P/L	426	benign
rs754332141	C/T	T/I	429	possibly damaging
rs779158730	T/A	M/K	434	benign
rs748337517	C/T	A/V	435	benign
rs778202316	C/T	T/I	439	benign
rs771178920	C/T	P/L	440	benign
rs745802542	G/C	A/P	441	benign
rs769562382	C/A	P/Q	443	benign
rs200890084	G/A	G/R	456	benign
rs150232826	A/G	M/V	463	benign
rs767036498	C/T	P/L	464	benign
rs375419124	G/C	A/P	465	benign
rs11541353	C/T	S/L	471	benign
rs753291106	C/T	S/F	472	benign
rs764579373	G/A	D/N	474	benign
rs756255193	G/A	V/I	484	benign
rs528544389	G/T	Q/H	486	benign
rs148668573	C/T	T/M	488	benign
rs778685112	G/A	A/T	490	benign
rs748004766	C/G	A/G	490	benign
rs139882603	C/G	P/A	491	benign
rs200963442	A/G	M/V	492	benign
rs778881458	T/A	F/Y	495	possibly damaging
rs530175072	C/T	S/L	496	benign
rs140242316	C/G	Q/E	498	probably damaging
rs746700349	G/C	Q/H	498	probably damaging
rs770292855	C/G	F/L	499	benign
rs769261008	A/G	K/R	506	probably damaging
rs569811925	A/G	E/G	510	probably damaging
rs762042441	A/G	Q/R	511	possibly damaging
rs767945700	C/T	R/W	514	probably damaging
rs370501805	G/A	R/Q	514	probably damaging

rs766577230	A/G	N/S	519	benign
rs753902734	T/G	I/S	520	probably damaging
rs755101176	G/A	R/Q	521	benign
rs765129798	C/G	H/Q	528	benign
rs752666027	G/T	K/N	529	probably damaging
rs777640948	G/T	Q/H	533	probably damaging
rs756916445	G/A	V/I	542	benign
rs751341349	A/G	M/V	544	benign
rs757053262	T/C	M/T	544	possibly damaging
rs780945587	G/C	V/L	551	benign
rs755619536	A/G	T/A	558	benign
rs190648743	G/A	R/Q	560	benign
rs748806872	G/C	E/D	562	benign
rs778182952	G/A	R/K	570	benign
rs747375488	G/C	R/S	570	possibly damaging
rs776791526	G/A	A/T	573	benign
rs145408736	C/T	T/I	575	benign
rs769803607	C/A	P/H	577	benign
rs368846782	G/A/C	G/R	580	benign
rs368846782	G/A/C	G/R	580	benign
rs751476774	C/T	A/V	581	benign
rs767425647	G/A	G/S	582	benign
rs755815520	C/G	P/R	583	benign
rs559977621	G/A	G/E	587	benign
rs753356704	T/G	I/S	589	possibly damaging
rs754493741	C/T	S/F	590	benign
rs778291961	C/T	T/I	595	benign
rs200112782	G/A	S/N	596	benign
rs757547524	C/T	L/F	600	probably damaging
rs781547387	T/C	I/T	606	benign
rs764655773	A/G	K/E	612	benign
rs143362961	G/A	S/N	616	benign
rs200722501	G/A	R/H	625	benign
rs781710928	T/C	S/P	626	benign
rs746214178	C/T	S/F	626	benign
rs146053755	C/T	P/L	633	benign
rs749478359	C/A	F/L	634	benign
rs200492145	G/A	S/N	636	benign
rs369584757	G/A	A/T	637	benign
rs772104477	C/T	A/V	640	benign
rs770660671	C/T	P/L	642	benign
rs759121548	G/A	S/N	644	benign
rs764993831	T/C	L/P	645	possibly damaging
rs752194246	C/T	T/I	648	benign
rs767967015	C/T	S/F	652	benign
rs750962223	A/T	T/S	653	benign
rs755152575	G/T	Q/H	661	benign

rs748216483	A/G	S/G	663	benign
rs373640373	C/G	S/R	663	benign
rs777811242	T/G	F/V	666	benign
rs746945274	A/C	D/A	669	benign
rs770699838	C/T	R/W	670	possibly damaging
rs150614730	G/A	R/Q	670	benign
rs537257287	G/T	R/S	673	possibly damaging
rs769666587	C/A	P/H	682	probably damaging
rs748955496	A/C	M/L	683	benign
rs768357374	G/T	M/I	684	benign
rs761426802	G/A	G/R	686	possibly damaging
rs58728948	G/A	A/T	690	benign
rs765698936	C/T	S/L	694	benign
rs751558229	A/G	R/G	698	benign
rs149857680	C/T	T/M	699	possibly damaging
rs141762291	C/T	R/W	701	possibly damaging
rs779814155	G/A	R/Q	701	benign
rs749148751	T/A	V/D	703	benign
rs769150682	G/A	A/T	706	benign
rs772909964	G/A	V/M	711	benign
rs767702332	T/C	V/A	711	benign
rs760794820	C/G/T	A/G	717	benign
rs760794820	C/G/T	A/V	717	benign
rs754701464	A/T	H/L	718	benign
rs760458330	C/A	P/T	719	benign
rs555995735	C/A	P/H	719	benign
rs141749026	G/A	A/T	720	benign
rs143542914	C/A/T	S/R	724	possibly damaging
rs202116734	C/T	P/L	726	benign
rs769103203	G/A	V/I	729	benign
rs555104961	G/A	G/E	733	probably damaging
rs773444775	C/T	A/V	735	possibly damaging
rs753716965	C/A	H/Q	738	benign
rs759454041	C/G	F/L	741	benign
rs765152742	G/C	A/P	743	benign
rs371339230	C/T	S/F	744	possibly damaging
rs751284957	C/T	S/L	747	benign
rs780841096	G/T	A/S	754	benign
rs759505480	C/T	R/W	755	benign
rs113107029	G/A	R/Q	755	benign
rs779340212	A/G	Q/R	757	benign
rs748498924	C/T	P/L	759	benign
rs773356795	A/G	Q/R	760	benign
rs558168215	C/G	L/V	763	benign
rs769792961	A/C	Q/P	766	probably damaging
rs775429015	G/C	Q/H	766	probably damaging
rs762790005	A/C	T/P	769	benign

rs764196824	C/A	T/N	769	benign
rs761752855	T/G	S/A	778	benign
rs767231151	C/T	S/L	778	benign
rs765822281	A/G	Q/R	787	benign
rs753444490	G/T	G/V	789	possibly damaging
rs367662228	C/G	L/V	791	benign
rs751895331	C/A	P/H	794	unknown
rs781349278	C/G	P/R	797	unknown
rs528422017	C/A	P/T	798	unknown
rs551720531	C/G	Q/E	802	unknown
rs768696753	C/T	R/C	805	unknown
rs774452911	G/A	R/H	805	unknown
rs761660915	G/A	R/Q	808	unknown
rs201591122	G/T	V/F	810	unknown
rs772864295	G/A	S/N	811	unknown
rs760230086	T/A/C	S/T	814	unknown
rs760230086	T/A/C	S/P	814	unknown
rs530536274	C/T	S/L	816	unknown
rs764533479	G/A/T	G/D	818	unknown
rs764533479	G/A/T	G/V	818	unknown
rs80034641	C/T	P/L	822	unknown

Appendix 3: Clock - NPAS2 Alignment.

```
                                                  BHLH Domain
CLOCK       MLFTVSCSKMSSIVDRDDSSIFDGLVEEDDKDKAKRVSRNKSEKKRRDQFNVLIKELGSM
NPAS2       -------------------------MDEDEKDRAKRASRNKSEKKRRDQFNVLIKELSSM
                                     ::**:**:***.********************.**

CLOCK       LPGNARKMDKSTVLQKSIDFLRKHKEITAQSDASEIRQDWKPTFLSNEEFTQLMLEALDG
NPAS2       LPGNTRKMDKTTVLEKVIGFLQKHNEVSAQTEICDIQQDWKPSFLSNEEFTQLMLEALDG
            ****:*****:***:* * **:**:*::**:: .:*:*****:*****************
               PAS-A Domain
CLOCK       FFLAIMTDGSIIYVSESVTSLLEHLPSDLVDQSIFNFIPEGEHSEVYKILSTHLLESDSL
NPAS2       FIIAVTTDGSIIYVSDSITPLLGHLPSDVMDQNLLNFLPEQEHSEVYKILSSHMLVTDSP
            *::*: *********:*:* ** *****::**.::**:** **********:*:* :**

CLOCK       TPEYLKSKNQLEFCCHMLRGTIDPKEPSTYEYVKFIGNFKSLNSVSSSAHNGFEGTIQRT
NPAS2       SPEYLKSDSDLEFYCHLLRGSLNPKEFPTYEYIKFVGNFRSYNNVPSPSCNGFDNTLSRP
            :******..:*** **:***:::***  ****:**:***:* *.* * : ***: *:.*
                                                  PAS-B Domain
CLOCK       HRPSYEDRVCFVATVRLATPQFIKEMCTVEEPNEEFTSRHSLEWKFLFLDHRAPPIIGYL
NPAS2       CRVPLGKEVCFIATVRLATPQFLKEMCIVDEPLEEFTSRHSLEWKFLFLDHRAPPIIGYL
             *    ..***:**********:**** *:** **************************

CLOCK       PFEVLGTSGYDYYHVDDLENLAKCHEHLMQYGKGKSCYYRFLTKGQQWIWLQTHYYITYH
NPAS2       PFEVLGTSGYDYYHIDDLELLARCHQHLMQFGKGKSCCYRFLTKGQQWIWLQTHYYITYH
            ***************:**** **:**:****:****** **********************

CLOCK       QWNSRPEFIVCTHTVVSYAEVRAERRRELGIEESLPETAADKS---QDSGSDNRINTVSL
NPAS2       QWNSKPEFIVCTHSVVSYADVRVERRQELALEDPPSEALHSSALKDKGSSLEPRQHFNTL
            ****:********:*****:**.***:**.:*:   *:  ..:   : *. : * .  :*

CLOCK       KEALERFDHSPTPSASSRSSRKSSHTAVSDPSSTPTKIPTDTSTPPRQHLPAHEKM--VQ
NPAS2       DVGASGLNTSHSPSASSRSSHKSSHTAMSEPTSTPTKLMAEASTPALPRSATLPQELPVP
            . . . :: * :********:******:*:*:*****: :::***   :  :  :   *

CLOCK       RRSSFSS-QSINSQSVGSSLTQPVMSQATNLPIPQGMSQFQFSAQLGAMQHLKDQLEQRT
NPAS2       GLSQAATMPAPLPSPSSCDLTQQLLPQTVLQSTPA--PMAQFSAQFSMFQTIKDQLEQRT
              *. ::  :   .  ...*** :: *:.    *      *****:. :* :********

CLOCK       RMIEANIHRQQEELRKIQEQLQMVHGQGLQMFLQQSNPGLNFGSVQLSSGNSSNIQQLAP
NPAS2       RILQANIRWQQEELHKIQEQLCLVQDSNVQMFLQQPAVSLSFSSTQRPEAQQQLQQRSAA
            *:::***: *****:****** :*: . :******   .*.*.*.*  ..:..  *: *

CLOCK       INMQGQVVPTNQIQSGMNTGHIGTTQHMIQQQTLQSTSTQSQQNVLSGHSQQTSLPSQTQ
NPAS2       V-TQPQLGAGPQLPGQISS-AQVTSQHLLRESSVISTQG--PKPMRSS--QLMQSSGRSG
            :  * *:    *: . :.:    *:**::::.:: **.    : : *.  *  .  .::

CLOCK       STLTAPLYNTMVISQPAAGSMVQIPSSMPQNSTQSAAVTTFTQDRQIRFSQGQQLVTKLV
NPAS2       SSLVSPFSSATAALPPS--LNLTTPASTSQDASQCQPSPDFSHDRQLRLLLSQPIQPM--
            *:*.:*: .: .   *:    :  *:*  *:::*.     *::***:*:  .* :

CLOCK       TAPVACGAVMVP---------------------------------STMLMGQVVTAYPTF
NPAS2       -MPGSCDARQPSEVSRTGRQVKYAQSQTVFQNPDAHPANSSSAPMPVLLMGQAVL-HPSF
              * :* *                                      .:****.*  :*:*

CLOCK       ATQQQQSQTLSVTQQQQQQSSQEQQLTSVQQPSQAQLTQPPQQFLQTSR--LLHGNPSTQ
NPAS2       PASQPS----------------------PLQPAQ-ARQQPPQHYLQVQAPTSLHSEQQDS
             :.* .                      **:*    ****::**..    **.: . .

CLOCK       LILSAAFPLQQSTFPQSHHQQHQSQQQQQLSRHRTDSLPDPSKVQPQ-------------
NPAS2       LLLST-YSQQP----------------------GTLGYPQPPPAQPQPLRPPRRVSSLSE
            *:**: :  *                       * . *:*  .***

CLOCK       ---------
NPAS2       SSGLQQPPR
```